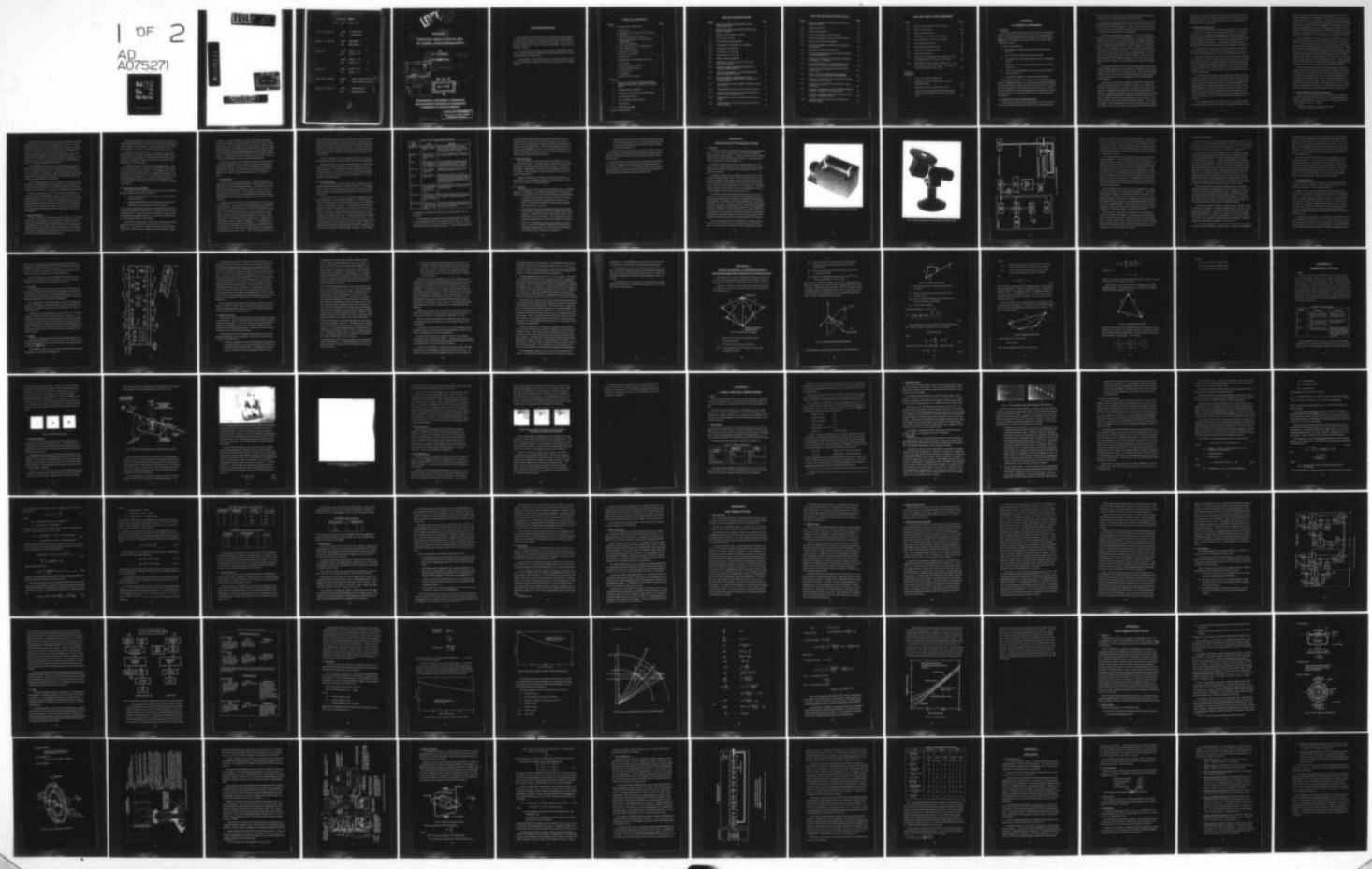
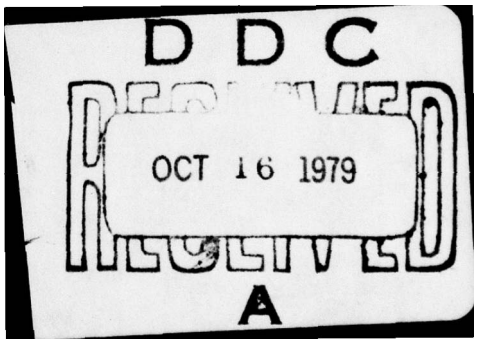
AD-A075 271 MASSACHUSETTS INST OF TECH CAMBRIDGE EXPERIMENTAL AS--ETC F/G 17/7
POSITION INDICATION AT SEA BY ASTRO-PHOTOGRAMMETRY,(U)
NOV 63 A C CONROD N62306-1168
UNCLASSIFIED RE-5 NL




DDC
OCT 16 1979
A

ERRATA SHEET

EAL MIT RE-5

page 19, line 31	read	17,500 watts
	for	5,000 watts
page 37, line 29	read	Appendix C
	for	Appendix II
page 49	read	Table C-1
	for	Table C-2
	read	Table C-2
	for	Table C-3
page 50	read	Table C-3
	for	Table C-4
page 84 footnote	read	. . . other sponsored projects.
	for	. . . other approved projects.
page 86, line 18	read	. . . approximate. . .
	for	. . . appropriate. . .

LEVEL II

(14)

REPORT RE-5

(6)

POSITION INDICATION AT SEA BY ASTRO-PHOTOGRAMMETRY

BY

(10) A. C. CONROD

(12) 131

(11) NOVEMBER 1963

(15) N62306-1168

Accession For
NTIS GRA&I
DDC TAB
Unannounced
Justification
By letter on file
Distribution/
Availability Codes
Dist | Avail and/or special
A

DDC
RECEIVED
OCT 16 1979
A

EXPERIMENTAL ASTRONOMY LABORATORY
MASSACHUSETTS INSTITUTE OF TECHNOLOGY
CAMBRIDGE 39, MASSACHUSSETTS

DISTRIBUTION STATEMENT A
Approved for public release;
Distribution Unlimited

387 140

LB

ACKNOWLEDGMENT

The contents of this report are the result of the work of the staff of the Experimental Astronomy Laboratory of the Massachusetts Institute of Technology, especially the Laboratory Director, Prof. Winston Markey, and Messrs. Bernard Blood, Thomas Egan, David Eto and Charles Lothrup.

The work described herein was performed under DSR Contract 9444, sponsored by the United States Naval Oceanographic Office under Contract Number N62306-1168.

The publication of this report does not constitute approval by the Naval Oceanographic Office of the findings and conclusions contained therein.

TABLE OF CONTENTS

Chapter		Page
I	STATEMENT OF PROBLEM	1
	1. Introduction	1
	2. Location of a Ship at Sea by Astro-Photogrammetry	1
	3. Method and Pertinent Geometry	3
	4. Recent Developments in Fixed-Camera Photography	4
	5. Need for stabilization	5
	6. Self-contained and Intervisible Modes	6
	7. Time Determination	7
	8. Sources of Uncertainty	8
	9. Outline of the Report	10
	10. Conclusions	10
II	DESCRIPTION OF PROPOSED SYSTEM	12
	1. Description	12
	2. Camera, Shutter and Timer	17
	3. The Stabilization System	18
	4. Control Panel	19
	5. Packaging	19
	6. Operation of the System	21
APPENDIX		
A	SIMPLE GEOMETRIC CONSIDERATIONS IN PHOTOGRAMMETRIC POSITION DETERMINATION	26
B	EXPERIMENTAL STUDIES	32
C	CAMERA, SHELTER AND PROGRAMMER	40
D	THE TIMING SYSTEM	54
E	THE STABILIZATION SYSTEM	72
F	PACKAGING	85
G	GYROCOMPASSING	90
LIST OF REFERENCES		122

LIST OF ILLUSTRATIONS

Figure		Page
1	Model of the Astro-Photogrammetric Ship Positioning System	13
2	Model of the Stabilization System Gimbals with Ballistic Camera	14
3	System Functional Block Diagram	15
4	System Control Panel	20
A-1	Four-Camera Vector Diagram	26
A-2	Photographic Plate-Position Coordinates	27
A-3	Components of Vector $\overline{S}_{ij}$	28
A-4	Components of Vector $\overline{R}^{r}_{j}$	29
A-5	Construction of Vector $\overline{P}^{r}_{4}$	30
B-1	Shutter Diffraction Effects	33
B-2	Roll Motion of Camera Axes with Two-Axis Stabilization System	34
B-3	Stargazer Telescope Stabilization System on Single Axis Swing Platform	35
B-4	Star Trail Photograph – Two-Axis Stabilization, with Misalignment in Train	36
B-5	Photomicrograph of Star Image on EG & G Type X-R Film, through (a) blue, (b) green and (c) orange filters	38
C-1	Photomicrograph of Star Images on Eastman Kodak 103-F Plate	43
D-1	Communications Net for Camera Synchronization	60
D-2	Communications Equipment for Synchronization of Cameras to Flashing Satellites	62
D-3	Position Error in Feet as a Function of Errors in Timing	65
D-4	Position Error in Feet as a Function of Errors in Orbital Position	66

LIST OF ILLUSTRATIONS (Cont.)

Figure		Page
D-5	Error in Geographical Position Due to Error in Satellite Position	67
D-6	Transmission Time	70
E-1	Gimbal Configurations	74
E-2	Mechanical Assembly, Train Gimbal	76
E-3	Mechanical Assembly, Roll and Pitch Gimbals	78
E-4	Sketch of a Three-Gimbal System	79
E-5	Functional Diagram of a Single Axis Integrating Drive System	82
F-1	Stabilization System Control Panel	89
G-1	Functional Diagram for an Acceleration-Coupled Gyrocompassing System	93
G-2	Orientation of Platform Coordinates with Respect to Geographic Coordinates	94
G-3	Functional Diagram of a Simplified Model of an Acceleration-Coupled Gyrocompassing System	100
G-4	Variation of Gyrocompassing Time With Initial Azimuth Error	105
G-5	Variation in Gyrocompassing Time Between + and − Values of $A_z(0)$ with Loop Gain Ratio	107
G-6	Variation in Alignment Time with Initial Conditions on Platform Error Angles	108
G-7	Variation of Alignment Time with $A_y(0)$ for Gyrocompassing	109
G-8	Variation in Alignment Time with Initial Conditions with Rate Limiting for the Azimuth Gyro	111
G-9	Variation of Platform Error Angle Magnitude with Frequency of Heading Wander	120
G-10	Variation of Alignment Time with Latitude on a Stationary Base	121

LIST OF TABLES AND SUMMARIES

Table		Page
I-1	Errors in Photographic Plate Reduction	9
B-1	Shutter Comparisons	32
C-1	Camera Characteristics	40
C-2	Light Intensity for Given Trace Widths	49
C-3	Star Magnitude for Given Trace Widths	49
C-4	Star Density Distribution	50
D-1	Timing System Specifications	63
E-1	Stabilization System Parameters	84
G-1	Glossary of Symbols	91
G-2	Variation of Leveling and Gyrocompassing Time with Sign Reversal of Initial Azimuth Error . . .	104
G-3	Steady-State Platform Error Angles (A_x, A_y, A_z) as a Function of Gyro Drift (E_{gx}, E_{gy}, E_{gz}) and Accelerometer Bias (E_{ax}, E_{ay})	115

Derivation Summary		
1	Derivation of System Equations	97
2	Derivation of the Transient Behavior of the Simplified Model	101
3	Alignment Errors on a Stationary Base	113
4	Derivation of Performance Functions Relating Platform Error Angles to Northerly Accelerations	116

CHAPTER I

STATEMENT OF PROBLEM

1. Introduction

The Experimental Astronomy Laboratory of the Massachusetts Institute of Technology, acting under U.S. Naval Oceanographic Contract Number N62306-1168, as amended, has prepared the following study of a method of locating a ship at sea by astro-photogrammetric methods.

Included in the study are:

1. The design of a stabilization system for a ship-borne camera
2. The selection of suitable camera parameters
3. Consideration of photographic exposure from a stabilized camera
4. The selection of a suitable timing system for ship-borne applications
5. A study of the propagation of errors in the collection and reduction of data
6. A suggested design for a complete system package.

The system described in this report is a surveying instrument and not a navigational device. It consists of an inertially stabilized photo theodolite with which one can accurately locate aids to navigation and make geodetic observations from a ship at sea. Like all direct-observation surveying techniques, good observational weather is required for its use, and results are only available after data processing.

2. Location of a Ship at Sea by Astro-Photogrammetry

If the precise location of an orbital vehicle is known relative to earth-fixed coordinates and if the direction of a line through that

position is known, then the point of intersection of that line from the satellite, with the Earth's surface will also be known.

This study is concerned with the construction of that line by photographing a satellite against a star-field and by an accurate determination of the time of each photograph. Given: 1) the location of a satellite relative to the stars, and 2) the time, the position of the camera on the surface of the Earth can be determined.

There are, from a geodetic standpoint, two kinds of satellites that may be used for astro-photogrammetry. One is the passive satellite, such as ECHO which is visible whenever sunlight is reflected from the surface of the satellite to the earth, provided the observer is on the nighttime side of the earth and the satellite is in twilight, Ref. (1). Any orbiting body may be used as a passive target when it is visible from the observer's station. The second is the active satellite, of the ANNA type, which carries a flashing light. The light may be turned on by command whenever desired, so that it may be observed even when in the Earth's shadow. The use of active satellites requires the support of a ground station to control the flashing light.

While opportunities for passive satellite photography may be had merely by selecting a target, active satellite photography requires that a specially built vehicle be launched into orbit. With active satellites, however, there will probably be ground observation stations planned as part of the project, with a consequent promise of good geodetic survey support.

The orbits of either active or passive satellites will determine their usefulness as targets for geodetic surveying. The higher the satellite's orbital altitude, the greater the range over which it can be seen, and consequently the longer the base line between observing stations. A satellite travelling in an orbit 1000 miles high will, under the proper lighting conditions, be visible at stations up to 3000 miles apart. Another important orbital parameter is the inclination, the angle between the orbital plane and the Earth's equator. The inclination angle is also the approximate North-South latitude limit of satellite travel. Thus, an 83° orbit will travel from 83°N latitude to 83°S

and could be visible from almost any point on the Earth, while a 30° orbit, being limited to the band from 30°N to 30°S, would not be visible much further north or south than the 35th to 40th parallels, depending on the orbital altitude.

3. Method and Pertinent Geometry

There are two methods of determining the position of a satellite at a given time; by means of an accurate ephemeris, or by triangulation from two or more observing stations. Once the satellite location has been determined, the position of an observing station may be derived after the orientation of the photographic plate at the time of photography is determined. A description of the geometry of photogrammetric position determination is contained in Appendix A.

Because of the uncertainties in present techniques of satellite ephemeris prediction, the method of simultaneous observations is the only one recommended for serious consideration at this time.

This method requires the use of three or more ballistic cameras (1 at sea and 2 or more on land) of the quality used by the U.S. Coast and Geodetic Survey for geodetic research, plus supporting timing and communication equipment. In addition, the camera aboard ship must be supported on a stable platform in order to isolate it from the ship's motion. This necessitates a system of gimbals and a stabilization subsystem.

A minimum of two cameras are mounted at precisely known locations on shore and pointed to the approximate location in the sky where the satellite will be at the time of exposure. The stable platform on the ship is leveled and a line on the platform aligned with geographic north through the technique of gyrocompassing. From this orientation the camera is slewed in azimuth and lowered in coelevation to point in the predicted direction of the satellite at the time of passage. The local station clocks will have been synchronized to each other by one of several techniques described in Appendix D.

At preselected times, from signals from their respective station programmers, the shore cameras are stepped through a series

of precalibration exposures, to provide a photographic record of camera orientation. The shipboard camera will not perform this precalibration since its orientation will be continually changing due to gyro drift. The orientation of the shipboard camera is determined directly from the stars in the background of the photographic plate when the photographs are taken. The position of the stars at the times of the satellite exposures are identified through the aid of programmed variations in the star trails; i.e., a variation in exposure sequence will provide a time code index on the photographic plate.

After completion of the shore camera precalibration the shore station camera shutters are closed until the satellite comes into view, at which time the shutters of the cameras will be actuated in a predetermined manner through their station programmers. There will be only one photographic plate produced in each camera. The photograph will contain multiple images of the stars and the satellite so that measurements of star-satellite separation can be made. A typical shore camera photograph may be seen in Ref. (2), and a shipboard camera plate is shown in Appendix B, Fig. 4. After passage of the satellite the shore cameras will go through a postcalibration sequence to verify the orientation of the photographic plates.

Following careful processing of the photographic plates the image coordinates are read on a Cartesian coordinate comparator and this data is processed for use in the data reduction procedure. The result of the reduction of the shore camera photographs is a construction of a portion of an orbit, in which the position of the satellite versus time is known. Then, since the time of each exposure of the shipboard camera is known, the line in space connecting the satellite and the ship can be constructed and the intersection of that line with the Earth's surface is the ship's position.

4. Recent Developments in Fixed-Camera Photography

The concepts of photogrammetric techniques as a means of missile tracking and the application of astro-photogrammetry to geodesy are largely due to the work of Dr. Helmut Schmid* and, more recently, Duane C. Brown.**

---

* *Ballistic Research Laboratory, Aberdeen Proving Grounds.*

** *Duane Brown Associates, Inc., Melbourne, Fla.*

Experiments in geodetic surveying with rocket flares have been performed at the Atlantic Missile Range (3), and the U.S. Coast and Geodetic Survey has been attempting to use artificial earth satellites to improve the accuracy of the 1st order triangulation network (2). In both cases, fixed cameras were used. The U.S. Naval Oceanographic Office has conducted field tests with a stabilized camera at AMR, in which preliminary tests indicate a position accuracy of 2 feet when using an airplane at 40,000 feet altitude as a simulated flashing light satellite. (4)

In the AMR fixed-camera test, Brown attempted to locate the island of Bermuda by simultaneous photography of rocket flares from two known positions on the U.S. mainland and from one camera on the island. The latitude, longitude and height of the Bermuda camera were treated as the unknowns. The methods of reducing the data are described in the reference.

While the published results of the Bermuda tie have been questioned on the methodology of the data reduction, the methods of observation were proven sound. All three cameras recorded flare images, and the basis for a successful triangulation was established.

The survey program of the U.S. Coast and Geodetic Survey, being conducted by LCDR Eugene Taylor, is using fixed cameras in portable stations to attempt to improve the accuracy of 1st order triangulation of the U.S. mainland by simultaneous observation of Earth satellites. Results of the data analysis are not available at the time of this writing, but a number of successful two and three station simultaneous observations have been made over the past few months.

5. Need for Stabilization

Fixed, shore-based cameras are rigidly mounted to a relatively stable base, and possible camera orientation changes are easily checked by photographing star fields before and after an event. On a moving base, e.g., a ship, camera axes would be in continuous angular motion unless the camera were stabilized, and it would be impossible to determine the orientation of the camera at any given time solely by examining photographic plates.

The ship-board camera will therefore be mounted on an inertially stabilized platform, to isolate the camera from angular base motion; ship's roll, pitch and yaw. Because of the extreme range of the satellite, there will be no parallax from ship's motion.

Aiming of the camera will be accomplished by allowing the stable platform to first gyrocompass, and then by setting in azimuth and elevation angles for the predicted satellite pass. By so doing, the acquisition of targets by the camera system is made independent of ship's heading.

A stabilized camera will produce photographic plates, from which it will be possible to measure the orientation of the camera for each of several instants of time. The orientation will be determined by the gyroscopic units in the stabilization system, and will be held to approximately 0.15 arc second per second of time. The photographic images will be expanded on the plate by the method explained in Appendix C, in order to facilitate the reading of the plates.

6. Self-contained and Intervisible Modes

Two methods of determining the position of a ship from photography of satellites have been mentioned:

1. Deriving ship's position from orbital data contained in an orbital ephemeris.
2. Deriving ship's position from orbital data obtained by triangulation of the satellite from shore cameras.

The use of an orbital ephemeris allows ship's position determination with the shipboard camera only, and will be termed the "self-contained mode". When location of the satellite is determined by simultaneous photography from two or more shore stations, the term "intervisible mode" will be used.

In the self-contained mode, the accuracy of the derived ship's position is directly dependent on the accuracy of the orbital ephemeris. In geocentric coordinates, an error in sub-satellite position of 1 arc-second will result in an error of ship's position

of 100 feet. Current satellite prediction techniques are yielding errors of 20 to 50 arc-seconds topocentrically referred for a single orbit period, and topocentric errors over several days may exceed 200 arc seconds. At a satellite slant range of 1000 n. miles, a 200 arc second observation error could result in an error in ship's position of 1 nautical mile, about 30 times greater than the desired system accuracy. The reader is directed to Appendix D and to Ref. (5) for an analysis of observation errors in deriving ship's position.

In the intervisible mode the satellite may be accurately located, under ideal conditions, by two cameras operating simultaneously from known positions. Measurement uncertainties in deriving the satellite's location will be reducible by increasing the number of observations, either by multiple exposures, more cameras, or both.

7. Time Determination

The real time of each photograph of a satellite must be determined to locate the satellite's position on the constructed orbital path described in the preceeding sections. The effects of an error in time determination are identical to those of an error in the orbital position of the satellite. The magnitude of those errors is dependent on the time error and the range and coelevation angle of the satellite from the observer's station, and the satellite's orbital velocity.

Satellites usually travel at 25,000 feet per second, or 25 feet per millisecond. An error in time determination of 1 millisecond would result in a maximum error of 25 feet in orbital position, or about 1 arc seconds at 1000 n. miles. This would result in a maximum error of 25 feet on the Earth's surface (satellite at zenith), which would be reduced as the slant range and coelevation angles increased. It is possible to determine time to 0.1 millisecond, using commercially available components. The techniques for accomplishing this are described in Appendix D. By limiting time errors to ± 0.1 millisecond, we may limit the resulting errors in ship's position to 2.5 feet, which is small enough to be neglected in comparison with the other errors. This is discussed in Ref.(5). In

the intervisible mode there is an added operational requirement of synchronizing the clocks of several stations to a single reference so that the timing differences between cameras can be determined. Time will ultimately be derived from UT-2, the international reference time, but each station will include a means of maintaining an independent clock, either an accurate crystal oscillator or an atomic clock.

Periodic checks of local clocks against UT-2 may be made through one of several techniques that are described in Appendix D.

The station clocks are used to generate signals for the station programmers, whose function is to control the operation of the camera shutters. A recording device will register the output of the station clocks, as real time, and the shutter position signals, in order to provide a permanent record of exposure vs. time for the data reduction process.

8. Sources of Uncertainty

The principle errors inherent in the astro-photogrammetric system previously described are listed in Table I-1. The magnitudes of the errors should be treated with some caution inasmuch as the majority have been determined by analysis rather than by experiment.

The use of the word "error" is somewhat misleading since, by strict definition, errors are determinable. In the present case, even though some errors could be determined, each is considered to be a 1σ uncertainty. Further, if each source is assumed independent, a standard deviation of 4.5 seconds of arc can be established. Using Fig. 5 from Appendix D this number can be converted into a 1σ value for the ship's position uncertainty under varying conditions of satellite geometry. If the slant range to the satellite is 1000 nautical miles the worst case would yield 135 feet. This number is the result of one measurement on the photographic plate. Normally twenty such measurements would be made. If all measurements are assumed independent the resulting uncertainty in the ship's position could be reduced by $\sqrt{20}$. However, in the absence

Table I-1. Errors in photographic plate reduction.

TYPE OF ERROR	ORIGIN	MAGNITUDE
Human error	Primarily comparator operator reader errors	With a calibrated comparator and a skilled operator, the limit of accuracy is about ± 3 microns (with a camera of 12" focal length this is equivalent to 2 arc seconds).
Lens distortion	Unknown or uncompensatable distortions and aberrations	With a properly designed and calibrated lens these should be held to within ± 3 microns.
Timing	Uncertainties in real time determination or in multiple camera synchronization	For reasons explained in Appendix D, a timing error of 100 microseconds is assumed, and the equivalent error in arc seconds is negligible in terms of this error analysis.
Orbital data	Errors in the post event synthesis of an orbit	Current practice yields topocentric angular errors between 20 and 50 sec of arc.
Position	Imperfect geodetic survey data	The magnitude is subject to the extent to which the shore stations have been surveyed. In the present study it is assumed the ship's location is to be determined relative to the shore network. Consequently position errors are not considered.
Stabilization	Gyro drift and imperfect stabilization in the presence of ship's roll and pitch.	The error budget here is complex. For reasons explained in Appendix E, 2 seconds of arc will be assumed.
Atmospheric	Image dancing of star and satellite and stellar scintillation due to air mass motion	With a 4-inch aperture camera, a value of ± 2 arc seconds is assumed, for reasons explained in references (3) (6) (7) (8) and (17).
Star Catalogue	Uncertainties in incorrect inital cataloguing and proper motion	The current technology, as described in Refs. (6) and (7), is such that the assumption of 2 arc seconds is reasonable.

of quantitative statistical models such a reduction will not be postulated.

The preceeding analysis should not be interpreted as a specific error analysis since such is not possible at this time. For example, twenty percent of the sum of the 1σ value in Table I-1 is made up of human error and stabilization error. The actual performance

of a stabilization system cannot be predicted except in the most general terms, and must be measured in testing. Also, the human errors in reading plates reflecting imperfect stabilization are subject to future experiments. If the error resulting from the interaction of stabilization system errors and plate reduction errors could be reduced by a factor of four the 1σ value of uncertainty in ship's position could decrease 20 percent.

9. Outline of the Report

The preceeding has consisted of general information of a primarily tutorial nature. The study program described in this report consisted of both analytical and experimental parts. These are described in Appendices A through G and are outlined in the table of contents. Each appendix is self contained and may be read for specific information.

Chapter II contains a description of the complete system as designed from the conclusions reached in the appendices. A summary of the principle conclusions follows:

10. Conclusions

The location of a ship at sea by astro-photogrammetric methods appears to be feasible. The design and construction of a system to perform this function will have to satisfy the following requirements:

1. A ballistic camera equal to or better than those currently available from several commercial sources will be required. The camera should have uncertainties in distortions of less than 3 microns.

2. The camera will require stabilization sufficient to isolate it from ship's motion and to prevent image blurring during exposure. Stabilization should be accurate to about ± 2 arc seconds over a 5 second period. This requirement is discussed in Appendices C and E, and in Chapter II, Section 3.

3. The choice of stabilization system performance requirements, camera parameters, exposure times and system operating techniques are to be considered simultaneously in the design and/or selection of components.

4. A method of time determination whose characteristics and calibration requirements are consistent with operation at sea for relatively long periods of time should be chosen, according to Appendix D.

The results of this study indicate that these conditions can be met, and that no developmental efforts beyond the design engineering will be required to buy or build the components required for such a system.

It has also been concluded that the technique of data handling now in use is capable of producing accuracies approaching the 50 - 100 feet contained in contract N62306-1168 when the system is operating under acceptable conditions, although the techniques of reading and analyzing plates warrants further study.

CHAPTER II

DESCRIPTION OF PROPOSED SYSTEM

1. Description

The proposed Astro-Photogrammetric Ship Positioning System, Fig. 1, will be a self-contained unit, with all sub-assemblies housed within a single shelter. No ship's facilities will be required to operate the system except electrical power, and possibly electrical connections to radio antennas, etc.

It will be possible to perform all of the operations of a conventional shore based ballistic camera station aboard ship without direct support from shore except plate reading and periodic reference time checks.

A ballistic camera will be mounted on a three gimbal, three axis stabilization system, Fig. 2, whose functions will be to control the orientation of the camera and to provide isolation of the camera's axes from the angular motion of the ship. The camera is described in the following section, and in Appendix C. The stabilization system is described in Section 3 and Appendices E and G. A block diagram of the system is shown in Fig. 3.

The camera will be held fixed to approximately ± 2 arc seconds per 5 seconds, the actual figures being dependent on the interval between exposures as mentioned in Section 6 following and in Appendix D. The method of achieving stabilization is described in Section 3 following. Stabilization of the camera will be possible under sea conditions causing ship's motion of up to ± 20° regardless of camera orientation. Camera aiming will be possible from 0° to 90° elevation, and in azimuth at any point over 360°, except that a vignetting by the system shelter and ship's superstructure will impose some limitations on the area of the sky that can be covered.

The camera shutter will be controlled by a programming console, which is described in Section 4, following, and in Appendix C and F. The function of the console will be to operate the camera

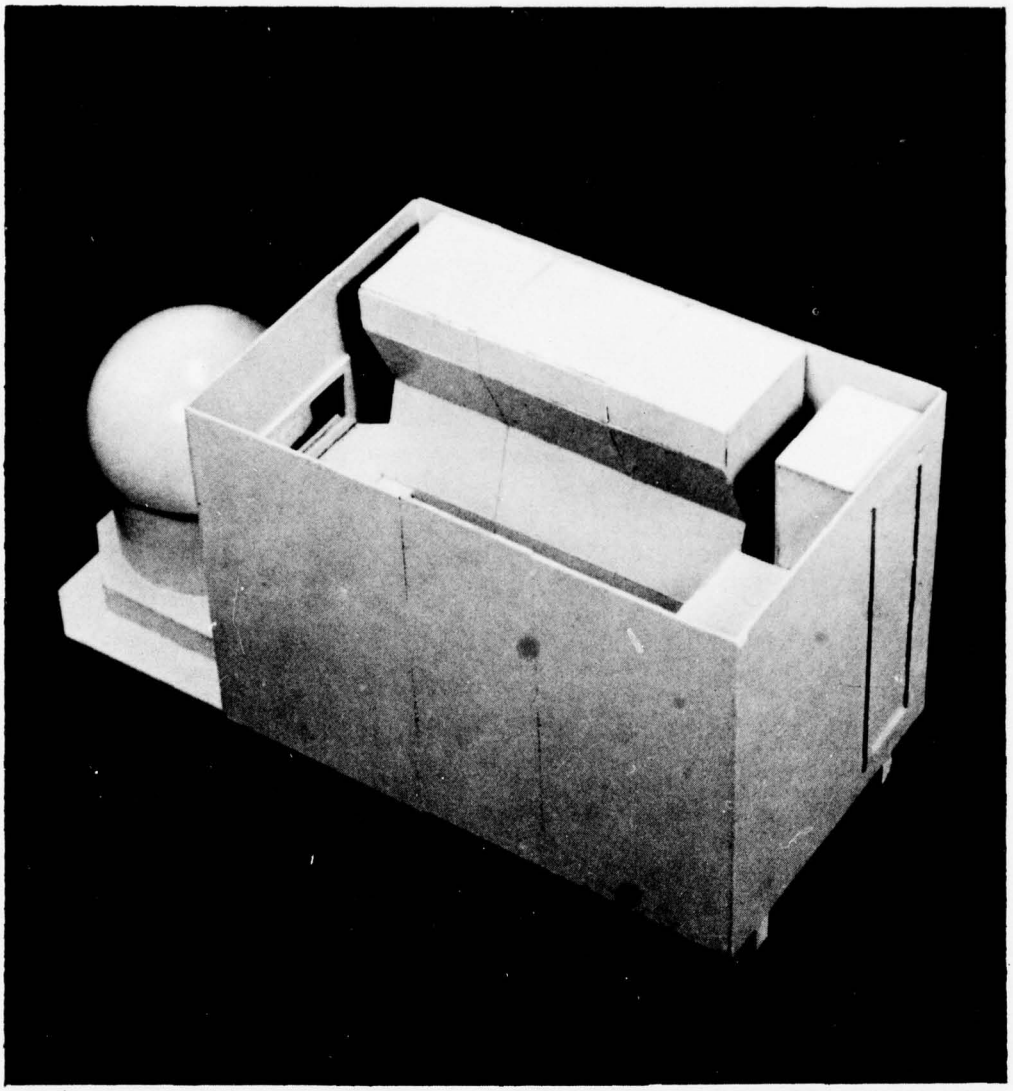


Fig. 1. Model of the astro-photogrammetric ship positioning system.

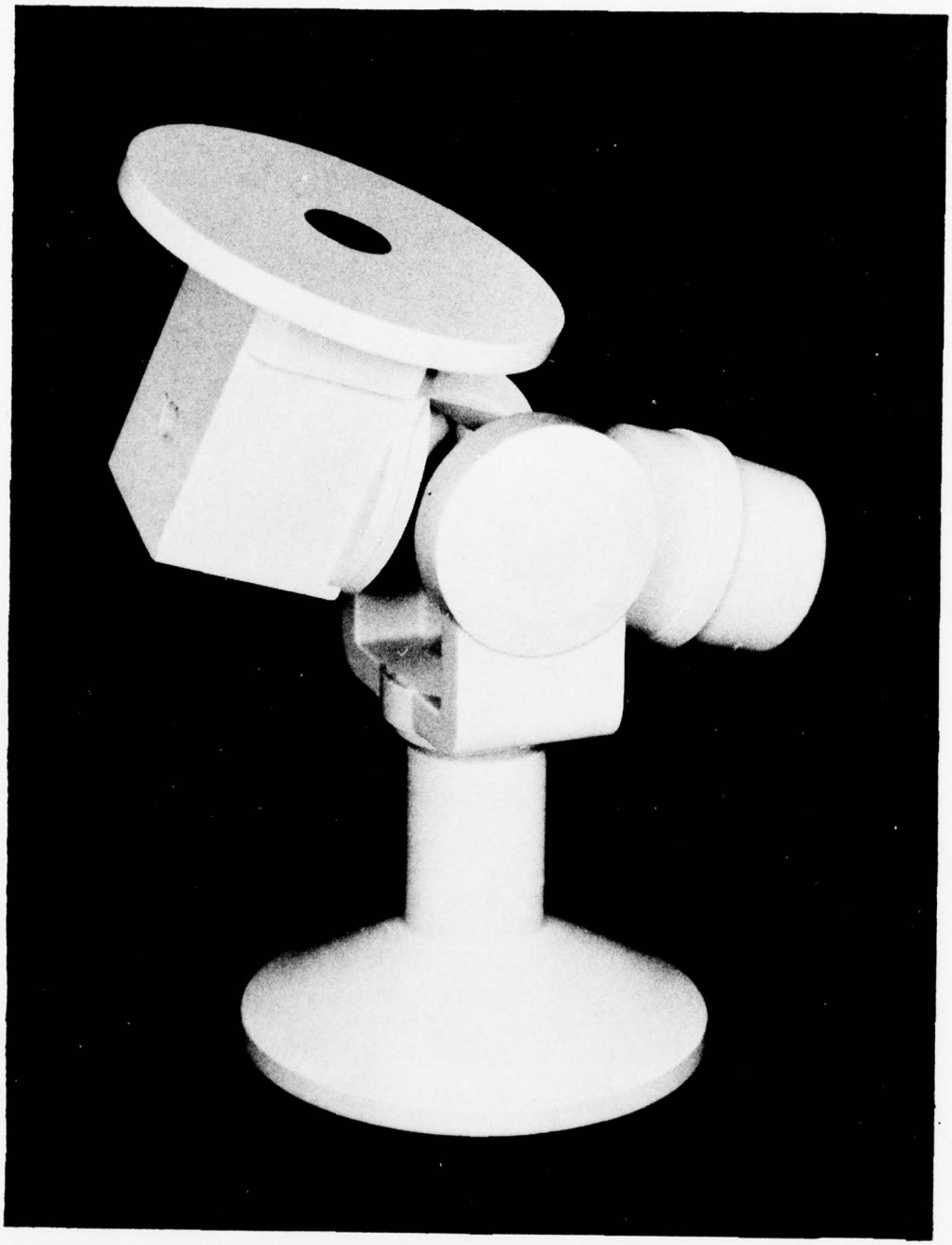


Fig. 2. Model of the stabilization system gimbals with ballistic camera.

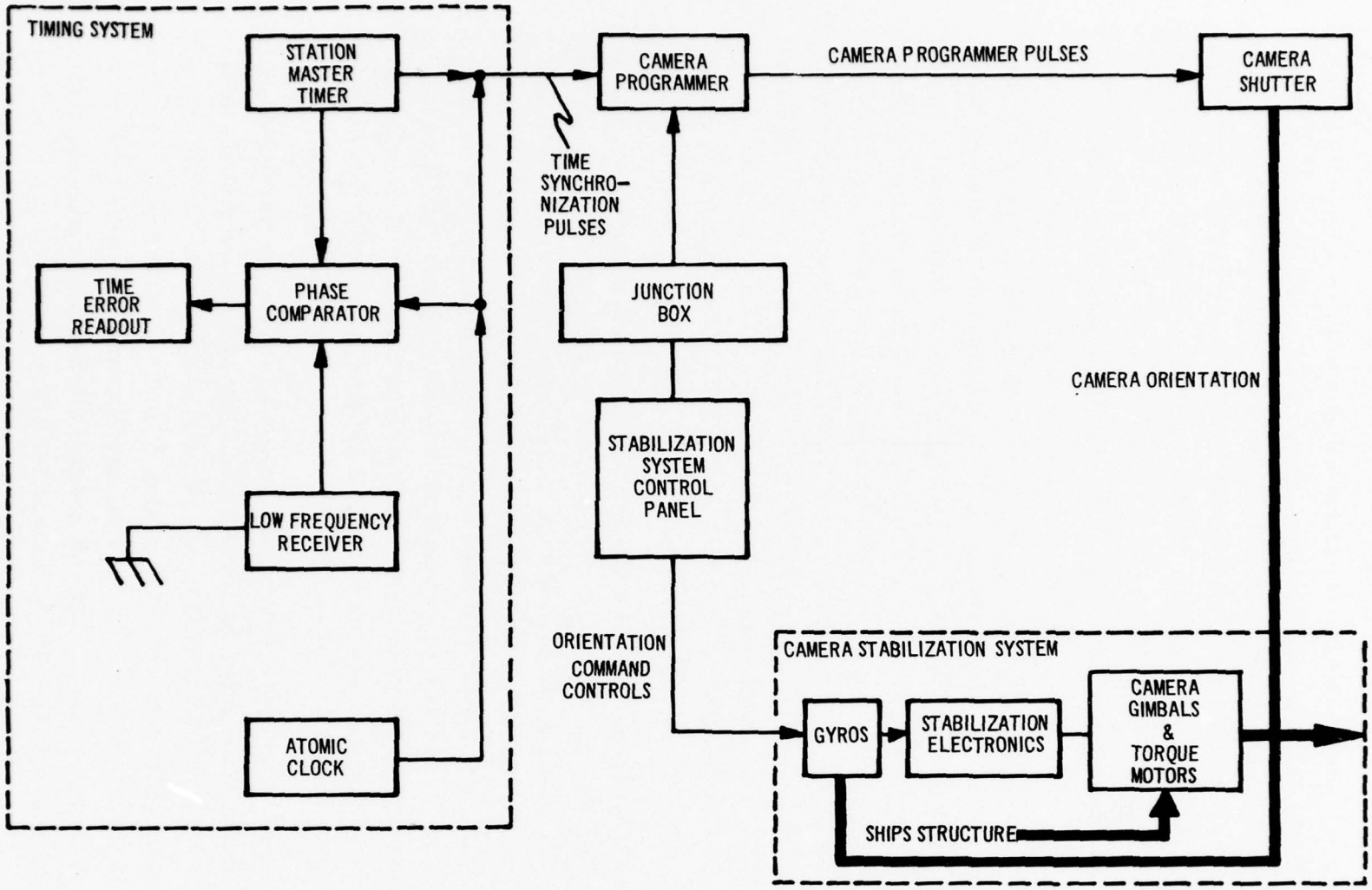


Fig. 3. System functional block diagram.

shutter and record the time of each shutter opening. The camera programmer may be considered adjunct to the system control panel in this case, in that the two encompass all of the electrical interfaces for the system. Control functions will be distributed so that the programmer will contain the elements used in camera system calibration and checkout, and the control panel will provide the system operation controls.

The timing system must satisfy the criteria described and defined in Appendix D. The accuracy of the clock must be determinable, readout must be to a precision of 100 microseconds, and calibration at sea is required. For shore-based equipment these conditions may be met with commercially available parts. The only problem unique to the system under consideration is calibration while at sea. Clock setting by radio link (WWV and VLF stations) can give the required accuracy, but reception may be unreliable at certain places and times. The proposed system should include an atomic clock, probably of the cesium vapor resonator type, to provide an on-board primary time standard and to act as a stand-by station clock.

Environmental control of the camera and equipment compartment will be necessary, as explained in Appendix F. The camera compartment temperature and relative humidity will have to be controllable to match the outside ambient prior to use, while the equipment shelter will have to be maintained at constant conditions. With careful design, a single air conditioning unit should be able to handle both requirements. Environmental control is important for proper camera operation and for equipment reliability, and an adequate air conditioner must be used regardless of cost.

The complete system will be installed in a portable shelter, which is described in Appendix F. The camera and stabilization system will be housed in one compartment, and the timing equipment, a master control panel, and environmental control equipment in the operator's area. Tools, instruments and spares will be provided for. The shelter will provide all-weather protection to all subsystems when the system is not in use.

2. Camera, Shutter and Timer

The system camera will be similar to the Wild BC-4 or ICF PC-1000 in concept. The camera will be fitted with a shutter assembly designed to be synchronized by an electronic timing system. For a description of the proposed designs, the reader is referred to Appendix C.

The proposed camera focal length will be nominally 12 inches, with a maximum lens aperture of f/4.0 to f/2.0. Aperture control to f/32 would be desirable. The lens would preferably be of the so-called aplanatic type; i.e., a lens free of spherical aberrations and coma for point objects. The lens distortion characteristics are of primary importance, (3, 6 and 7). The common method of specifying ballistic camera lenses has been to state that radial distortion should be a continuous function, and tangential distortion should be held to some acceptably small amount, usually a micron. It is possible that these requirements cannot be met in manufacturing. Since lens distortion is an important part of the data reduction procedure, (5) and (6), it will be necessary to completely test all lenses and plot the actual distortion contours over the entire format.

The camera will be a precision casting or built up assembly, designed to maintain the photographic plate or film in very close relation to the lens focal plane and optic axis. In addition to the lens cell mount and film plane positioning assembly, the camera body will house fiducial markers and a data card assembly. It might be desirable to include a binary-coded lamp readout to print index and time data directly onto the emulsion during photography.

The shutter assembly will be a between the lens, variable speed, interrupter type shutter. A separate capping shutter will allow using the camera as a fixed, conventional ballistic camera, or for single exposure photography. There are commercially available shutters that would satisfy the present requirements, but it may prove, after more study, that a shutter design effort will be justifiable. Suitable designs are described in Appendix C and in Ref. (7).

The timers, Appendix D, will consist of a time reference device, such as a crystal oscillator or atomic clock, a means of independently

checking the time reference, a synchronized shutter command device and a means of graphically recording time and shutter data. Existing camera timers use a crystal clock, a VLF and WWV receiver and a strip chart recorder for these functions (9). The only major changes suggested for the shipboard application will be the addition of a second, redundant clock, preferably an atomic clock, for better reliability and for relative independence from WWV or VLF reception failures.

The interconnection between the timer and shutter will be a shutter programmer. This device will provide the shutter commands at the intervals and in the order required, and will maintain synchronism between the timer and the shutter. Time, programmed commands and shutter response will be fed into a monitoring oscilloscope display, and will be recorded on an oscillograph. For maximum flexibility, the input to the programmer should be on punched tape rather than manual settings.

3. The Stabilization System

The stabilization system consists of a set of gimbals which support the camera relative to the ship, gyroscopic units, a set of servo electronics, and an operating console.

Figure 2 shows a model of the gimbal stabilization system. The camera is mounted on the innermost gimbal of a three gimbal system. The gimbals are identified as pitch, roll and train starting on the inside. The gyro units are mounted in the cylindrical core on one end of the pitch gimbal and sense any angular motion of the camera. Signals, generated by the gyros, are processed by a set of servo electronics (not shown in the figure) and converted into currents which drive motors mounted on the gimbals. Through this process the camera is stabilized relative to inertial (stellar) space.

In addition to stabilization, it is necessary to provide a system for orientational control of the camera. For example, prior to use the camera will be stored in a vertical position. When the gimbals are unpinned the camera will be positioned in azimuth and elevation for interception of the satellite. Finally, during photography

the camera will be slewed at pre-selected rates as explained in Appendix C. All of these functions are accomplished by introducing appropriate signals to the gyros on the gimbal drive system. The camera will rotate at an angular velocity about each axis proportional to the signal introduced to the appropriate gyro.

The control panel, from which operation of the system is accomplished, is described in the next section. Details of the stabilization system design are presented in Appendix E.

4. Control Panel

The integrated Astro-Photogrammetric Ship's Positioning System has been designed so that the actual photographic operation can be performed by one man at a central operating position. The loading of the camera preparation of the shutter program will have been completed beforehand. (See Section 6 following.)

The control panel will be comprised of a central operating position for controlling the stabilization system and camera shutter, instruments to monitor the operation of all subsystems and the system junction box.

A tentative control panel design is shown in Fig. 4. The panel is further described in Section 6, following, and in Appendix F. The majority of the control panel functions have to do with the stabilization system, since the commercially available timer-programmer assemblies already include the control functions necessary to themselves. There will be modifications required on the presently available timer-programmers in order to make them compatible with a central control.

5. Packaging

The Astro-Photogrammetric Ship's Positioning System will be housed in a portable shelter and will be entirely self-contained with the exception of ship's-service electrical power requirement of approximately ~~5,000~~ 17,500 watts.

The shelter is shown in Fig. 1, and the requirements and design parameters are discussed in Appendix F.

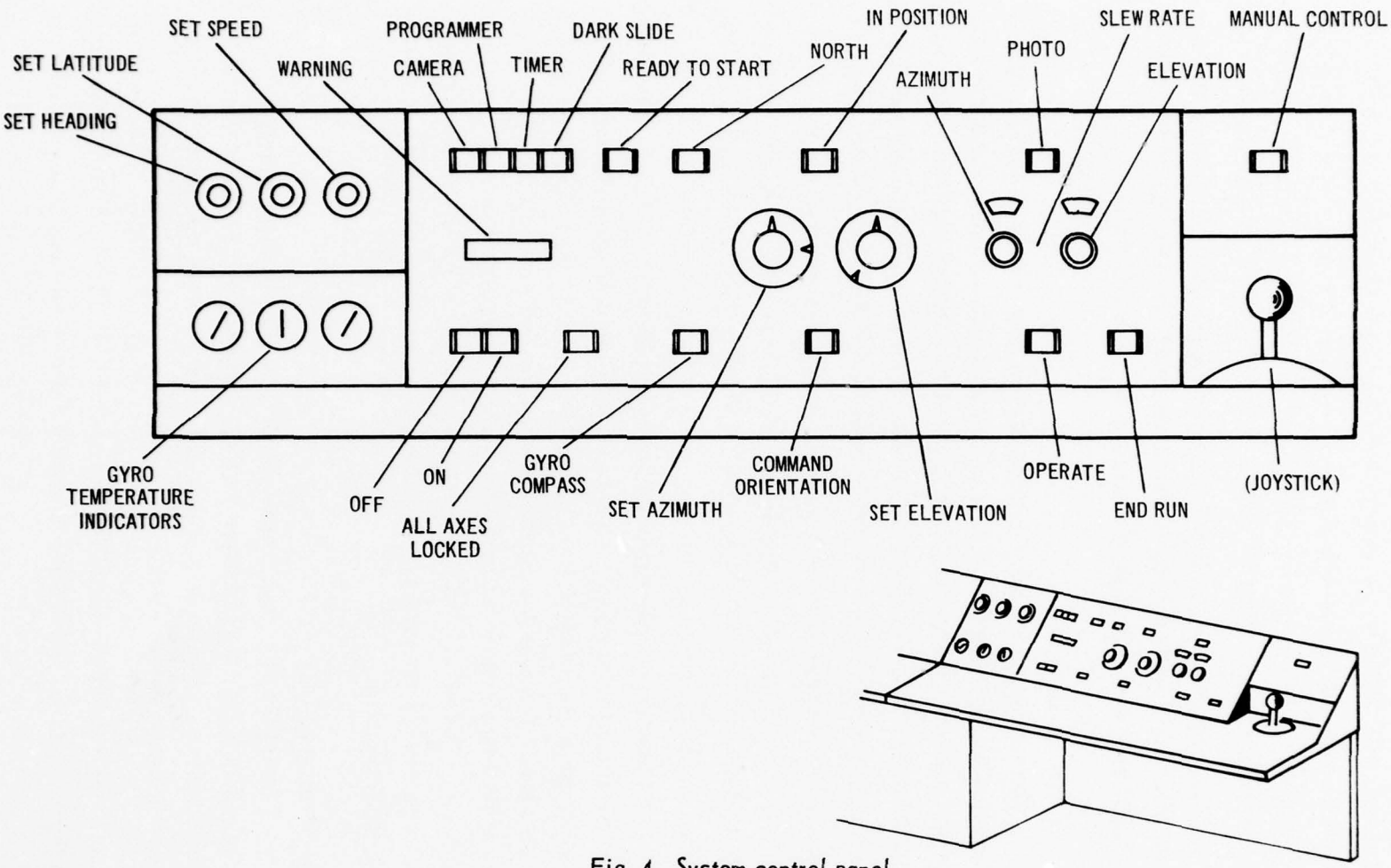


Fig. 4. System control panel.

The shelter will provide a weather tight, environmentally controlled enclosure for the entire system and the system operator(s). The camera and stabilization system will be mounted on an enclosure that is separate from the operating area, so that the camera dome may be opened for photography without exposing the operator's area. The dome, when opened for photography, will act as a wind break, for reasons discussed in Appendix E. Duct work in the base of the gimbal enclosure will provide conditioned air, so that the camera compartment can be brought to outside temperature and relative humidity before being opened. This is necessary to prevent condensation and thermal air currents. The temperature control for the dome will be separate from the equipment enclosure, since the dome may have to be brought to any temperature for 0°F or less to over 100°F, and the equipment, especially the timer and servo electronics, will probably be designed for an ambient temperature of about 70°F.

The approximate dimensions of the shelter, overall, will be 14' long by 6' wide by 7' high. This will provide mounting and protection for the equipment and space for one or two operators, and also room for special tools and spare parts.

6. Operation of the System

The operation of the proposed system may be thought of as being in three stages. The first is the calibration of the timing equipment described in Appendix D. Second, the preparation of the system for operation; the loading of the camera and the presetting of the programmer and the stabilization system. Finally, there is the actual operation of the system during the event.

The reader may refer to the appropriate appendices for more detailed descriptions of the equipment, and for the reasons behind the steps described below.

1. The actual calibration of the timing equipment is performed at periodic intervals, but the performance of the master oscillator should be checked daily. In calibration, the oscillator is compared with a time standard, either by direct

comparison or by radio links, and the oscillator's clock is set to agree with the standard (actually, the station clock is slightly offset, as described in Appendix D). The daily check, which is made to determine consistent oscillator operation, consists of a comparison of the oscillator output with the frequency of a VLF station. By comparing the phase shift of the local oscillator relative to VLF the operator can determine whether the drift of the local standard had remained constant, and thereby verify the calculated time display correction.

2. If the recommended atomic clock is carried aboard the system, it may be used in one of two ways. The recommended use is that of a standby source of both constant frequency, duplicating the VLF transmissions, and real time, as a backup to the crystal oscillator. Used this way, an atomic clock provides redundancy for both functions. The alternate method of use would be as the local station timer, with the crystal oscillator relegated to the role of a backup device. If this is decided upon, the daily checks of frequency shift will not be necessary, for the average shift of an atomic clock from its center frequency is zero. Periodic checks against a primary time standard will still be required, since frequency dividers and registers may skip or add counts.

3. At some time before an event the preparation of the system will be done against a check list. The time at which preparations must be made will be governed by temperature considerations. For example, Eastman Kodak recommends that 103-F plates be allowed 4 hours to come to ambient temperature. Gyroscopes require 15 to 30 minutes of pre-heat before their wheel supplies may be turned on.

4. The satellite pass will dictate the settings of the camera and camera programmer. The stabilization system will be prepared according to ship's position, heading and speed at the time of the pass.

5. The camera will be inspected at the same time that it is loaded and checked, and the inner lens cap and dark slide removed. In the case of gear-driven shutters, reduction gear cases should be checked, and changed if necessary. The outer lens cap can be removed at this time if weather conditions permit.

When these steps are completed, the camera shelter should be closed and the compartment environmental control turned on in order to bring the compartment interior to the temperature and relative humidity of the outside air at the time of the event as explained in Appendix F. If condensation or frosting is expected the camera internal heater should be turned on. Next, a punched tape will be prepared with the input commands for the camera programmer. The tape will contain the commands for the shutter sequence, so that photography will take place automatically when the tape reader is started by the control panel "slew" control. The flexibility possible with punched tape should be adequate for any desired photographic sequence.

Finally, the camera slew, which will have been determined, is set into the dials on the control panel as arc seconds per second of train and/or elevation, as described in Appendices C and E.

When the remaining routine checks have been made, such as loading strip chart recorders and so on, the system will be ready for operation.

If an event is to take place at time "T", and 20 minutes each is required for gyro warm-up and for gyrocompassing, a typical event will be photographed in the following sequence.

At about T-55 minutes, the operator will turn on the system main power switch and the gyro heaters. While the gyros are coming up to temperature, the camera compartment internal temperature will be checked and the camera compartment opened.

At about T-35 minutes, or when the gyros are at their operating temperature, the stabilization system will be ready to turn on. At this time, the ship's latitude, heading and speed will be set into the

appropriate dials on the control panel. The stabilization system may be turned on and set into the gyrocompassing mode. At the end of the predetermined (20 minutes) period, the control panel will indicate "North", at which time the stabilization system will be aligned North and down to within the limits discussed in Appendix G.

The time should then be about T-15 or T-10 minutes. The operator will then shift the system into the aiming mode after setting the true azimuth and elevation of the satellite into the appropriate control panel dials. Then the system will be ready for photography, and when the satellite appears, the operator, when satisfied that it is in the camera's field of view, may place the system in the slew mode. When the slew control is actuated, the camera will be fixed in its orientation and will begin its controlled drift. Photography will be automatically begun by the programmer tape reader when the "slew" button is pressed.

The camera slew will be set at a rate to insure that the images of each exposure will be spread over the plate in a manner to permit easy spot reading and star identification. The direction of slew should be chosen so that the motion of the camera is about at right angles to the path of the satellite through the field of view. The rate of slew should be sufficient to provide a spread of about 1/2 to 1 millimeter between star images. Then, if exposures are to be taken at intervals of 5 seconds, the slew rate will be between 60 and 120 arc seconds/second, (assuming a 12" focal length camera where 2" arc = 3 microns). This is discussed in Appendix C.

In the event of an error in aiming, the operator will be able to override the automatically commanded orientation of the camera with a manual control. This will be done by switching the camera from the acquire mode to the manual mode and re-positioning the camera with a joystick. When the camera has been correctly oriented, photography may be begun as before, by pressing the "slew" button. As stated above, when the system is placed in the slew mode the camera will be fixed in position. Any corrections to the orientation of the camera must therefore be made before the beginning of photography.

The photographic sequence will be ended by actuating the stop control. This step will terminate camera slew and stop the camera

programmer. The stabilization system may then be shut off or placed into any operating mode, including gyrocompassing.

The stabilization system will be de-energized by the off button. If desired, it might be possible to instrument the stabilization system so that the gimbals will return to their "caged" position and automatically lock in place before system power is removed.

The equipment will be secured by removing the photographic plate from the camera, replacing the lens caps and re-covering the camera compartment.

APPENDIX A

SIMPLE GEOMETRIC CONSIDERATIONS IN PHOTOGRAMMETRIC POSITION DETERMINATION

This appendix is concerned with the elementary geometry associated with photogrammetric position determination; a detailed method for the reduction of photographic data is given in Ref. (5).

Figure A-1 defines the vectors between four camera locations, the center of the reference coordinate system, and the control points. The notation used is:

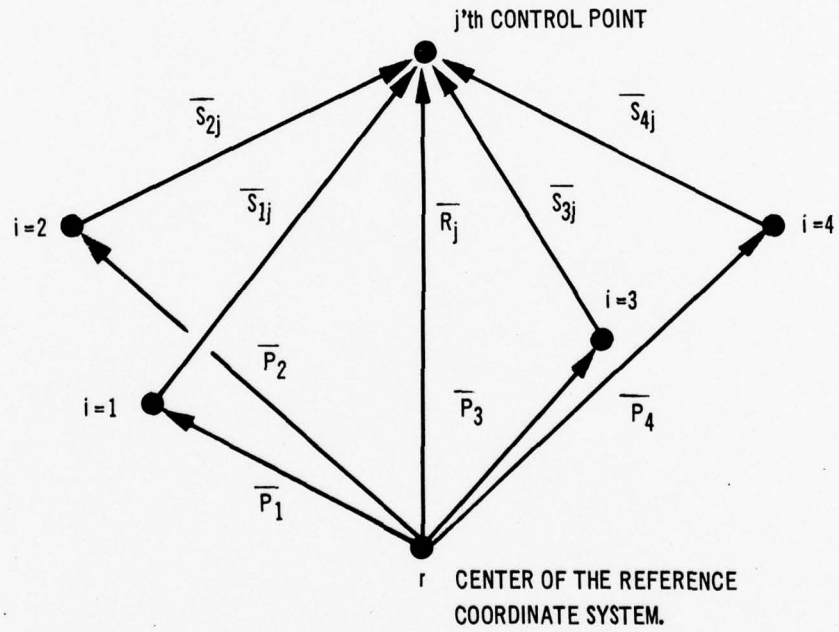


Fig. A-1. Four-camera vector diagram.

r - Center of the reference coordinate system

i - i^{th} camera location

j - j^{th} control point (a star or a satellite)

$\bar{P}_i^r$ - Vector location of the i^{th} camera written in the r-coordinate system

$\bar{S}^i_{ij}$ - Vector from the i^{th} camera to the j^{th} control point written in the coordinate system associated with the i^{th} camera.

$\bar{R}^r_j$ - Vector location of the j^{th} control point written in the r-coordinate system.

Q_{ir} - Matrix for transforming vectors from the i^{th} to the r-coordinate system i.e. $\bar{A}^r = Q_{ir}\,\bar{A}^i$

The reference coordinate system is arbitrary, but we presume that star coordinates (from the catalog) as well as $\bar{P}^r_1$, $\bar{P}^r_2$, and $\bar{P}^r_3$ are known. $\bar{P}^r_4$ is the unknown location. The i^{th} coordinate system is established by the photographic plate; the x and y axes are parallel to the plane of the plate and the z axis is perpendicular to the plate. Figure A-2 shows this arrangement.

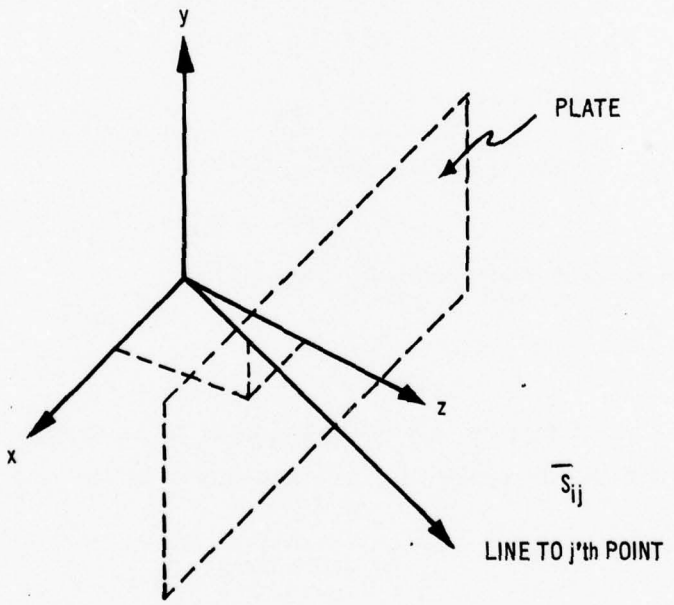


Fig. A-2. Photographic plate-position coordinates

The components of $\bar{S}_{ij}$ are shown in Fig. A-3, in which we have

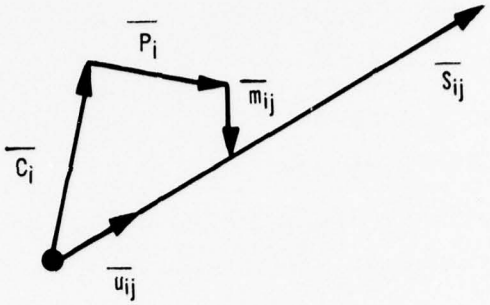


Fig. A-3. Components of vector $\bar{S}_{ij}$.

$\bar{c}_i$ - Perpendicular from the center of projection to the plate

$\bar{p}_i$ - Vector in the plane of the plate from $\bar{c}_i$ to an arbitrary zero

$\bar{m}_{ij}$ - Vector measured in the plane of the plate from $\bar{p}_i$ to the image of the j^{th} point

$\bar{u}_{ij}$ - A unit vector along $\bar{S}_{ij}$

Using matrix notation, we can write

$$\bar{u}^i_{ij} = \frac{1}{\sqrt{m_{ij}^2 + p_i^2 + c_i^2}} \begin{vmatrix} m_{ijx} + p_{ix} \\ m_{ijy} + p_{iy} \\ c_i \end{vmatrix} . \tag{A-1}$$

The first step in our calculation is to determine the Q_{ir}'s. The "infinite" distance of stars allows us to assume

$$\bar{S}_{ij} \text{ parallel to } \bar{R}_j .$$

Then

$$\bar{u}^i_{ij} = Q^{-1}_{ir} \frac{\bar{R}^r_j}{R_j} = Q^{-1}_{ir} \bar{\ell}^{\cdot r}_{j} \tag{A-2}$$

in which $\bar{\ell}^r_j$ is a unit vector along $\bar{R}^r_j$. Further we have

$$\bar{u}_{ij} = \bar{u}_{ija} + \delta \bar{u}_{ij} \tag{A-3}$$

in which

$\bar{u}_{ija}$ - the assumed unit vector, gotten from the initial plate measurements and the camera constants

$\delta\bar{u}_{ij}$ - is the vector which accounts for errors in the plate measurements and camera constants

Then

$$\delta \bar{u}_{ij} = Q_{ir}^{-1} \bar{\ell}_{j}^{r} - \bar{u}_{ija} . \tag{A-4}$$

The solution to this equation can be obtained by an iterative least-squares adjustment, in which the elements of Q_{ir} are adjusted to minimize $\sum \delta\mu^2$. The equation contains 3 unknown elements of $\delta\bar{u}_{ij}$ and 3 unknows associated with Q_{ir}. Since each star (each j-point) provides 2 independent equations, at least 3 stars are required for a solution.

The second step in the calculation is the determination of $\bar{R}_j^r$, *in which the j-control point is the satellite.* The following diagram Fig. A-4 shows the situation for 2 known camera locations. We know the $\bar{u}_{ij}^i$ from plate

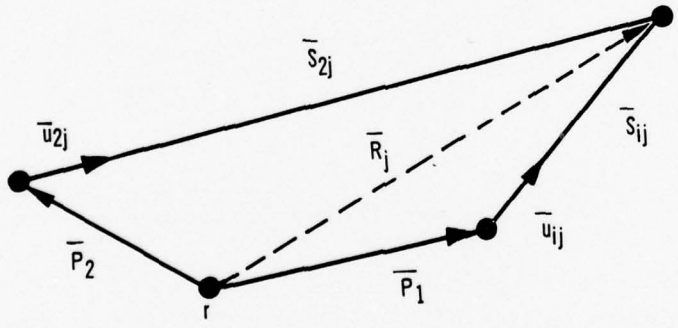


Fig. A-4. Components of vector $\bar{R}_j^r$.

measurements and can calculate

$$\bar{u}_{ij}^r = Q_{ir} \bar{u}_{ij}^i$$

Then, since the $\bar{P}_i^r$'s are known, we can write

$$\bar{R}_i^r = \bar{P}_i^r + \frac{(\bar{P}_i^r \times \bar{P}_k) \cdot \bar{u}_{ki}^r}{(\bar{u}_k^r \times \bar{P}_i^r) \cdot \bar{u}_{ij}^r} \bar{u}_{ij}^r$$

in which $i \neq k$

$$i, k = 1, 2, 3.$$

This is one of many possible equations for $\bar{R}_j^r$, and again we can get a solution by a least squares technique.

The final step in the calculation is the determination of $\bar{P}_4^r$, using $\bar{R}_j^r$ and Q_{4r}. The diagram in Fig. A-5 shows the situation. We know $\bar{R}_j^r$ and can get $\bar{u}_{4j}^r = Q_{4r}\, \bar{u}_{4j}^4$

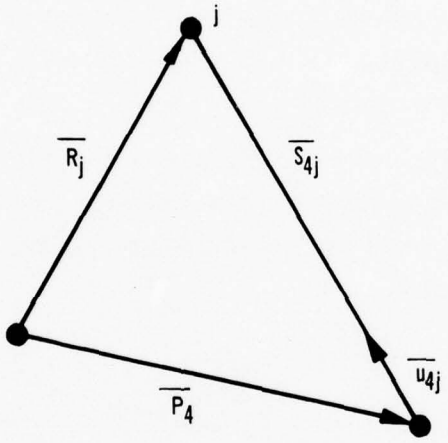


Fig. A-5. Construction of vector $\bar{P}_4^r$.

however, this is insufficient information to get $\bar{P}_4$ (unless we have more than one j point). We can get a solution if we assume a value for P_4 (this essentially means that we know the figure of the earth and the altitude of the station). Then we have

$$P_4 \begin{vmatrix} \alpha_1 \\ \alpha_2 \\ \alpha_3 \end{vmatrix} = R_i \begin{vmatrix} \ell_1 \\ \ell_2 \\ \ell_3 \end{vmatrix} - S_{4i} \begin{vmatrix} u_1 \\ u_2 \\ u_3 \end{vmatrix}$$

in which

a's are the direction cosines of $\bar{P}_4^r$

ℓ's are the direction cosines of $\bar{R}_j^r$

u's are the direction cosines of $\bar{u}_{4j}^r$.

APPENDIX B

EXPERIMENTAL STUDIES

1. Shutter

The form of the camera shutter came under consideration early in the program. There are three basic designs to choose from; the conventional iris diaphragm shutter, the mask shutter, or the louver or venetian blind shutter. The iris diaphragm needs no description. The mask shutter consists of a disc or discs in which openings are made. The discs are moved so that the lens is opened and closed as the openings traverse the optic paths and is similar in concept to the curtain shutter. Louver shutters may be parallel or radial arrangements of shutter blinds that rotate about 90° to open. Each shutter has certain advantages, and these are enumerated in Table B-1:

Table B-1. Shutter comparisons.

SHUTTER TYPE	ADVANTAGES	DISADVANTAGES
Iris	Small size - conventional design - no aperture stopping when open - inexpensive	Limitations on speed - time-to-open may not be same as time-to-close
Mask	Precise speed control possible. No aperture stopping when open - inexpensive	May be physically large - with high inertias
Louver	Rapid operation - small size - wide range of speeds.	Some aperture stop always present. Shutter diffraction effects may be noticeable - expensive and difficult to achieve perfect light seal.

Some photographs were made of a point source through stretched wires to illustrate the diffraction effects of radially arranged louvers. One photograph, Fig. B-1a, shows the affect that

a parallel blade shutter would give. Figures B-1b to B-1c show patterns for symmetrically arranged 4, and 12 spoke shutters respectively. In every case, the diffraction pattern is clearly visible, as it would be for the brighter star and satellite images photographed through a louver shutter. This effect, together with the unavoidable loss in light that would result from an opened louver assembly in front of the lens, would tend to make this unit a second choice after a mask or iris shutter. If a venetian blind is considered, the parallel blade shutter would probably be the best choice.



a. b. c.

Fig. B-1. Shutter diffraction effects.

2. Stabilization Experiment

A government furnished K-37 camera was mounted on the Stargazer Telescope Stabilization System in possession of the Experimental Astronomy Laboratory in order to perform experimental studies of the effect of stabilization system performance on photographic accuracies.

The stabilization system used for the experiments was originally designed to guide a Cassegranian telescope on top of a balloon gondola. At the time of the experiment, there were approximately 3000 hours on the system, and the expected life of the gyros is only about 2000 hours. In consequence, its performance was not that of a system in good condition.

Stargazer is a two-axis system only, with control in train and elevation. This means that, while the optic axis of the camera is held in aim, there will be an angular motion of the camera axes

about the optic axis if the gimbals move in both train and elevation. This may be seen in the diagrammatic sketch of Fig. B-2.

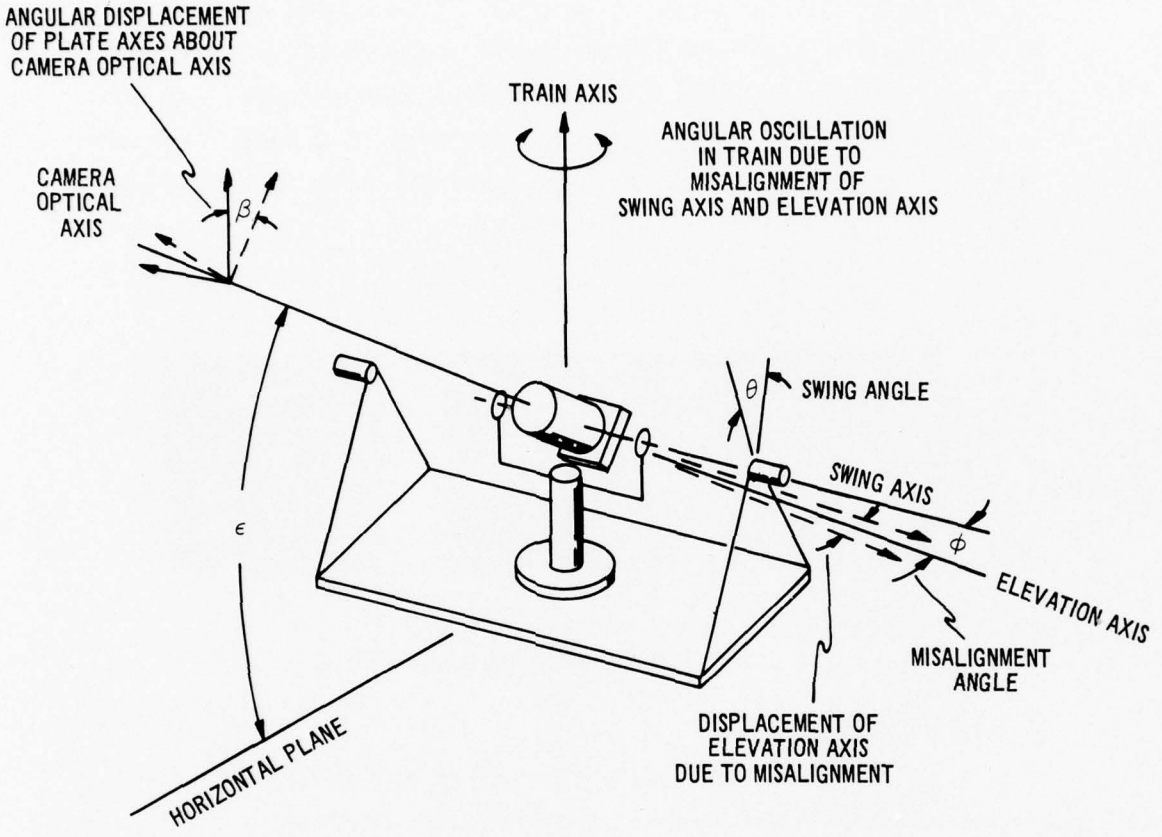


Fig. B-2. Roll motion of camera axes with two-axis stabilization system.

The stabilization system was mounted on a swing platform, shown in Fig. B-3. The swing platform simulated base motion in one axis. The stabilization system was oriented in train so that the elevation axes were parallel to the swing's axes. If this alignment were correct, there would be no correcting motion in train due to the motion of the swing. The camera was then aimed by pointing with the elevation gimbal.

The swing platform was driven at angles of up to ±5° and at rates of 3 to 10 cycles per minute, to simulate ships roll. The

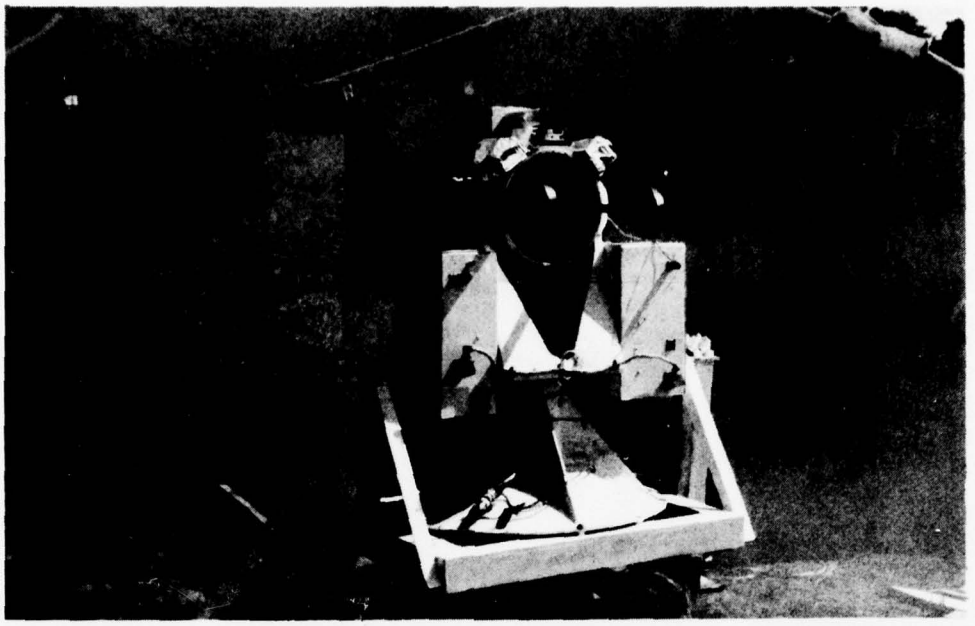


Fig. B-3. Stargazer telescope stabilization system on single axis swing platform.

elevation gimbal drive corrected the orientation of the camera during this motion, so that the camera was aimed at the same portion of the sky. However, for reasons discussed in Appendix II, the camera was intentionally slewed in elevation at about 100 arc-seconds/second. The resulting photographs, like that shown in Fig. B-4, contained a series of star images arranged vertically on the plate.

Note that the star trails in Fig. B-4 do not form a straight line in the photograph, but contain oscillations that increase in amplitude as the trails move further from the center of the format. This was the result of a misalignment in train, as mentioned previously and as shown in Fig. B-2. The rotation of the photographic plate, β is the product of the roll amplitude θ, the sine of the misalignment angle ϕ and the cosine of the elevation ϵ. The displacement, ω, of the image trails about the optic axis (the line normal to the plate through the center of the plate) the product of the plate rotation and the distance of the trace from the plates center, r-:

$$B = \theta \sin \phi \cos \epsilon \qquad \text{(B-1)}$$

$$W = r \beta \qquad \text{(B-2)}$$

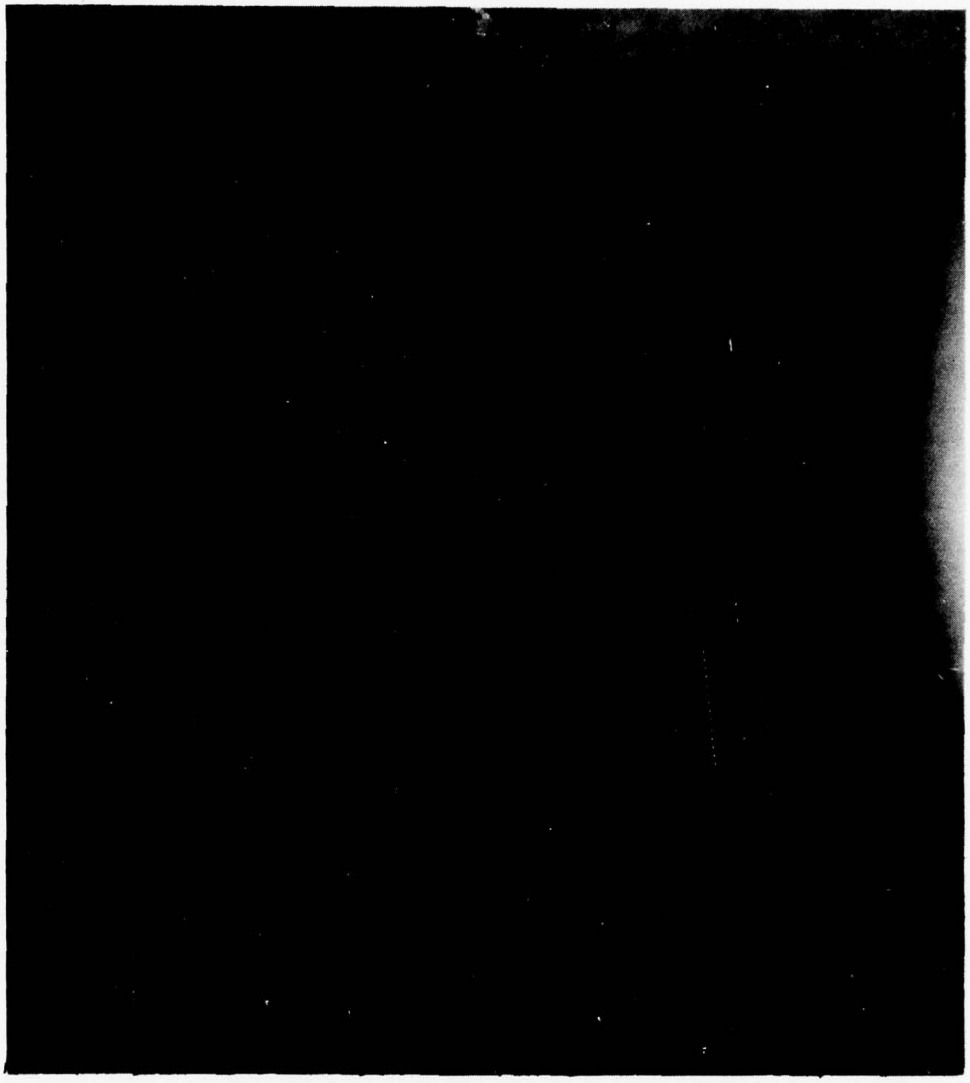


Fig. B-4. Star trail photograph - two axis stabilization, with misalignment in train.

A second plate was exposed with the camera rigidly fixed to the earth while pointing at the same general area of the sky.

The locations of the star images on the two photographic plates were read on a travelling stage microscope, and the x and y coordinates of the images determined. Three stars were selected, and located on the two plates. Their apparent angular separations were then derived from their x and y coordinates on the respective plates. The apparent separation of the three target stars differed by 1 minute of arc to 1 minute 20 seconds of arc when comparing measurements between the stabilized camera and the static camera plates. At the time of this writing, the Naval Oceanographic Office was in possession of the lens calibration plate, and data had not been processed. Therefore, it is not known what part of the measured error was due to the camera lens errors, and analysis of the results is not justified.

3. Exposure Experiments

Some exposure experiments were performed on Eastman Kodak 103-F plates, to check the statements contained in Appendix II. The star trace widths were measured on plates that had been slewed at rates from 60 to 120 arc seconds/second, as well as on plates taken in fixed cameras; where stars trail at Earth's rate — 15 arc seconds/second. Fairly good agreement was obtained with Table C-2 and References (6), and (7) both in trace width vs magnitude and in limiting magnitude vs camera slew rate. These are mentioned in Appendix C.

4. Emulsion Experiments

An experimental photographic emulsion was tested, to examine the effects of emulsion diffusion on image formation. Mention is made in Appendix C, Section 4 of the problems of reading large or distorted images. The experiment described below will illustrate that problem.

The film used was Edgerton Germeshausen & Grier Co. X-R. This is a three layer color film and is described in Reference (10). Each of the three layers has a different ASA speed rating; yellow, ASA 400, magenta, ASA 40 and cyan, ASA 0.01. As a result,

when a white-light image is formed on the film, an image of a different density appears on each layer of the emulsion. Then, when the correct colored light or colored filters are used to separate the three-color emulsions of the X-R film, only one emulsion at a time will be seen. For example, in the photographs, Figs. B-5a to B-5c, the film was photographed through blue, green and red-filters to allow viewing of the yellow, magenta and cyan film layers respectively. The spot has been magnified about 16 times.



a. b. c.

Fig. B-5. Photomicrograph of star image on EG & G Type X-R film, through (a) blue, (b) green and (c) orange filters.

In this experiment a photograph of the star Vega (α-Lyra) was taken on 35 mm X-R film with a 400 mm f/5.6 telephoto lens. The camera was sidereally driven during the 8 second exposure. Vega is a -1 magnitude AO star; a very bright star whose light spectrum is nearly that of our sun. At the time of the photographs, Vega was nearly on the zenith, so atmospheric effects were minimized.

Figure B-5a shows the image viewed through a blue filter, bringing out the high-speed yellow layer. The image is what one would see if white light were used for viewing. In Fig. B-5b, the medium speed magenta layer appears in green light, and a slight shift in density distribution over the spot begins to appear. In Fig. B-5c, the slowest emulsion has been viewed with orange light. Here the shift in density distribution is more pronounced and the effects of guiding error are suggested in the elongation of the densest region of the spot.

The experiment just described demonstrates one source of error in locating the centroid of an image, due to the effects of diffusion in an emulsion. The results also suggest that this and other special emulsion films deserve investigation for their use in satellite photography.

APPENDIX C

CAMERA, SHELTER & PROGRAMMER

1. General

The recommendations of the Experimental Astronomy Laboratory are for the selection of a camera of 300 mm nominal focal length with a two-section shutter, one interruptor type and one conventional iris type.

The shutter will be driven from a timing system, in the manner already in use by USC & GS and others. Camera timing will be controlled from a master station clock. Timing system redundancy is recommended, by supplying both a crystal oscillator and an atomic clock as time references.

2. Camera Selection

The selection of a camera for stationary use has been treated by Hendrikson (11) and Brown (6). Each has presented his case in terms of the camera metrics required to achieve a desired accuracy; Hendrikson for world-wide mapping, and Brown for mapping AMR to 1 in 10^6 with eventual extension of the resulting net to world-wide observations.

The proposals of the two authors are shown in Table C-1.

Table C-1. Camera characteristics.

PARAMETER	HENDRIKSON ARMY MAP SERVICE	BROWN RCA - AFMTC
Focal length	600 mm	1200 mm
Field	20° × 20°	10° × 10°
Plate	9½" × 9½" × 1/8"	190 mm × 210 mm × 6 mm
Aperture	f/2.5	f/4.0
Plate Reading Error	± 0.5 μ	± 3.0 μ

Note that each has assigned a different value to the accuracy of plate reading, which accounts for the differing choices of focal length. Of the two, the 3μ value quoted by Brown is more reasonable.

Brown has offered the best discussion of the factors involved in selection of camera parameters (3,6). His comments do not apply solely to cameras operating from a fixed base, but his discussions center on that application.

The basic premise in Brown's selection of a 1200 mm focal length was the ultimate accuracy of 1 part in 10^6 to be gained in the measurements. This figure is dependent on some redundancy in observations.

For a 1200 mm focal length 1 micron is equivalent to 0.173 sec. of arc, so that a plate reading accuracy of ± 3μ would provide image positions good to 0.5 sec. of arc. If this were added to the error budget postulated by Hendrikson, the results would be:

Measurement	0.5"
Emulsion shifts	1.0"
Camera errors*	2.0"
Star catalog	1.0"
Atmospheric effects**	2.0"
RMS error	3.2 arc-seconds

Of these, only the measurement error can be effected by camera focal length. If Hendrikson's figures are accurate, and they seem consistent with data available from other sources, the net error in image position would be effected little by increasing focal length beyond 1200 mm, justifying Brown's selection of this as a maximum. However, when lower focal lengths are employed, the image errors become:

600 mm	RMS Error = 3.35 arc-seconds
300 mm	RMS Error = 3.74 arc-seconds

and the desirability of a very long focal length becomes less clear. The error in plate reading of ± 3μ becomes a position error of ± 2 arc-seconds with a 300 mm camera, but the uncertainties of star position data, processing and atmospheric effects remain the same.

Camera errors unspecified, but presumably due to distortion calibration errors and lens aberrations.

**Atmospheric effects would be dependent on exposure time and atmospheric conditions at time of photography.*

3. The Stabilized Camera

All of the treatments found to date have dealt entirely with the problem of a camera on a fixed base. For cameras with dynamic rather than static restraints the effects of instrument limits becomes a limiting factor on focal lengths.

To examine the proposed 600 mm and 1200 mm geodetic survey cameras, assume a base motion frequency low enough to have no effect (relative to exposure times) but a noise figure of 2 arc-seconds about all axes and of a frequency equal to or greater than the exposure time.

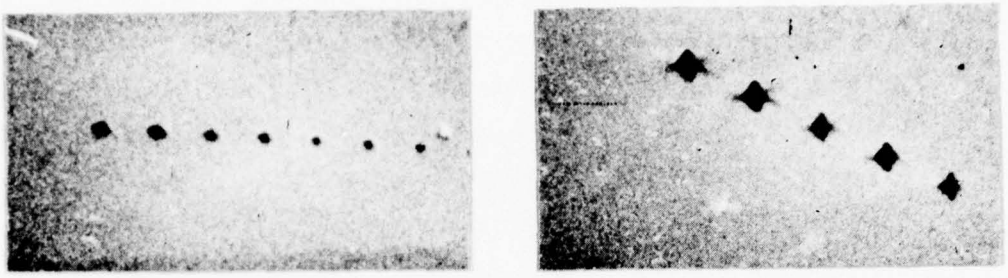
At 600 mm, 2 arc-seconds equals 6 microns, at 1200 mm, 2 arc-seconds equals 12 microns. With a reading accuracy of ± 3 microns on the plates, the effects of stabilization accuracy become serious at longer focal lengths, so that, at least for our intended application, the question of focal lengths much greater than 300 mm does not even warrant discussion. Furthermore, the added mass and higher moments of the long focal length cameras would impose requirements on the stabilization gimbals and servos such that the stabilization errors might not even be reducible to the ± 2 arc-second figure quoted.

The degree of stabilization that is obtained will effect the photographic sequence, as explained in Section 5 following.

4. Film Reading

The first step in the data reduction procedure is the reduction of the photographic plates to numerical data. There is less known about this step than any other part of the operation, especially with regard to the "man-machine interaction" of the operator and plate.

In any optical system in which aberrations are present, the images produced by points of light will be distorted. So long as the images are on axis, the image distortions are symmetrical and there is no difficulty in locating the centroid of the image. Off axis asymmetry, though, introduces a judgement by the operator, requiring the location of the centroid of an asymmetric, inhomogeneous area. Probably, this means that an error will be introduced into the spot readings. An example of off-axis distortion can be seen in Figs. C-1a and C-1b. Figure C-1a is a 16X enlargement of images about 3° off axis and are seen to be relatively even. The images in Fig. C-2b were about 15° off axis, and the effects of coma and distortion are evident.



a. b.

Fig. C-1. Photomicrograph of star images on Eastman Kodak 103-F plate.

The most obvious solution would be to obtain the best lens possible and then to limit plate reading to the center of the plate format, and this is, in fact, the practice today. To do this is to throw away the advantages of a wide field system, although it is still possible to use the outer areas of the format if one will accept a lower confidence in data. But this is an evasion of the problem rather than a solution. It is recommended that one or both of the following be considered.

1. Scanning microdensitometer – Several firms manufacture scanhead instruments with small-aperture microdensitometers for reading photographic plates. Reading resolution compatible with system accuracy requirements are obtainable. For example, the David Mann Co. instrument was developed for A.R.P.A., and will accept standard ballistic plates. The X and Y coordinates of the spots are automatically read out and may be stored immediately on punched cards or tape. Resolution is about 5 μ, the aperture size. So far as is known, no available instrument has provision for storage of density data, but this should be possible to add to the equipment, so that an integration could be performed to precisely locate the centroid of each image on the plate. (Even in its present form, in which the machines duplicate the functions of a human operator, they are worth consideration because they are faster and more reliable.)

2. Human Factors Study – All of the likely sources of information on the human factors in plate reading have been surveyed, with no success. Apparently, no work has been done in this area, nor is any in progress to the writer's knowledge. We have gained some opinions from persons in the field, based on their

experience and preferences, but no factual data exist to substantiate their opinions. A psychological study of the reading and interpretation of photographic plates would help to finally determine such matters as optimum spot size, effects of asymmetry in operator judgement, and optimum methods of measuring star trails.

5. Exposure Time Determination

At present, all users of fixed, shore based ballistic cameras have adopted a more or less uniform operating technique. A series of pre and post event calibration exposures are taken to establish camera orientation and to provide reference stars for the event. In this mode of operation, star photographs may be typically taken at exposure times of 2, 1, 1/2, 1/4 and 1/10 seconds. The event itself may be photographed at times as short as 1/50 second or less, depending on the photographic magnitude of the object or the intensity of the flashing light or flares. The entire sequence of the operation, from the first pre-calibration exposure, through the event, to post-calibration photography, requires ten minutes or more.

It is unlikely that the stabilization system can remain within tolerance during this long a period of time, at least with regard to drift. For this, and other reasons mentioned elsewhere, the method of photography used will differ from the techniques used ashore. For one, the camera will not be earth-fixed, since the inertial stabilization system will lock the camera's axes to inertial or stellar space, and the locations of the images of the stars on the photographic plate will be fixed, except for system noise and gyro drift effects. This might present difficulties in data reduction if star images became too large for reliable reading due to diffusion in the emulsion. It is intended, therefore, to slew the camera at a rate sufficient to expand the stellar images into a series of short traces or individual spots. The slew rate will be determined by the interval between exposures.

Drift values for the gyros will run to about 10 MERU, or 0.15 arc-seconds/second. The camera will be slewed at a rate of up to 150 arc-seconds/second.

As the slew rate is increased, the density of the trace will decrease, since the total integrated light per unit area will be reduced. Camera slew is discussed in Section 6.

Using data contained in Refs. (6) and (7) the following estimate of the effects of camera slewing may be derived.

From examinations of several photographic plates taken with the K-37 camera, the minimum useful trace width for a star trail is approximately 20 microns. (Fifty microns is considered optimum.)

With a 300 mm, f/2.6 camera (Wild BC-4), a twenty micron trace supplied by a star of magnitude 8.0 under ideal seeing conditions, at the zenith, when the rate of image motion is that produced by Earth Rate only; i.e., 15 arc-seconds/second at the equator. As the seeing and co-elevation angles become less ideal, the magnitude required for a 20 micron trace increases to about 4.0 at a 60° co-elevation and poor seeing.

It would be well to note here that in this discussion of sensitivity, image size and exposure time, the arguments quoted are valid only for so-called AO spectral class stars on panchromatic film for which the visual and photographic properties are identical. For stars of other spectral classes, or for lenses or films of limited bandpass, corrections must be made to correlate the power spectral density of the stars with the spectral sensitivity of the photographic emulsion.

The exposure required to generate lines of a given width is

$$E_d = p\,(2.51)^{-m}\,d^{-2} \text{ meter candle seconds} \qquad \text{(C-1)}$$

where

E_d = exposure in meter candle seconds (M.C.S.) to to produce spot of diam "d"

m = stellar magnitude

d = image diameter.

Now

$$p = 1.91\,(2.51)^{-\Delta m}\,D^2\,T_L\,\Delta t \times 10^{-6} \qquad \text{(C-2)}$$

where

Δm = atmospheric extinction, in stellar magnitudes

D = lens diameter

T_L = lens transmission

Δt = exposure time.

Substituting Eq. (C-2) into (C-1) we have

$$E_d = [1.91\,(2.51)^{-\Delta m}\,D^2\,T_L\,\Delta t \times 10^{-6}]\;[(2.51)^{-n}\,d^{-2}]\text{, meter candle seconds}$$

or (C-3)

$$E_d = 1.91\,(2.51)^{-(m\,+\,\Delta m)}\,D^2\,T_L\,\Delta t\,d^{-2} \times 10^{-6}\text{ meter candle seconds}$$

which is valid for zenith exposures (sec z = 1) of short duration (no image trailing).

This states that the exposure to produce a spot of "d" microns is dependent not only on the magnitude of the star or object, but also on the astronomical "seeing" and the camera lens diameter and T/number. In the expression above, atmospheric transmission has been expressed in the "Δm" term in the exponential.

When an image is allowed to trail, either by sufficiently long exposures to allow trailing at earth's rate or by moving the camera during exposure, the expression above is no longer valid, since the total integrated light input per unit area is reduced in proportion to the image velocity. This is treated in Ref. (3) and is summarized below.

Referring to (6) and (7), and beginning with Brown's plot of image density vs. illumination on a 103-F plate, an expression may be derived for spot size, d, of:

(C-4)

$$F_d\,\Delta t = \frac{\pi D^2}{4}\,(1.9 + 0.00012\,d^2) \times 10^{-14}$$

and

$$d = \sqrt{\frac{1.9}{00012\,F_d\,\Delta t}}$$

where

F_d = luminous flux, lumens, to produce the spot size "d" microns.

and the expression for exposure is now in a form that can be related

to the brightness of the object, and the quantity F_d can also be expressed as

$$F_d = E_m T_a T_\ell \frac{\pi D^2}{4} \tag{C-5}$$

where:

E_m = illuminance from star of magnitude "m"

T_a = transmission of atmosphere

and again, as in (C-3), we can express T_a in terms of the apparent decrease in visual magnitude of a star. Then:

$$E_m T_a = (2.43)(2.51)^{-(m + \Delta m \sec z)} \times 10^{-6} \text{ lumens/meter}^2$$
$$= (2.43)\, e^{-0.92 (m + \Delta m \sec z)} \times 10^{-6} \text{ lumens/meter}^2 \tag{C-6}$$

Combining the expression for Brown's experimental curve (C-4) with (C-6), we have an expression relating exposure and spot size to atmospheric conditions as well as lens parameters,

$$(2.43)\, e^{-0.92 (m + \Delta m \sec z)} \times 10^{-6} T_\ell \frac{\pi D^2}{4} \Delta t =$$
$$\frac{\pi D^2}{4} (1.9 + 0.00012\, d^2) \times 10^{-14} \tag{C-7}$$

which we may rewrite as

$$\Delta t = \left(\frac{d}{D}\right)^2 \frac{1.9 + 0.00012\, d^2}{2.43\, T}\, e^{0.92 (m + \Delta m \sec z)} \times 10^{-8}, \tag{C-8}$$

which is an expression for exposure time that is valued for short exposures only (unless siderial tracking is used).

For trailing images, either by trailing at Earth's rate or by slewing a camera, the effects of image velocity must be taken into account. It has been shown in Ref. (3) that the lumens required to produce a trace of width "2a," where "a" is one-half the trail width, can be expressed as:

$$F \cong 4.8 \times 10^{-18} V a \sqrt{a^2 + 4000}\, (a + \sqrt{a^2 + 4000}) \tag{C-9}$$

where:

F = luminous flux - lumens

a = half of trace width - microns

V = image velocity - microns/second

and, using this expression, we can prepare plots of predicted star trail width for given illuminance and image velocity, or conversely to determine the lowest magnitude object that will provide a trace of a minimum acceptable width for a given velocity.

Tables C-1 and C-2 show the minimum star magnitude for star trails of 20 microns and 50 microns for various image velocities. The flux, F, must be related to corresponding magnitudes by the use of (C-5), in which the effects of atmospheric and optical losses are accounted for, where:

$$F_d = E_m T_a T_\ell \frac{\pi D^2}{4} \qquad \text{(C-5)}$$

First, using (C-9), the luminous flux required can be computed for trails of 20 μ and 50 μ respectively as

$$F_{20} = 22.7 \times 10^{-14} V \text{ lumens} \qquad \text{(C-10)}$$

$$F_{50} = 75.8 \times 10^{-14} V \text{ lumens} \qquad \text{(C-11)}$$

with the values of F being the luminous flux at the emulsion, after attenuation of objects by atmosphere and lens, and the velocity being read in microns/second.

Then, applying these values to (C-5) and (C-6), we can derive the image magnitudes required to generate the traces for a given set of optical characteristics.

For average "good seeing" of $\Delta m = 0.26$, and a lens transmission of $T_\ell = 0.5$ in a 300 mm, F/2.6 camera (D = 115 mm, 4.54 inches), the required intensities are as tabulated in Table C-2. By using (C-5) and (C-6) combined, with $T_\ell = 0.5$, D = 115 mm, $\Delta m \sec z = 0.26$, $F_d = 2.43\, e^{-0.92\,(m + \Delta m \sec z)} \times 10^{-6} \times 0.5 \times \pi(115)^2/4$, Table C-3 may be prepared.

Table C-1. Light intensity for given trace widths.

ANGULAR VELOCITY ARC SEC/SEC	LINEAR VELOCITY MICRONS/SEC	F, LUMENS FOR 20 μ TRACE	FOR 50 μ TRACE
15"	22.5 μ	511×10^{-14}	1705×10^{-14}
30"	45	1022	3410
60"	90	2044	6820
120"	180	4088	13,640

Table C-2. Star magnitude for given trace widths.

ANG. VELOCITY ARC SEC/SEC	MAGNITUDE REQUIRED, 20 μ TRACE	50 μ TRACE
15"	8.6 m	7.4 m
30"	8.0	6.7
60"	7.3	5.9
120"	6.6	5.2

These figures were checked by experiment with the stabilization equipment previously mentioned. One might expect a variation of plus or minus a half magnitude under the conditions stated; $T_\ell = 0.5$, $\Delta m = 0.26$, and the variation will be even greater under poor "seeing", lower lens transmission, or stars of a spectral class other than type AO. In general, though, fairly good agreement was obtained between the data in the table above and spot-readings of several plates.

6. Star Image Distribution

The loss of images from slewing leads to another consideration; whether there will be enough stars in the field of view to allow sensible data reduction. A minimum of three star images are required to establish the plane of the photographic plate.

Stellar density, in the number of stars of a given magnitude per square degree is known and the number of stars per photograph may be predicted. The density will vary with the portion of the sky being photographed. There are in general fewer stars at the galactic pole than at the galactic equator, and there are local variations in star density also. (7)

If we take the worst case from the preceding table, where stellar magnitude equals 5, the number of stars of magnitude 5 or higher in the field of a 30° × 30° photograph will be, for the orientations stated:

Table C-3 Star density distribution.

GALACTIC LATITUDE	NUMBER OF STARS
0°	42
90°	11
Average	20

It is obvious then that there will be enough stars on the photographic plates to determine plate orientation under the worst conditions postulated in the section preceding.

7. Exposure Control

It has been stated (in Section 5) that the minimum readable star image will be 20 microns wide, and that the optimum spot size will be 50 microns. Neglecting for the moment the questions raised in Section 4, we may assume that star and satellite images are to be limited to a diameter not to exceed 50 microns.

In order to achieve an image of 50 μ or smaller for an object very much brighter than the limiting magnitude of the camera, the total light reaching the film must be controlled by means of an aperture stop, shutter speed control or both.

The exposure must also be controlled to give useable spot size images for stars of varying magnitudes, for ease in data reduction.

Restrictions on the choice of f-stop or exposure time will be imposed by the nature of the satellite or flare being photographed. A very bright object will demand both small aperture and short times. Fast moving, relatively dim objects will require large f-stops and short times, to provide a number of images on the plate.

The method of photography under consideration, that of taking simultaneous star and target photographs from a slewing camera, will require an exposure program for each photograph, with the lens openings times being governed by the brightness of the satellite.

If a satellite of equivalent magnitude zero were photographed at 0.1 second exposure time, the lens would have to be stopped to f/75 to produce an image of 50 microns diameter, by using (C-4), (C-5), and (C-6). In order to achieve the desired image size at a more reasonable f-stop of f/32, the shutter speed would have to be about 0.017 seconds, or about 1/60 second.

Since gyro drift will be about 1/100 of earth's rate, or about 0.15 arc-seconds/second, giving a mean camera drift of about 0.2 arc-seconds/second. The optic axis of the camera will move 1 arc-second in 5 seconds of time, and this becomes the limit of time that we may allow to elapse between the photography of reference stars and of a target. It will be necessary in many cases to adjust exposures in less than 5 seconds from stars to target and back to stars. This will be necessary because the location of the satellite relative to the star background must be measurable to an accuracy approaching 1 arc-second, and we can neither measure gyro drift nor assume its characteristics to be constant.

From the foregoing, the following requirements exist:

1. The photography of an event cannot follow the procedures used for shore-based cameras, but rather star backgrounds and targets must be photographed within a very few seconds of each other.
2. The ranges of star magnitudes and of target brightness will have to be accommodated for within these few seconds by varying diaphragm and/or speed settings over a range sufficient to render useable images of all objects to be photographed, or;
3. A fixed or variable neutral-density filter or cross-polarized device will have to be fitted into the camera to adjust the light reaching the plate, or;
4. A film emulsion of variable sensitivity will have to be acquired, to cover the range of target brightnesses.

Of the solutions offered, neither 2 or 3 would be easy to mechanize, but they could be achieved at the expense of some camera performances. The suggestion in 4 is being pursued, with an experimental emulsion from the Edgerton, Germeshausen and Grier Company (10).

The simplest mechanical solution would be to drive an aperture stop in a continuous, cyclic fashion, varying asynchronously with the exposure repetition rate. This would allow coverage of a range of stars bracketing or approaching the satellite's magnitude, by setting in an appropriate exposure time for the exposure sequence. Thus, by varying the f-setting from f/2.4 to f/32 at 1/50 second, useable star images from magnitude zero to about 4 would be obtained, and a satellite with a magnitude in this range would be photographed successfully. The only restrictions on this method, beyond limiting the number of useful stars, is that the shutter repetition rate must be known precisely.

Filters, either variable or fixed, would reduce the brighter satellite and star images to the point where they were of useful sizes, but either the operator must position the fixed filter accurately beforehand or the losses attendant on a variable filter's maximum transmission will have to be accepted.

8. Camera Slewing

Camera slew rate will be determined by the interval between exposures. Exposure interval is in turn limited by other system parameters; the interval between exposures cannot exceed the time dictated by stabilization tolerance and camera focal length, and cannot be less than the time required to adjust exposure f-stop.

For a 12 inch focal length camera, three microns is equivalent to two seconds of arc. As has been discussed, three microns is also the generally accepted limit of reading accuracy of an optical comparator.

If it is decided to make the exposure adjustments mentioned in Section 5 in four seconds, we must maintain a stabilization accuracy of two arc seconds in four seconds, or 0.5" arc/second time. Then, star field images will be occurring at 8 second intervals on the plate. A separation of 1 mm (1000 microns) between sets is arbitrarily chosen, so that the camera must be slewed at 2/3 (1000) ÷ 8 = 83.4 or about 85 arc-seconds/second for the conditions stated. Different conditions will require other slew rates, but the choice will be made in the manner just described. Rates of 0* to 150 arc-seconds/second will be made available.

Excluding gyro drift

The system will have the capability of slewing in both train and elevation. The choice of direction of slew will be determined by the path of the satellite across the field. Normally, a slew at right angles to the satellite track will be selected. Slewing with the satellites direction might cause bunching of images, while motion opposite to the satellite path will shorten the total time that the target is in the field of view.

Mechanization of the slewing mode is discussed in the sections of the report dealing with stabilization.

9. Shutter and Programmer

The shutter, programmer and timer operate as a single subsystem, in that the shutter is sychronized to the station timer by commands generated in the programmer. Any shutter can be made compatible with any variety of timer by appropriate programmer design.

Shutter design was touched upon in Appendix B. The only stringent requirements on the shutter are; time-to-open equal to time-to-close, shutter mid-open time to be precisely determinable, and a speed range of approximately 1/10 to 1/50 second be obtainable. Within these limits, any suitable design will be acceptable. A comprehensive discussion of shutters for ballistic cameras is available in Ref. (7). Descriptive literature is available from the Fred C. Henson Company and from the Instrument Corporation of Florida, among others.

The shutter programmer will be designed to generate signals that are compatible with the characteristics of the shutter decided upon. Its functions will be to accept command inputs and, after synchronization with the time standard, to generate appropriate shutter commands.

A second function of the programmer is to monitor and record the operation of the camera shutter. Monitoring is accomplished by comparing the command signals generated in the programmer with the time synchronizing signals. A permanent record of shutter functions versus time is provided by a strip chart recorder.

Programmers, like shutters and timers, are available commercially, and good descriptive literature is available from the vendors. For the proposed system, the only important changes that will be required in existing programmers will be those involved in integrating the programmers with a system control panel. The overall system block diagram in Fig. 3 reflects this requirement.

APPENDIX D

THE TIMING SYSTEM

1. The Timing System

Each of the proposed modes of position determination by photogrammetric means will impose specific requirements on the system for station time determination and camera synchronization.

For the "self-contained" system, the final outcome will be dependent on an accurate satellite ephemeris and a knowledge of time.

When flashing light satellites are used, the problem of time determination may not be so severe if the characteristics of the flashing light satellite are known. The chief problem would then become synchronizing the ship's camera interrupter shutter with the arrival of the satellite flashes.

In the "intervisible mode," when triangulation techniques are used, the time synchronization of multiple stations must be accomplished. In the case of passive satellites, it will be necessary to orient all cameras properly, synchronize all shutter rates against a common reference, and to key all cameras simultaneously, or to know the exact mid-exposure time of each camera for later data reduction corrections. For intervisible mode photography of flashing light satellites or rocket-borne flares, all camera shutters will have to be opened at the time of the flashes. For the shore-based cameras, this is accomplished by simply opening the camera shutters for the whole duration of the event. For the shipboard camera, however, the method of orientation determination by simultaneous star and satellite photographs makes this impossible. Therefore, the interruptor shutter of the shipboard camera must be set so that the shutter mid-openings occur close to the expected times of the flashes. The shutter mid-openings are recorded by the systems oscillograph, and the time of the satellite or flare flashes is known, or can be determined. Differences in time between the shipboard camera shutter openings and the flashes can be determined and the data adjusted accordingly.

In reading the following sections, the attention of the reader is called to the difference between operation in synchronism, in which stations are referred to a common time base for comparison, and simultaneous operation, in which all stations operate at the same instant. Cameras operating simultaneously will be in synchronism, but synchronized cameras will not necessarily be operated simultaneously.

2. Methods of Timing

The basic timing system presently in use for secondary standards is comprised of an accurate local oscillator, a VLF or HF receiver and a phase comparator. Since there are propogation uncertainties in HF transmission, and the frequencies of the VLF stations are controlled more accurately than those of WWV, only VLF should be considered as the final reference in a radio link.

The VLF signals are matched to those of the local oscillator in a phase comparator after the frequency of the local oscillator is divided, where necessary, to agree with the VLF frequency. The record of local oscillator drift is recorded as a current output on a meter or chart. Oscillator drift will be essentially constant in a well designed oscillator. When integrated with respect to time, this constant drift will be reflected as a time error curve whose shape will be parabolic. When the direction of drift has been determined, the initial offset of local oscillator frequency can be made, when the local oscillator is set against a reference standard, to insure that the local oscillator's time will remain in tolerance for the maximum length of time.

Setting the station's local oscillator may be done either by comparing it with a broadcast transmission of sufficient accuracy (VLF) or by setting it against a "master clock". While the idea of a portable master clock may be attractive for shore based operation, for shipborne use VLF transmissions are more convenient. Another recommended method of comparison could use "Atomicron" cesium vapor clocks. The atomic clock could provide an accurate check on both oscillator frequency and drift. More important, the atomic clock will be independent of radio reception problems and will provide a redundant timing system.

3. Methods of Synchronization

Synchronization of cameras with their own station timers, with other stations, and with flashing satellites, both alone and in concert with several stations, may involve slightly different problems, but a single, compatible system could be devised to provide reasonable operating ease and reliability.

4. Self-Contained System Requirements

For observation of passive satellites with one camera, the time of observation and the ephemeris of the satellite will have to be known. Although it has already been stated that satellite ephemeris predictions are not sufficiently accurate at present, a method of timing these observations is discussed for possible future reference. Time synchronization can be accomplished by energizing the interrupter-type shutter and synchronizing it with the station's local oscillators. This can be monitored by means of an oscillator-keyed programming control device and a display, similar to the programmer and CRO display on the Electronic Engineering Company of California, Pickard and Burns Company or Hewlett-Packard/Dymec control devices. Then a separate capping shutter can be either programmed to open at a given time, via clock registers, or opened at any time and the time recorded on a strip chart or other readout.

An alternative method of obtaining a time record would be to display the time onto the photographic plate in binary form. A register in the camera body that was wired to the station's oscillator via suitable divider circuitry could indicate time directly on small indicator lamps. At a given time, for example, in conjunction with the n^{th} interrupter-shutter opening following the opening of the capping shutter, a switch closure would stop the lamp display input and, by switching the lamps to buffers, hold the lamps at the state they showed at the time of switching. An auxiliary shutter could be opened at any convenient time to project the display onto the photographic plate. This technique offers the advantages of a visible time display on each plate, and offers an opportunity to add further identification with additional registers, but at the expense of added circuitry and components.

In the case of active satellites, it is necessary to be prepared with an open shutter at the time of the flashes. If the camera is equipped with a shutter mid-opening indicator, the camera should be synchronized to the flashes so each flash coincides with a mid-point opening, if possible. If the predicted times of satellite flash are available, and the data accurate, the camera can be entirely preset. If there are large uncertainties in the satellite's program, then it will be necessary to either synchronize the camera with the satellite during the run, or to open the shutter fully for a known interval of time and derive accurate flash time data from another source after the event. In the latter case, star trails would be available whose beginning and end could be accurately placed in time, and point images of the satellite's flashes would be visible and could be related to the event times gathered elsewhere. Probably, it would be necessary to adjust the shutter f-stop to accommodate the background star field, but an experienced operator could do this by observation of sky conditions. This latter method would be preferable if satellite program prediction uncertainties were of an order comparable to the exposure interval of the camera where rotary-type shutters were being used for chopping. Obviously, in the case of rotary shutters large phase angle corrections could require large disc accelerations with consequent heavy power demands. Where vane or "venetian blind" chopping shutters were used, the change of mid-open points would involve nothing more than a shift in command signal time, and synchronization of the camera with the event would not be a problem.

Basically, the requirements of the timing system for either kind of self-contained camera station photography are the same. The only thing open to choice is the method of timing the capping shutter; opening the shutter at a predetermined time or recording the actual time of opening. It is recommended that the first stated method be used, to avoid having to retain auxiliary data records. If opening at a prearranged time proves unwieldly, then the binary lamp time register deserves consideration. In any event, the error in actuation time of the shutter must be measured, or known, so that the proper information can be put into the data reduction.

With proper design and operation, any of these methods can be made to provide results within acceptable limits of accuracy. The final choice, then, will be determined by the mode of operation, system control and data reduction favored by the operating personnel.

Each method involves some trade-off. Where stations operate independently, operator skill becomes a factor, both in operating cameras at the correct time and mode and in the setting of station clocks. If a central control mode is favored communications equipment must be provided similar to that described in the sections following.

Regardless of whether all stations operate independently, and hence all have clocks, or whether only the master control stations and the shipborne camera have station timers, the clocks at each station will have to be synchronized to the limit of accuracy of the allowable system time error. If this error is assumed to be one half millisecond between stations, then each station will have to be calibrated independently against the same source (VLF or master clock) at intervals not to exceed the time for which the poorest time standard can remain within specified limits. With the limit of one half millisecond, and assuming a maximum oscillator drift rate of five part in 10^{10} per day, recalibration will be necessary at about ten day intervals. With VLF available, it would be preferable to calibrate clocks during each day that an event was expected. If all oscillator rates were accurately known, and if frequent checks were made to verify station times, synchronism between stations might be held to 100 microseconds over short time intervals.

While synchronization of all stations is possible by radio links, high frequency radio transmissions are subject to propogation errors, as sky and ground waves have different path lengths and hence different times of transit between two points on the ground. Sky waves (reflected signals) begin to appear at ranges above one hundred miles. Differences in transit times of ground and sky waves may range from three milliseconds at short ranges (one to two hundred miles) to one millisecond at ranges beyond 1500 miles. If accurate propogation prediction charts are available, and if signals are monitored with an oscilloscope, there should be no difficulty in determining the exact

delay, but the possibility of error exists under conditions of poor reception. The delay in transmission to the furthest station should be introduced into the programmer of the originating station, so that camera synchronization will not be effected by transmission times. Intermediate stations will enter appropriate programmer time corrections, equal to the difference between the greatest path and their own distance from the transmitter. The correction at the most remote station would be zero. All stations on the net would have to discriminate, automatically or manually, between desired and unwanted transmissions. The use of land-line signals ashore would simplify this somewhat, since known delays could be introduced as desired into each station, leaving nothing to choice at the various stations. By using longer delays than necessary on the wire net, the transmitter operator could apply a transmitter delay to the signal to be sent to the seaborne station to bring all stations into synchronism. A block diagram of such a communications link is shown in Fig. D-1.

6. Active Satellites

For photographing active (flashing) satellites, or flares, all cameras must be synchronized with the event.

In order to successfully use a lighted object for a target, the program of the satellite must be known. Without the data, it would not be possible to pre-program the ship's camera shutter so that it will be open at the correct time.

There are three ways in which the shipboard camera could be synchronized with a flashing light satellite or a flare.

1) The camera could be run at a prearranged time, through accurate satellite program predictions.

2) The initial flash of a series of flashes could be detected by photo-electric devices, and the signal used to trigger the camera shutters.

3) A radio beacon signal from the vehicle, before or concurrent with the first flash, could be used to trigger the camera.

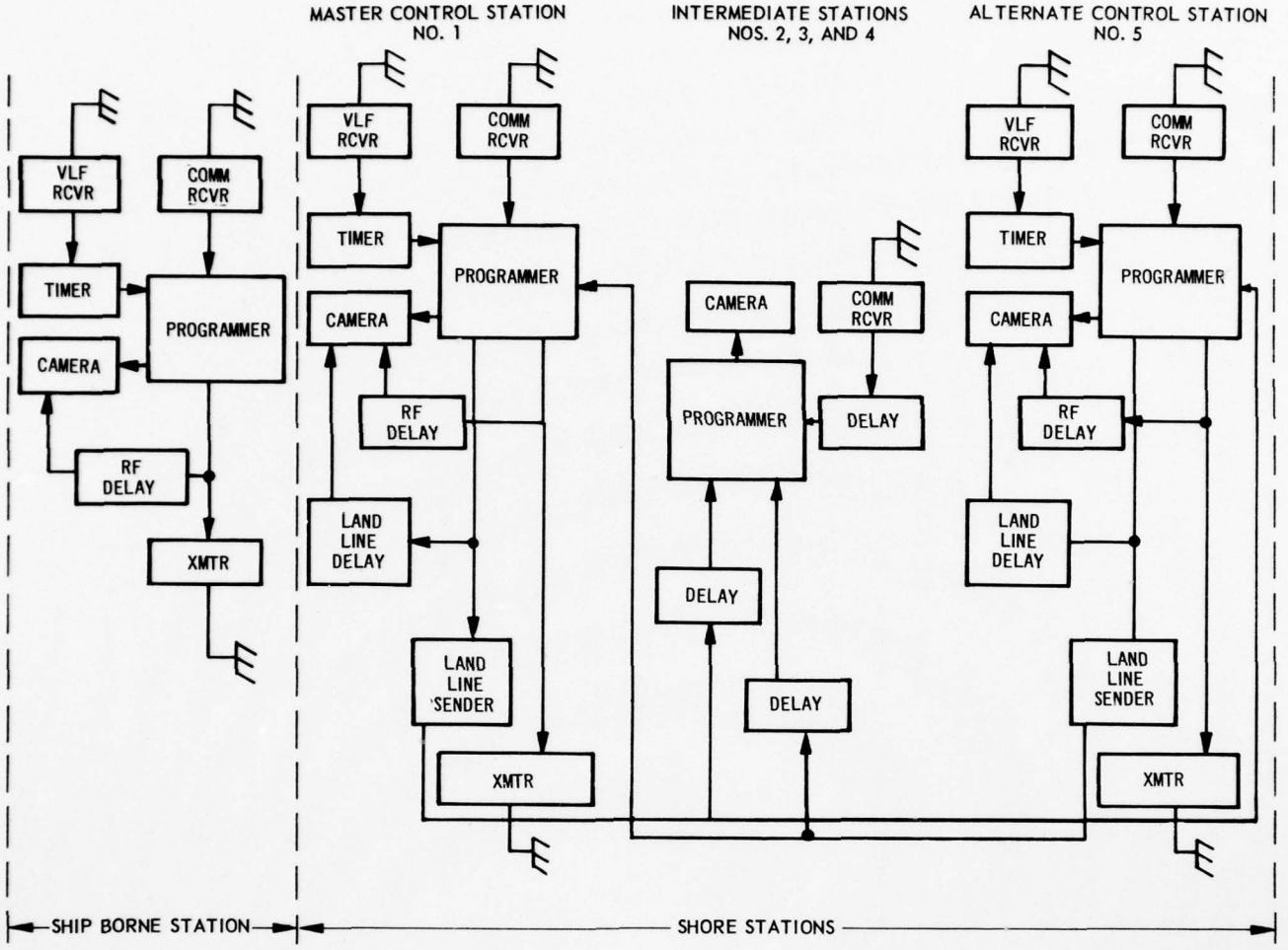


Fig. D-1. Communications net for camera synchronization.

From information presently available, the first method might not always be possible due to uncertainties in flash times but in the technique used at present. The second would probably require a prolonged engineering effort to develope the photo-electric device. The third method, the radio beacon, would involve some fairly complex operating techniques, but offers a feasible approach for photography with chopping shutters. The shutter would be run at a rate compatible with the expected intervals of the flashes. The time of the first flash, the error in predicted vs. actual event time would be determined by time comparator circuitry and the chopping shutter could, if flash intervals were not too short, be phased so that the next flash would occur at the time of shutter mid-opening. The equipment required for this operation may be seen in the block diagram of Fig. D-2. Note that the times of the flashes do not have to be known to determine position so that there would be no timing problems associated with shutter phasing.

There is little more that can be said concerning active satellite's triangulation without a fairly accurate knowledge of the plans for future geodetic satellites. However, it would be wise to include the capability for installing a telemetering receiver signal input and a means of adjusting shutter phase signal commands. This should cover most of the conditions likely to be encountered in the future.

7. Summary

From the foregoing, certain requirements of a comprehensive timing system, communications net, and camera shutter design may be specified. The requirements shown are for the maximum in system flexibility and attempt to cover all requirements. These are tabulated in Table D-1, first by function and then as partial equipment specifications.

From the foregoing, it becomes evident that the instrumentation of a system to cover any eventuality in satellite photography will be expensive and complex. From an examination of the current state of satellite prediction techniques, and in view of the uncertainties in plans for various programs, one may question the wisdom of planning such a complex arrangement at this time.

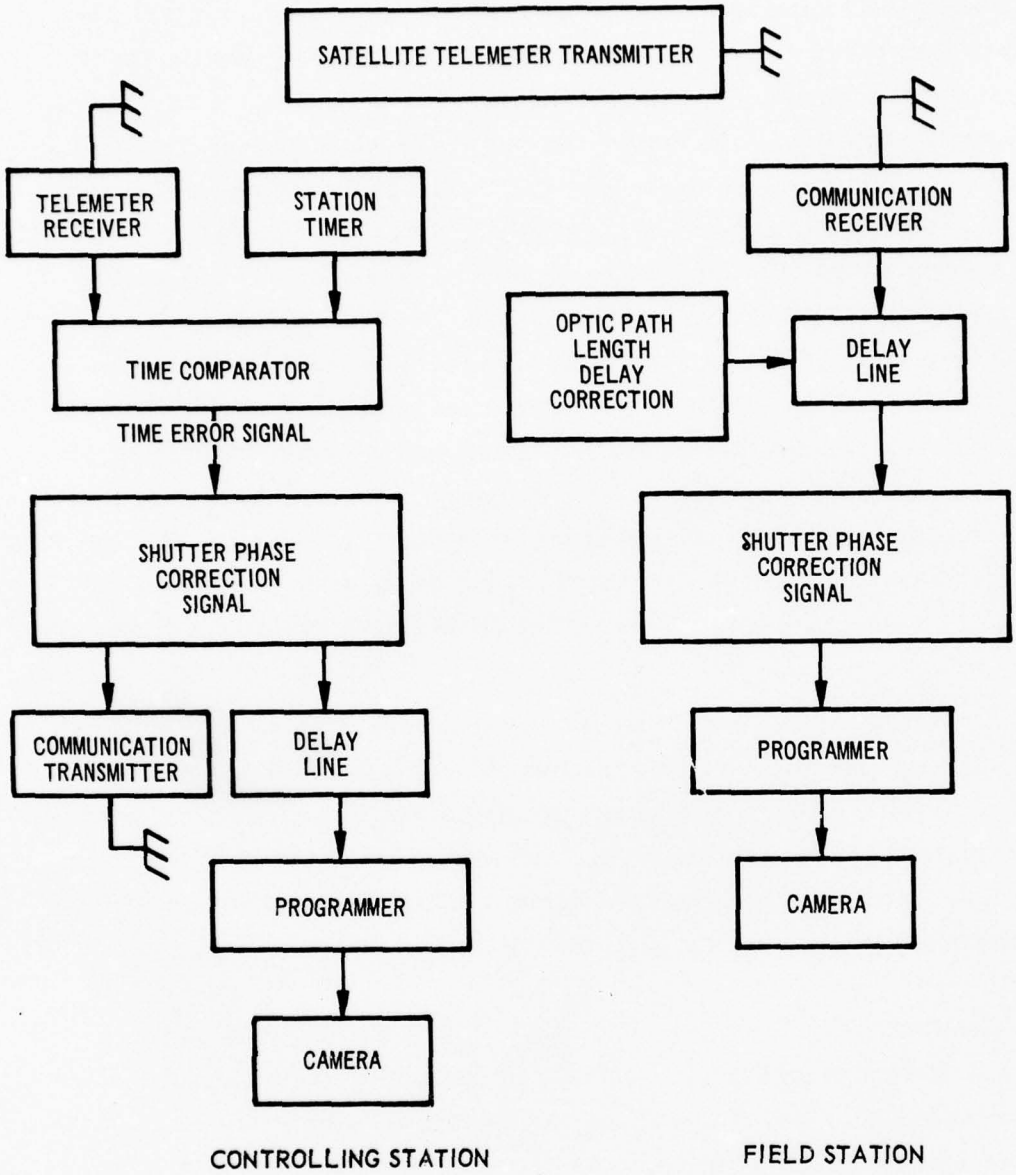


Fig. D-2. Communications equipment for synchronization of cameras to flashing satellites.

As already stated, the most promising technique at the present time will be that of intervisible mode observation of passive satellites. Camera stations could, for this mode of photography, be synchronized by reference to a common time base and operated independently at a prearranged time, or operated simultaneously by means of remote command signals. Simultaneity is, of course, implicit in the first stated case, for each camera operator will have started his camera at a prearranged time that is measured to milliseconds.

Table D-1. Timing system specifications.

Self-Contained Camera System

Passive Satellite

TIMER	SHUTTER	COMMUNICATIONS
Self-contained clock, with outputs for camera programming. Provision for checking against VLF, WWV, Atomicron, or master clock.	Chopping shutter, tied to clock. Capping shutter for pre and post calibration.	Not applicable

Active Satellite

TIMER*	SHUTTER	COMMUNICATIONS
Same as above, with addition of time comparator for correction chopping shutter signal and delay adjust from clock to programmer.	Same as above, with addition of provision for rapidly adjusting chopping shutter full-open time.	Telemetry from satellite, either by direct link or relay.

* An additional requirement for all cases is to provide a print-out of time, on an oscillograph or directly on film, of any convenient known point during the photographic sequence.

Triangulation System

Passive Satellite

TIMER	SHUTTER	COMMUNICATIONS
Same as self-contained system, but with addition of delay lines and provision for external synch signals where communications are used.	Same as self-contained system.	Land line and/or radio link ashore, and radio link to ship-borne system. Transmitters to include variable delays, both radio and land line. Provision for one or more transmitter stations ashore, and one afloat, to assume control of the entire system.

Active Satellites or Flares

TIMER	SHUTTER	COMMUNICATIONS
Same as self-contained system, but with added provision for variable delay adjust from external signal.	Same as self-contained system.	Same as above, and same as self-contained system. Additional requirement for insertion of correct delay for each camera station based on light transit time.

This method would lend itself to the proposed scheme of photographing a satellite from shore stations to establish an accurate path over a portion of an orbit, and then at some later (or earlier) time, photographing the satellite from shipboard. This would be a hybrid method, in which the ship's camera would act like a self-contained system, extracting positional data from the short-term "ephemeris" derived from the shore stations' triangulation. In this case, the synchronism of the ship's camera to the shore cameras would be by a common time reference, whether the shore cameras were independently run or run from a master control. A study should be undertaken to determine the length of time over which an observed segment of an orbit may be safely extended by extrapolation, to check on the validity of the proposal.

8. Timing Errors

An error in time determination will result in an error in position that will be directly proportional to time uncertainties and inversely to the slant range of the satellite.

Since an error in time may be interpreted as being analogous to an error in satellite ephemeris, the two may be treated in the same manner. For the simplest case, of small angular errors at the zenith, and if errors are considered as angular displacements relative to geocentric coordinates, then

Error in orbital position, feet = $(R_o + h)\gamma$

Error in earth position, feet = $(R_o)\gamma$

where;

R_o = earth's radius in feet

h = orbital altitude in feet

γ = orbital position error in radians

and the error in positional determination may be expressed in terms of the error in orbital position as;

$$\frac{\text{Position Error}}{\text{Orbital Error}} = \frac{R_o \gamma}{(R_o + h)\gamma}$$

$$= \frac{1}{1 + \frac{h}{R_o}}$$

$$\text{Position Error} = \frac{\text{Orbital Error}}{(1 + \frac{h}{R_o})}$$

and, since the term $1 + (h/R_o)$ is dimensionless, any units may be used in the final expression.

In Figs. D-3 and D-4, the curves show respectively position error in feet as a function of errors in time determination and in satellite ephemeris for the case of small angles about zenith satellite position. The plots show what one might expect; errors are reduced as orbital altitude increases, for a given set of conditions.

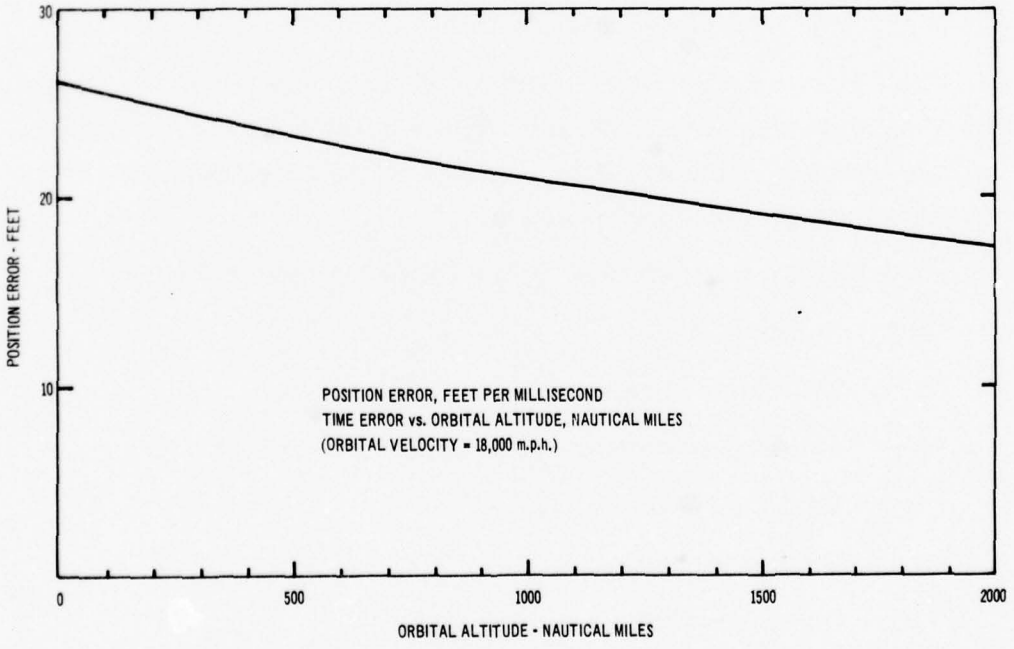


Fig. D-3. Position error in feet as a function of errors in timing.

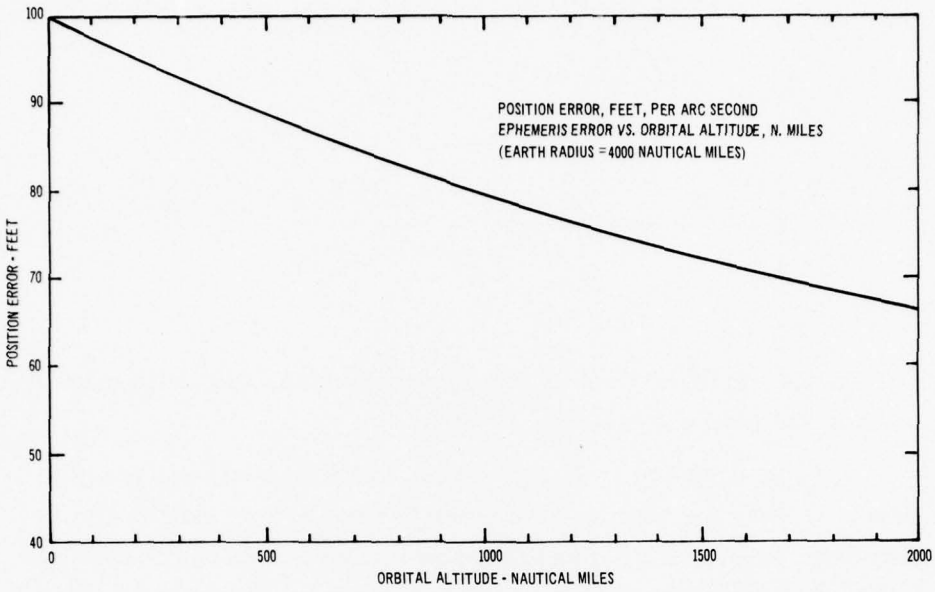


Fig. D-4. Position error in feet as a function of errors in orbital position.

The following derivation, extracted from reference (4) shows the relationship in the planar case between error in satellite position, zenith distance of the satellite, altitude of the satellite, and error in calculated geographical position.

The basic quantities used in the following derivation are:

e - Zenith distance

θ - Ship's position error angle, geocentric

ϕ - Satellite's position error angle, geocentric

R - Earth's radius

h - Orbital altitude

R+h - Orbital radius

CE - Slant range

d/dt is taken with respect to inertial space. If geometrical

Referring to Fig. D-5

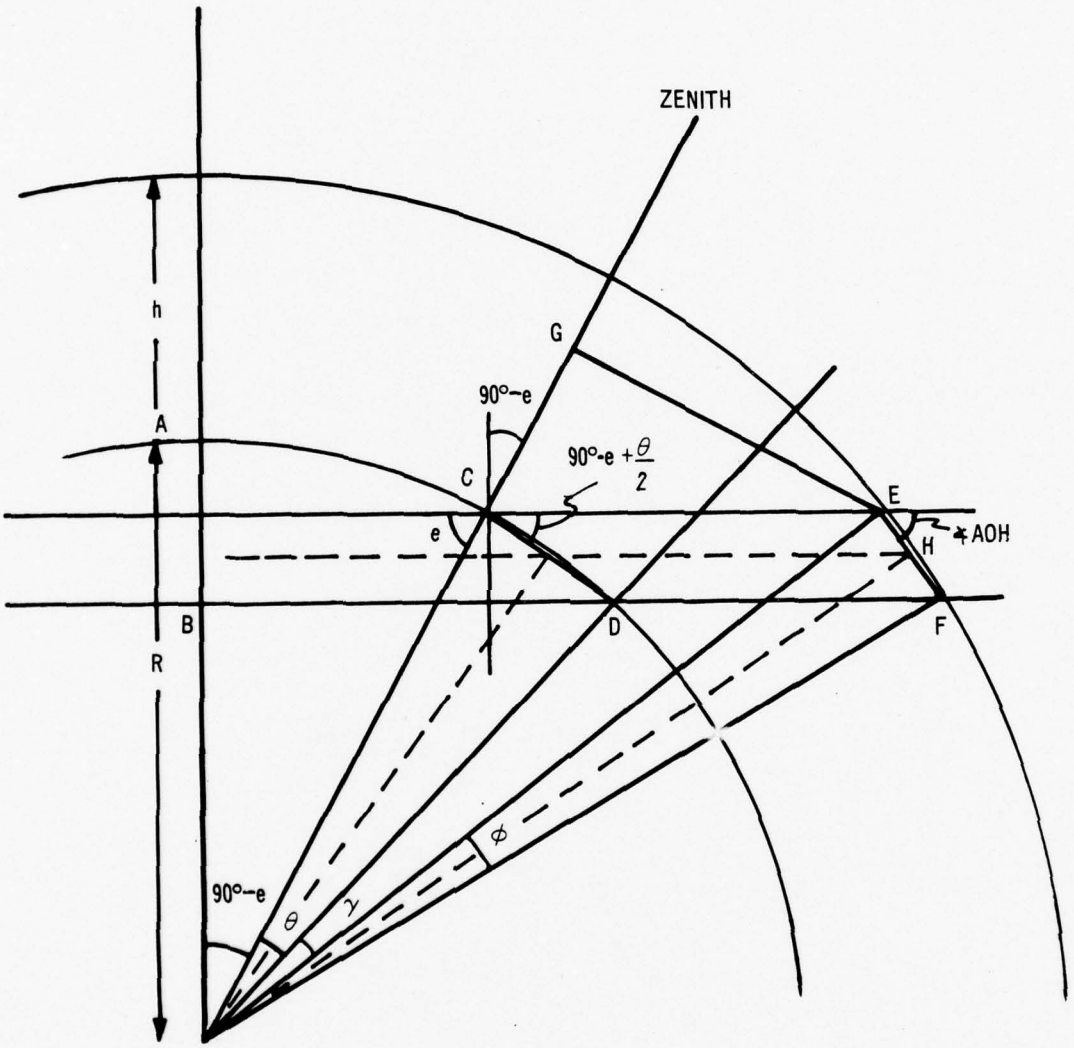


Fig. D-5. Error in geographical position due to error in satellite position.

$$\frac{\overline{GE}}{\overline{CE}} = \sin e$$

$$\frac{\overline{GE}}{(R+h)} = \sin(\theta + \gamma)$$

$$\overline{CE} = \frac{(R+h)\sin(\theta+\gamma)}{\sin e}$$

$$\overline{AB} = \overline{CD}\cos\left(e - \frac{\theta}{2}\right)$$

$$\overline{AB} = \overline{EF}\sin \angle AOH$$

$$\angle AOH = \angle AOE + \frac{\phi}{2}$$

$$\angle AOE = \sin^{-1}\frac{\overline{AE}}{(R+h)}$$

$$\overline{AE} = \sqrt{(R+h)^2 - (R\sin e)^2}$$

$$\frac{\overline{AE}}{R+h} = \sqrt{1 - \left(\frac{R\sin e}{R+h}\right)^2}$$

$$\sin^{-1}\left(\frac{\overline{AE}}{R+h}\right) = \sin^{-1}\sqrt{1 - \left(\frac{R\sin e}{R+h}\right)^2}$$

$$= \cos^{-1}\left(\frac{R\sin e}{R+h}\right) = \angle AOE$$

$$\therefore \angle AOH = \cos^{-1}\left(\frac{R\sin e}{R+h}\right) + \frac{\phi}{2}$$

and

$$\text{and } \overline{AB} = \overline{EF}\sin\left[\cos^{-1}\left(\frac{R\sin e}{R+h}\right) + \frac{\phi}{2}\right]$$

$$\overline{CD} = 2R\sin\frac{\theta}{2}$$

$$\overline{EF} = 2(R+h)\sin\frac{\phi}{2}$$

$$R\sin\frac{\theta}{2}\cos\left(e-\frac{\theta}{2}\right) = (R+h)\sin\frac{\phi}{2}\sin\left[\cos^{-1}\left(\frac{R\sin e}{R+h}\right)+\frac{\phi}{2}\right]$$

$$R\sin\frac{\theta}{2}\left(\cos e\cos\frac{\theta}{2}+\sin e\sin\frac{\theta}{2}\right)$$

$$= (R+h)\sin\frac{\phi}{2}\left[\sqrt{1-\left(\frac{R\sin e}{R+h}\right)^2}\cos\frac{\phi}{2}+\left(\frac{R\sin e}{R+h}\right)\sin\frac{\phi}{2}\right]$$

For ϕ small

$$R\sin\frac{\theta}{2}\left(\cos e\cos\frac{\theta}{2}+\sin e\sin\frac{\theta}{2}\right)$$

$$= (R+h)\frac{\phi}{2}\left[\sqrt{1-\left(\frac{R\sin e}{R+h}\right)^2}+\left(\frac{R\sin e}{R+h}\right)\frac{\phi}{2}\right]$$

For e = 0, satellite at zenith

$$\theta = \frac{R+h}{R}\phi$$

For e = 90° satellite on horizon

$$R\sin^2\frac{\theta}{2} \approx \frac{\phi}{2}\sqrt{2Rh+h^2}$$

Thus, for a thousand mile altitude orbit, with the satellite on the zenith, a topocentric error of 16 seconds of arc when viewed from the earth's surface will yield an error of 464 feet. If the satellite is at zenith distance of 60°, the error on the ground will be 620 feet.

As stated above, timing errors and ephemeris errors are similar in effect, and may be treated in identical fashion. It is also true that, unless the time is known to the observer, it is impossible to separate these errors, either by observation or by data reduction.

Another source of timing errors mentioned previously was that of radio wave propogation uncertainties. These are due chiefly to the path difference between a ground wave traveling on a great circle course, and a sky wave, which will travel in a series of straight line hops between the earth's surface and the ionospheric layers. This error is a maximum at points close to the transmitter and approaches a constant difference as range increases beyond 1000 miles. The curve in Fig. D-6, from ref. (9), shows the time delay between ground waves and sky waves making a single hop. Under conditions of reception (i.e., night, long range) where no ground wave is being received, the correction in transmission path time would be straightforward except that the signal received may not necessarily have

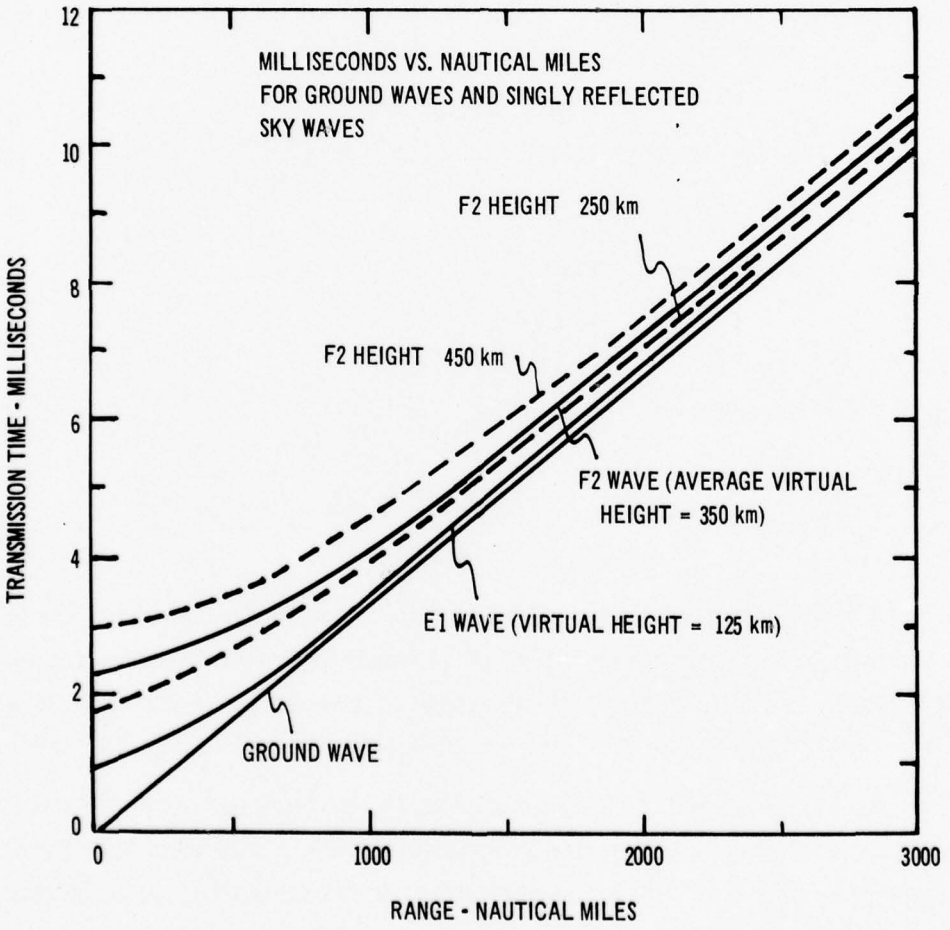


Fig. D-6. Transmission time.

experienced only one reflection, but may have been multiply reflected, in which case the delay may not be known with certainty. This difficulty could be overcome by transmitting the time of the master control station with pulses delayed by the expected transmission time. The receiving station could then compare the received time pulses with its own clock and by noting and counting any differences determine whether the first, second or third reflection was being received. (In practice, signals that have experienced four or more hops will have been attenuated beyond use and so need not be considered.) Obviously, such a modification would further complicate the communications system and add to its expense, but for long range synchronization the cost would be justified by improved system performance.

APPENDIX E

THE STABILIZATION SYSTEM

1. Introduction

Stabilization of the camera consists of mounting the camera in a set of gimbals so that it can be isolated from the ship's angular motion. In addition, a means of slewing the camera at pre-determined rates is to be provided.

These two functions – geometrical stabilization and response to commanded changes in orientation are the properties of a three axis integrating drive system developed by the MIT Instrumentation Laboratory. The equipment consists of a set of gimbals to support the object to be stabilized, gyroscopic units, torque motors and servo electronics. The gyroscopic units are mounted on the camera and sense any angular deviation of the camera relative to inertial (star) space, within the drift uncertainties of the gyros. For three axis stabilization either two two degree-of-freedom gyros or three single degree-of-freedom gyros can be used. Hereafter it is assumed that three SDF gyros will be used. Signals, proportional to the sensed angular deviations are produced by the gyros, processed by the servo electronics, and converted into torques by the torque motors mounted on the gimbals. Thus the gimbals are moved so as to restore the camera to its original orientation. If signals (commanded angular velocity components) are introduced to the gyros the camera will rotate relative to inertial coordinates at a rate proportional to the vector sum of the commands. Further detailed information may be found in Refs. (12) and (13).

The principal design problems are to determine 1) the number and arrangement of gimbals, 2) the size of the gimbal torque motors, and 3) a specific servo design. These are taken up in order in the following three sections.

2. The Gimbal System

Early in the program it was determined that

1) the camera's stabilized orientation could be anywhere between a vertical and horizontal position,

2) a specific camera design would not be known by the end of the study, and

3) ship's roll and pitch amplitude would be a maximum of twenty degrees.

The above served as boundary conditions for the design presented below.

Three gimbals are required for stabilization about three axes. Sometimes more than three gimbals are used if the vehicle carrying the stabilization system is expected to undergo large angular rotations (in excess of 90°). Since this is not the case with a ship it was decided to use three.

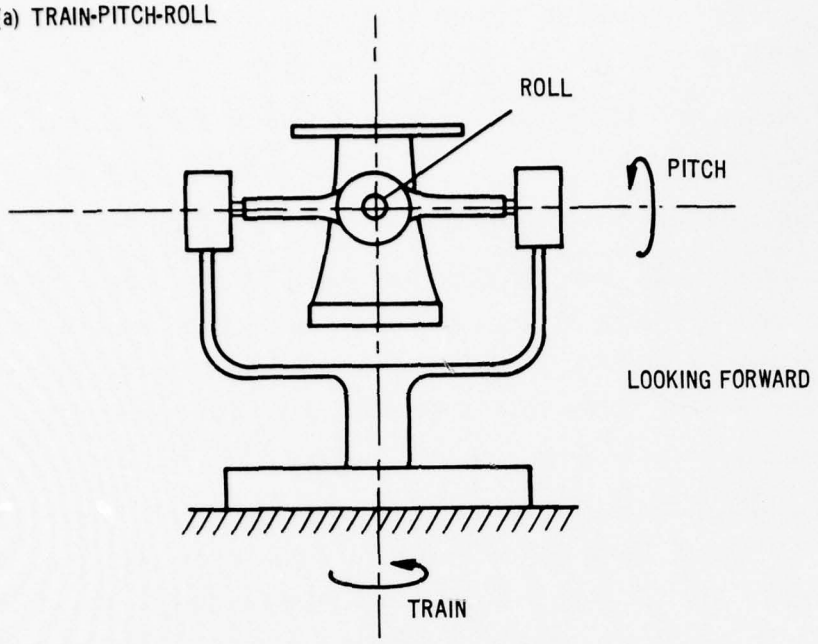
Six possible orientations can be instrumented and these are identified in Fig. E-1. Here the camera is always in the center of the gimbal system. In each case a condition of gimbal lock is possible, i.e., there is some orientation of the camera for which three axis stabilization is impossible. For example, in Fig. E-1a if the camera is to be used in the horizontal position the pitch gimbal will be rotated through 90° from its indicated position.* Then the yaw and train axes coincide and no roll stabilization is possible. Also in each case a coordinate transformation of the gyro output data is required in order to make the gain of the stabilization system about each axis invariant to relative gimbal orientations (12).

After a consideration of the above problems together with many others which will not be detailed here, it was decided to add a fourth articulation as shown in Fig. E-2. Motion of the camera about this axis is controlled by a motor drive thus allowing the camera to be set in co-elevation from 0 to 90 degrees. As a result the relative gimbal motion will be dependent only on the roll and pitch of the ship.

The gimbals, from the outside, are designated train, roll and pitch. The train gimbal is a shaft in a vertical base, and serves the dual function of providing motion for train stabilization and camera train. The roll gimbal is in a yoke mounted on the top of the train column. The gimbal is actually a ring which contains and supports the pitch gimbal. This last gimbal is the system's controlled member, and contains the camera

*The use of a mirror to alleviate this condition was considered unsatisfactory.

(a) TRAIN-PITCH-ROLL



(b) TRAIN-ROLL-PITCH

SAME AS (a) WHEN TRAIN GIMBAL IS TURNED 90°
HENCE DOES NOT CONSTITUTE DIFFERENT
MECHANICAL ARRANGEMENT.

(c) ROLL-PITCH-AZIMUTH

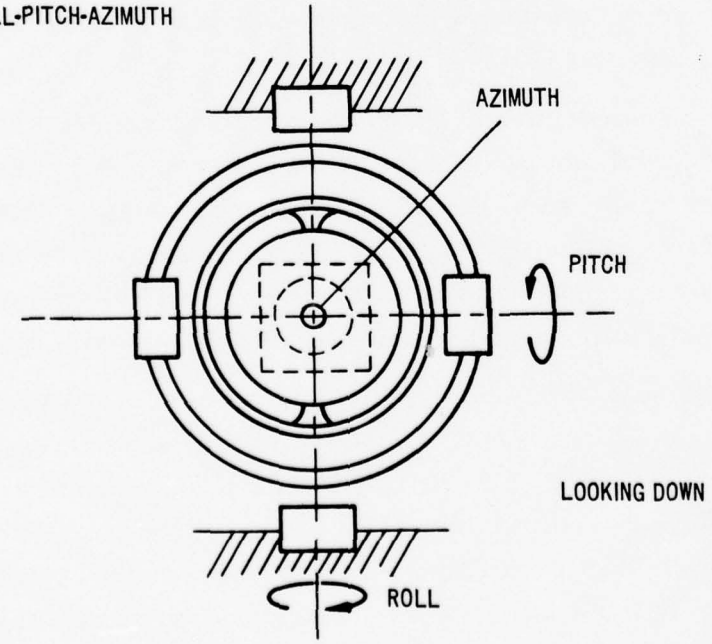


Fig. E-1. Gimbal configurations. (Page 1 of 2)

(d) PITCH-ROLL-AZIMUTH

SAME AS (c) EXCEPT PITCH AND ROLL AXES ARE TURNED 90° ABOUT DECK VERTICAL.

(e) ROLL-AZIMUTH-PITCH

SAME AS (c) EXCEPT ROLL GIMBAL IS TURNED 90°.

(f) PITCH-AZIMUTH-ROLL

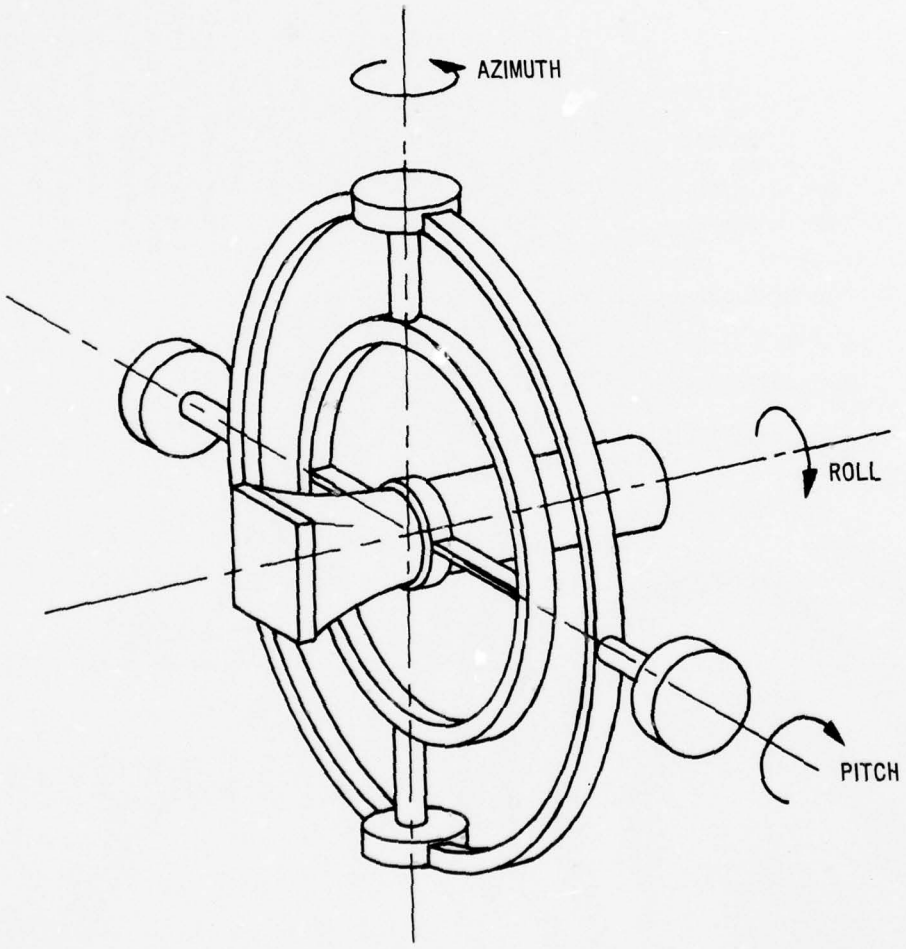
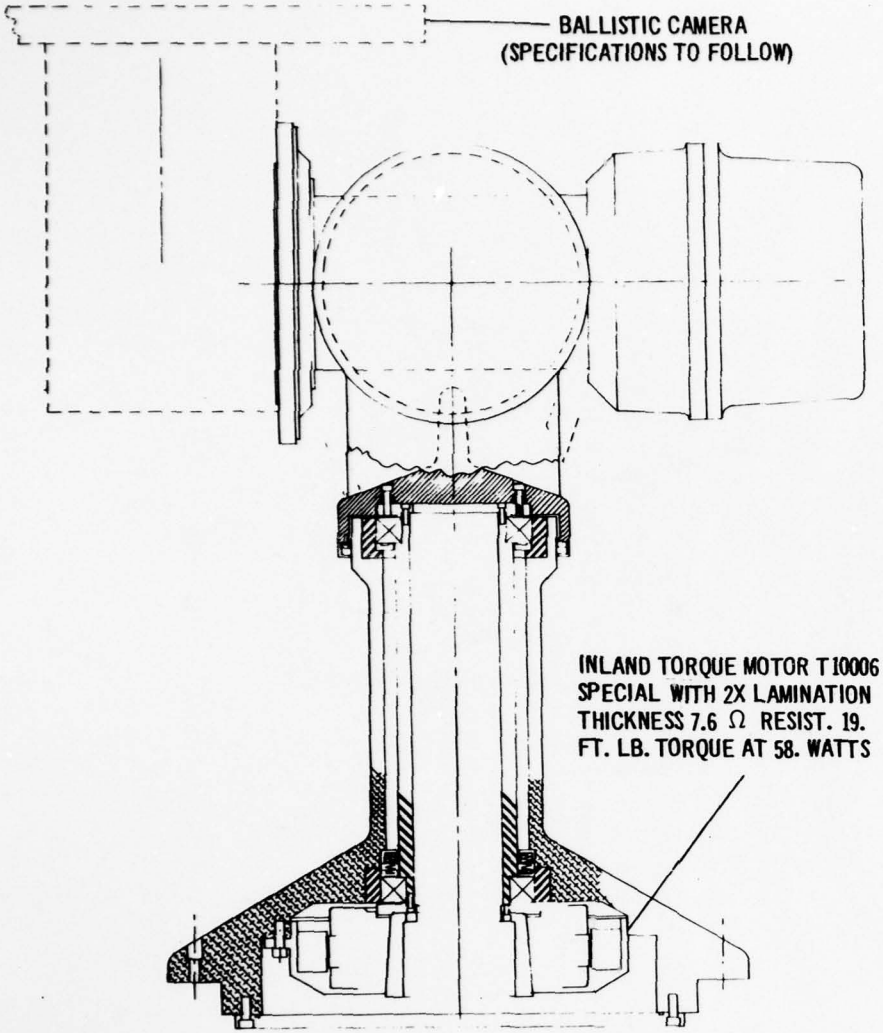


Fig. E-1. Gimbal configurations. (Page 2 of 2)



MATERIALS:

Alumimum castings ASTMCS22
Cast Iron yoke ASTMA 48-48 Class 30
Seamless Mechanical Steel tubing ASTM (to follow)

FINISHES:

On steel and cast iron use Endurion anti-corrosion treatment all over.
On alumimum parts etch and black anodize all over.
On all exposed surfaces use Profilm No. 3000 (a vinyl paint)
Both Endurion and Profilm 3000 are produced by: Rust Proofing and Metal Finishing Corp., Cambridge 42, Massachusetts.

The two horizontal servo controlled axes have an angular range of ± 20 degrees and the vertical servo train axis angular travel is ± 175 degrees from the centered (locked) position.

The camera elevation angle may be remotely set to any angle ± 90 degrees from the vertical and is independent of the servo controlled axis. The vertical train axis can be remotely preset ± 170 degrees from the centered position but the total angular travel is limited to ± 175 degrees from the centered position.

All angular rotations are limited by directionally sensitive limit switches.

Each gimbal axis is equipped with a remotely actuated solenoid lock (solenoid energized to unlock). The locks will engage only in the middle of each angular range, when all axes are orthogonal and are equipped with switches to remotely indicate the 'all axes locked' or 'all axes unlocked' condition.

With the camera in operating condition and at any preset elevation angle each gimbal axis is to be statically balanced to within 10 inch oz. and is to have a starting friction of less than 30 inch oz. neglecting torque motor hysterisis frictions.

Fig. E-2. Mechanical assembly, train gimbal.

and the stabilization system's gyros and accelerometers.* The camera mount pad, shown on the left side of the drawing will accept any shape or size camera when suitable adapters or mount pads are prepared.

A major advantage of the configuration shown is that of accessibility for construction and maintenance. Note that the gyro package, with its electronics, is mounted on the opposite end of the pitch gimbal from the camera.

The pitch and roll gimbals are each capable of unobstructed motion of ± 20 degrees. In all likelihood this amount will never be exceeded, or even approached, in weather suitable for satellite photography. The train gimbal is capable of motion over ± 175° from its center position, but the equipment shelter will limit motion to about ± 145° before vignetting occurs.

The salt spray and air environment was recognized in the design of the gimbal system, and careful attention was given to the placement of parts for ease of sealing and protection from spray. The choice of materials was primarily dictated by mechanical considerations, but due consideration was given to protective coatings, dissimilar metals and corrosion-resistant materials and components.

Figure E-3 shows the mechanical details of the design of the roll and pitch gimbals. The camera elevation angle is set by a motor drive that actuates the camera mount pad. Readout of camera angle is provided by a synchro transmitter in the drive gear train. The camera must be statically and dynamically balanced about the pitch axis for all settings; i.e., the camera weight distribution must be that of a disc or taurus. This requirement can be met at the possible expense of some additional weight.

The gimbals are equipped with solenoid-operated locking pins, for caging the system when not in use. Limit switches are provided on each gimbal, to prevent possible damage by exceeding the displacement limits.

Gimbal positioning is done by direct current torque motors. Train and pitch are controlled by one torquer each, while the roll axis has two torquers arranged at each end of the gimbal. The selection of these torque motors is taken up in the next section.

The use of accelerometers for gyrocompassing is discussed in App. G.

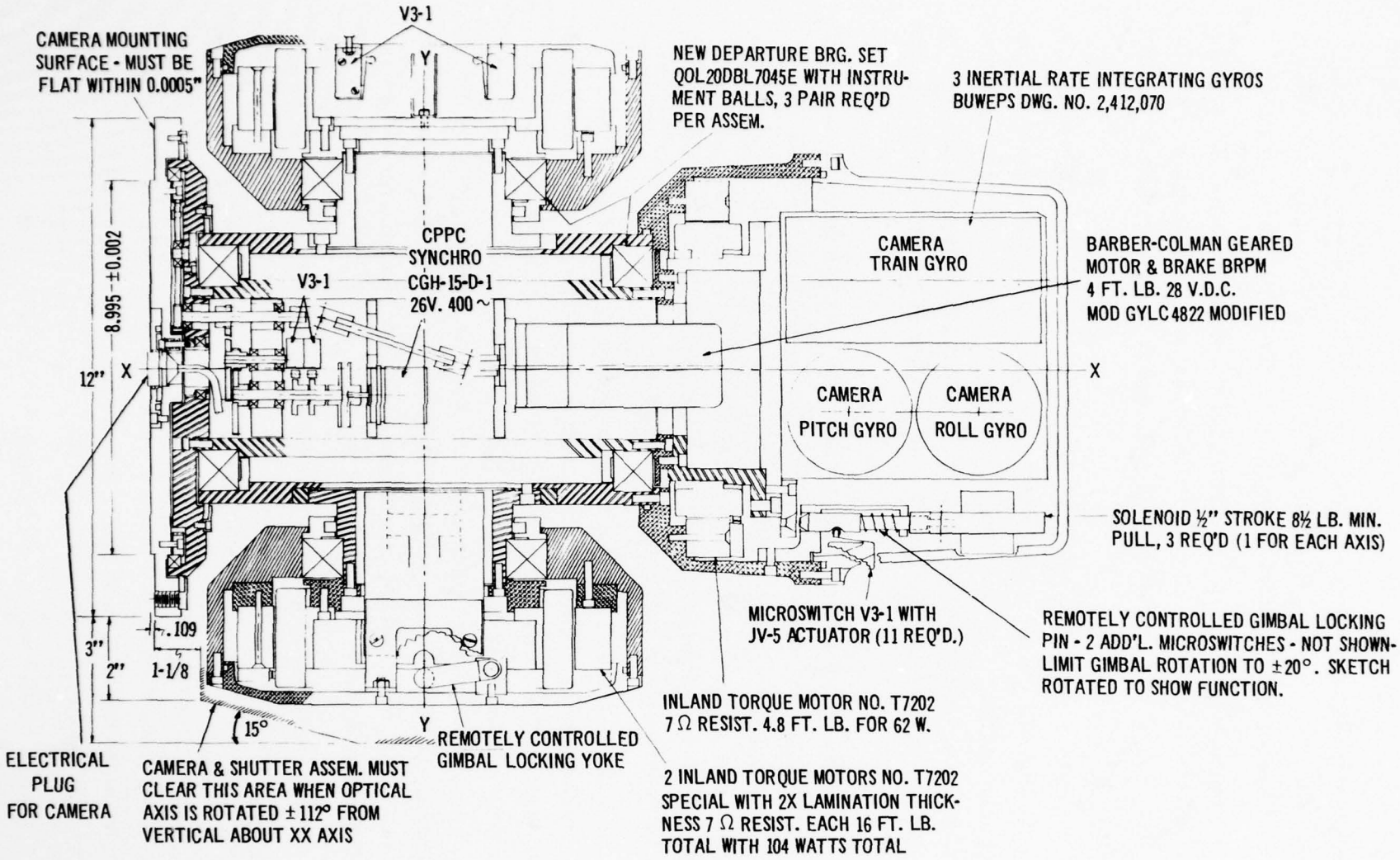


Fig. E-3. Mechanical assembly, roll and pitch gimbals.

3. Gimbal Torque Motors

As mentioned in Section 1, torque motors are mounted on each of the gimbal drive axes to re-orient the camera when it has been disturbed from a desired orientation. The following analysis shows how the torque motors are selected.

Figure E-4 shows a three-gimbal system supported by a base. A coordinate system is fixed to each of the gimbals. In this figure the gimbals happen to be mutually orthogonal, hence the coordinate system x, y, z represents the intersection of three gimbal fixed coordinates. In order to determine where torque motors should be placed so that corrective torques can be applied, the equations of motion of the system will be derived. At first it is assumed that 1) the bearings are frictionless, and 2) the gimbals are perfectly balanced.

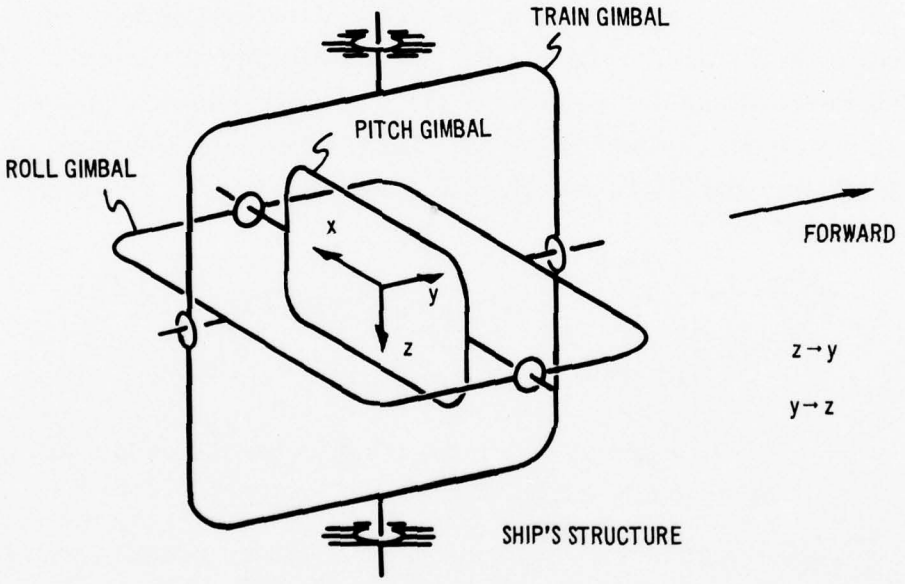


Fig. E-4. Sketch of a three-gimbal system.

Euler's equation for the pitch gimbal is

$$\bar{M} = \frac{d\bar{H}}{dt}$$

where

$\bar{M}$ is the torque applied to the pitch gimbal,

$\bar{H}$ is the angular momentum of the pitch gimbal, and

d/dt is taken with respect to inertial space. If geometrical stabilization is achieved

$$\frac{\overline{dH}}{dt} = 0$$

Thus a torque motor between the pitch and roll gimbal is not needed.

Writing Euler's equation for the roll gimbal yields

$$\begin{aligned} M_x &= I_x W_x - (I_y - I_z) W_y W_z \\ M_y &= I_y \dot{W}_y - (I_z - I_x) W_z W_x \\ M_z &= I_z \dot{W}_z - (I_x - I_y) W_x W_y \end{aligned} \qquad \text{(E-1)}$$

The angular velocity components are with respect to inertial space and the cross products of inertia are assumed to be zero. Since the angular velocity of the pitch gimbal is zero, only an ω_x of the intermediate gimbal can be permitted. An inspection of the above equation set will show that no torque motor is needed between the roll and train gimbals.

Finally, writing Euler's equation for the train gimbal yields a set identical to Eq. (E-1). Since an ω_x of the roll gimbal can exist, all three components of angular velocity of the outer gimbal exist in the presence of random base motion. If the necessary kinematic relationships are derived and substituted into Eq. (E-1) the following expression for M_z is obtained;

$$M_z = -\tan A \left[I_{x(r)} - I_{z(t)} \right] \dot{W}_{x(t)} - W_{x(t)} W_{z(t)} \left[I_{x(r)} \tan^2 A + \right. \qquad \text{(E-2)}$$

$$\left. - I_{z(t)} \sec^2 A \right] + \left[I_{y(t)} - I_{x(t)} \right] W_{x(t)} W_{y(t)}$$

where

A is the angle by which the train and roll gimbals are non-orthogonal, and

( ) is a subscript to identify the indicated quantity with either the train (t) or roll (r) gimbal.

Using an amplitude of 20 degrees and a period of 10 sec Eq. (E-2) can be evaluated, approximately, term by term. Using the estimated moments of inertia it can be determined that M_y would never exceed 1 ft-lb.

The conclusion is only one torque motor, on the train gimbal, is needed if the gimbal system is perfect. Recognizing, now, friction and stiction in the bearings, brush and torque motor friction, wind loads, and gimbal unbalance, a torque motor will be needed on all axes. Before

pursuing this matter further, however, some aspects of the servo electronics should be considered.

4. The Servo Electronics

Figure E-5 is the functional diagram of a typical single axis integrating drive system. As was mentioned in Section 1 the output of the gyro is a signal (generally an ac signal whose carrier frequency might be anywhere between 400 cps and 20 k cps) proportional to the angular displacement of the gimbal about its drive axis. A pre-amplifier near the gyro raises the level of the output before it is sent to an ac amplifier and demodulator. The dc amplifier contains networks which make the loop stable and determine the frequency response characteristics. The power amplifier converts the output of the dc amplifier into sufficient power to drive the torque motor.

As was mentioned in Chapter II the camera stabilization system has two functions; it must 1) isolate the camera from roll and pitch of the ship, and 2) permit the camera to be slewed at pre-determined rates. The mode selection block in Fig. E-5 show the various commands that can be introduced to the integrating drive system. Gyro compassing is discussed in Appendix G and the inter-relation of the other modes is discussed in Appendix F. A basic property of an integrating drive is the angular velocity response to a signal introduced to the gyro (13). Referring to Fig. E-5 the angular velocity of the gimbal, relative to inertial space, will be proportional to the magnitude of the input signal. For example, if the mode selection switch is in the operate position the gimbal will slew at pre-determined rates.

The camera stabilization system consists of three integrating drive systems identical to the one shown in Fig. E-5. Each axis operates independently. Perfect stabilization is not achieved because of gyro drift and gimbal friction.

Gyro drift is the result of imperfect manufacturing techniques and causes random drift of the camera about all three axes. In Appendix C it is shown that the camera should not drift more than 2 sec of arc in 5 seconds. Gyro drift is usually expressed in parts of the earth rate. The term meru is a contraction of milli-earth-rate-unit and is equal to 0.015

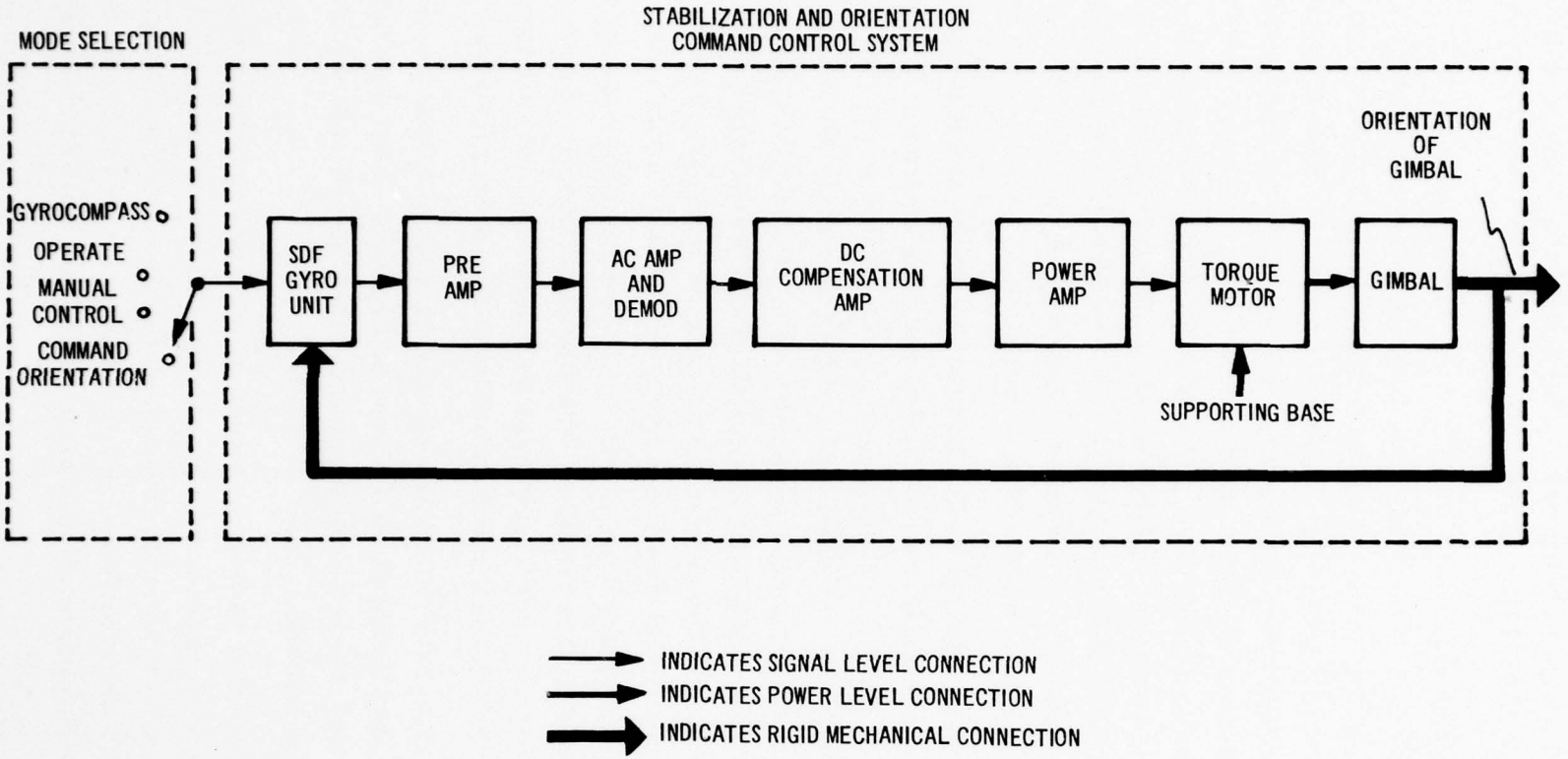


Fig. E-5. Functional diagram of a single axis integrating drive system.

degrees per hour. A drift of 2 seconds of arc in 5 seconds is 26 meru, but the specification of 10 meru is recommended in order to achieve the desired overall system performance. The reason is most gyro manufacturers express drift in terms of the standard deviation (1σ) of a set of data. In this case the 26 meru should be considered a 3σ value.

Gimbal friction causes disturbance torques about the drive axes. Due to the low frequency roll and pitch of a ship two types of torque interference can be identified. At the peak of a roll or pitch motion there will be a step torque equal to twice the gimbal friction. In between peaks the torque will be equal to the gimbal friction and will be almost constant. The former is more serious. In order to determine the angular perturbation caused by the torque interference a specific servo design should be analyzed. However, in the construction of the gimbal drive systems it is not always possible to achieve the desired performance. Current practice yields a static loop compliance of approximately 10 ft-lbs/mr. The effect of an interference torque will be a function of the dynamics of the dc compensation amplifier (Fig. E-5) and this is a matter of experiment in order to optimize the system.

The above considerations would then lead to minimizing the gimbal friction which means minimizing the size of the torque motor. However, if the ratio of torque to gimbal inertia is small it may be difficult to "stabilize" the gimbals when the servos are turned on. This is a problem of synchronization as discussed in Ref. (14). The conflict of minimizing gimbal friction and avoiding synchronization problems led to two design approaches summarized in Table E-1.

The torque to inertia ratio for the pitch axis is favorable and the friction is probably as low as is practical. Attempting to maintain a constant torque to inertia ratio for the other axes leads to higher gimbal friction. As may be seen, if constant gimbal friction is maintained the torque to inertia ratios decrease sharply. However, if the large torque motors are used it may be found that the camera shutter must be closed during periods of large servo error and a significant amount of data could be lost. The problem here is subject to experiment.

Reference (14) contains an analysis of the specific servo design assumed in this appendix.

Table E-1. Stabilization system parameters.

AXIS	X (PITCH)	Y (ROLL)		Z (TRAIN)	
Number of torque motors	1	2	2	1	1
Inland Motor type	T-7202	T-7202	T-4006	T-10006	T-7202
Resistance	7Ω	7Ω	7Ω	7Ω	7Ω
Stack	Std.	2x Lam.	Std.	2x Lam.	Std.
Stall torque (ft.lbs)	4.8	16	3.6	19	4.8
Inertia (±30%) ($Slug\text{-}ft^2$)	0.8	3.4	3.4	4.4	3.8
Stall torque Ratio inertia	6.0	4.7	1.1	4.3	1.3
Power (watts)	62	104	200	58	62
Sensitivity (ft-lbs/amp)	1.6	6.4	1.2	6.9	1.6
Friction-bearing, brush, and seal (ft-lbs)	0.08	0.12	0.07	0.09	0.07
Friction-hysteresis (ft-lbs)	0.07	0.26	0.07	0.38	0.07
Friction-total (ft-lbs)	0.15	0.38	0.14	0.47	0.14

The compensation effected by networks in the d-c amplifier (Fig. E-5) is often called "lag-lead compensation". It turns out that this design is more sensitive to interference torques than the other methods of stabilization commonly used in integrating drive systems. The other methods consist of 1) the use of "lead-compensation" or 2) the use of an ADA (angular differentiating accelerometer). In the latter case angular motion of the gimbal is sensed not only by the gyro but also by an accelerometer mounted on the gimbal, thus providing a stabilization loop inside the one shown in Fig. E-5. Of the three methods this instrumentation is least sensitive to interference torques.

Experiments* on methods 1) and 2) above are currently being conducted in the Instrumentation Laboratory. The results will be available within a few weeks from the date of this printing.

*In connection with other ~~approved~~ sponsored projects.

APPENDIX F

PACKAGING

1. Environmental Control

An integrated shelter, Fig. 1, is recommended for the Astro Photogrammetric Ship's Positioning System. The shelter will provide all-weather protection to the equipment, and a controlled environment for both equipment and personnel.

The ambient control problem will be different for the camera dome and the equipment compartment.

In the camera compartment, the power requirements of non-operating equipment will be zero, or nearly so, and the principle problem will be to maintain a low relative humidity inside the dome. This is a straightforward air conditioning problem. When the camera is being prepared for operation, the warm-up and operating power consumption could be as high as 1000 watts (maximum). The dome air conditioner must deal with this input while adjusting the dome temperature up or down to match outside ambient. Dome air humidity must be controlled during this operation to prevent condensation.

In the equipment compartment, there will be a constant heat load of about 2000 watts from the timing equipment, which runs continually. Peak load during operation could be as high as 4000 watts, including operators. Humidity and temperature in the equipment compartment will be kept at a constant level, at about 70°F and 50% R.H.

The air conditioning system to handle the loads described will have to have a capacity of at least 17,000 B.T.U.

Vibration and shock control will be required for reliable equipment operation. The timer's crystal oscillator will be particularly sensitive. Shipboard shocks and vibrations, as specified in Ref. (15), will be primarily low frequency. Precision equipment will be subjected to these and to possible higher frequency vibrations from

equipment in the shelter. Vibration isolation of individual consoles within the shelter is recommended since isolation of the entire shelter would require mounts of low stiffness and large deflections for a low resonant frequency, the shelter would rotate undesirably about its own axes when the ship rolled and pitched.

If the shelter is located on the main deck, above a main frame member, the vibration inputs will be less than if mounting is on a superstructure deck or between frames.

2. Power Consumption

Electrical power consumption is estimated. The input power to the shelter can be made compatible with any ship's service supply, including 400 cycles.

Stabilization System	500W
Timing Equipment	2000W
Lighting, etc.	1000W
Air Conditioning	14000W
Total	17,500W

These figures represent approximate peak demands.

3. Weight and Size

The complete system will weigh approximately 4500 pounds. The approximate overall dimensions of the shelter will be 14 feet long by 7 feet high by 6 feet wide.

4. Console Design

A central control panel, Figs. 4 and 1, is proposed to allow a central position from which a single operator can control or monitor all of the subsystems. (16)

The operator may energize and operate the stabilization system and camera with the controls on the panel, while malfunction indicators advise him of the status of the remaining subsystems.

Interlocks are provided, consistent with the operating procedure for the system, to prevent aborted runs and/or equipment damage from operator errors or equipment malfunctions.

The operating sequence is presented below, in the form of an outlined set of instructions. The presetting and calibration of the system's timer and the camera programmer and the setting of the train ring, are implicitly a part of the operating instructions, as described in Chapter II, Section 6.

1. Turn On Main Power. Power is applied to the gyro heaters. Warm-up time is 15-30 minutes.
2. "Ready to Start" lamp indicates that gyros are up to temperature. Power is applied to system electronics.
3. Set in Latitude Heading and Speed of the ship on the appropriate control panel dials.
4. Press "Gyrocompass" switch to unlock gimbals and connect North and East pendulums to stabilization loops. At the end of a pre-determined settling-in time the "North" lamp will light, indicating that the system has gyrocompassed to within the limits discussed in Appendix G
5. Set the azimuth and elevation of the satellite at the time of the event, with the set azimuth and set elevation dials.
6. Press "Command Orientation " switch to disconnect the stabilization system from the gyrocompass mode to the acquire or orient mode. The system will move to the true azimuth and elevation commanded, and stop. The "In Position" lamp will light when the camera is pointed properly. The azimuth and elevation indicators should agree with the settings of the corresponding dials.
7. Set the camera slew rate and direction with the "Elevation Slew Rate" and/or the "Train Slew Rate" dial. The dials will be calibrated in arc seconds/second.
8. Press the "Slew" switch to begin the motion of the camera and to start the camera programmer. When this control is depressed the camera programmer is turned on, starting the photography, and the camera is slewed as discussed in the section on exposure time determination.

9. Press the "End Run" switch to stop the camera slew and the camera programmer. The stabilization system locks in position until commanded otherwise.

10. Press the "Off" button to shut off the stabilization system. When this switch is operated, the stabilization system gimbals automatically return to their caged positions, the gimbals are pinned, and the power to the stabilization system is shut off.

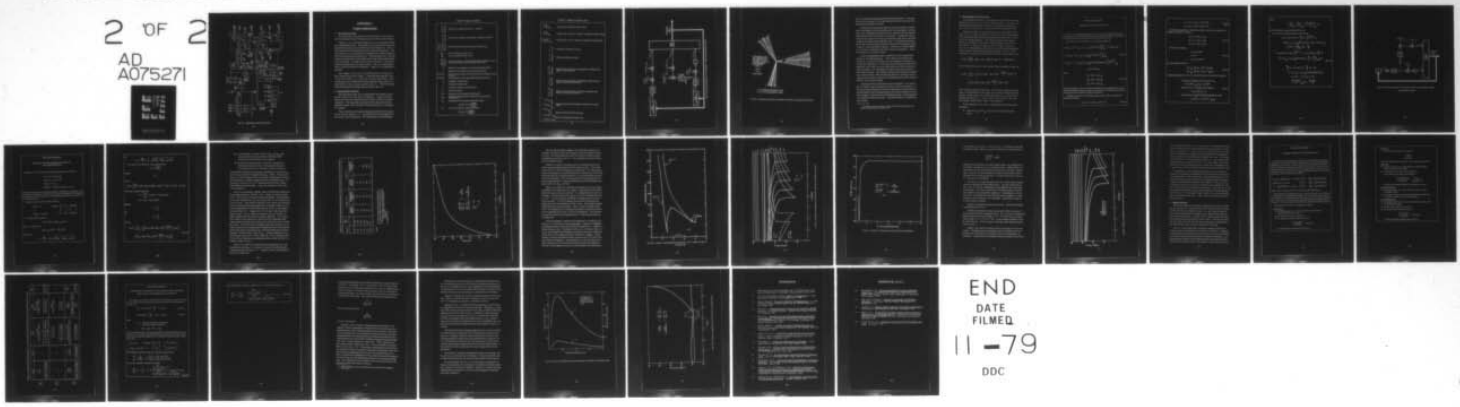
In addition to the controls and indicators mentioned in the outline above, there is a manual control for orientation and a series of malfunction indicators.

The manual control overrides the set azimuth and set elevation dials, and may be necessary in the event of a serious error in predicted satellite arrival, erroneous dial settings, changes in ships course and the like. Whenever the manual control switch is depressed, the control of camera orientation is switched to the joystick. The "In Position" lamp will remain on whenever the joystick is in its neutral position, and the "Slew" button may be depressed from any camera orientation.

The malfunction indicators and interlock are to monitor operation of subsystems and prevent photography in the event of malfunction, respectively. The indicators shown in Fig. F-1 are for the camera, programmer, timer and dark slide in place, but the actual system may well include more functions. An audible warning has been shown; this will be a horn or buzzer to alert the operator to troubles. The malfunction interlock relay will prevent operation of the slew circuits and camera programmer until the malfunction is corrected.

AD-A075 271 MASSACHUSETTS INST OF TECH CAMBRIDGE EXPERIMENTAL AS--ETC F/G 17/7
POSITION INDICATION AT SEA BY ASTRO-PHOTOGRAMMETRY,(U)
NOV 63 A C CONROD N62306-1168
UNCLASSIFIED RE-5 NL

2 OF 2
AD
A075271



END
DATE
FILMED
11-79
DDC

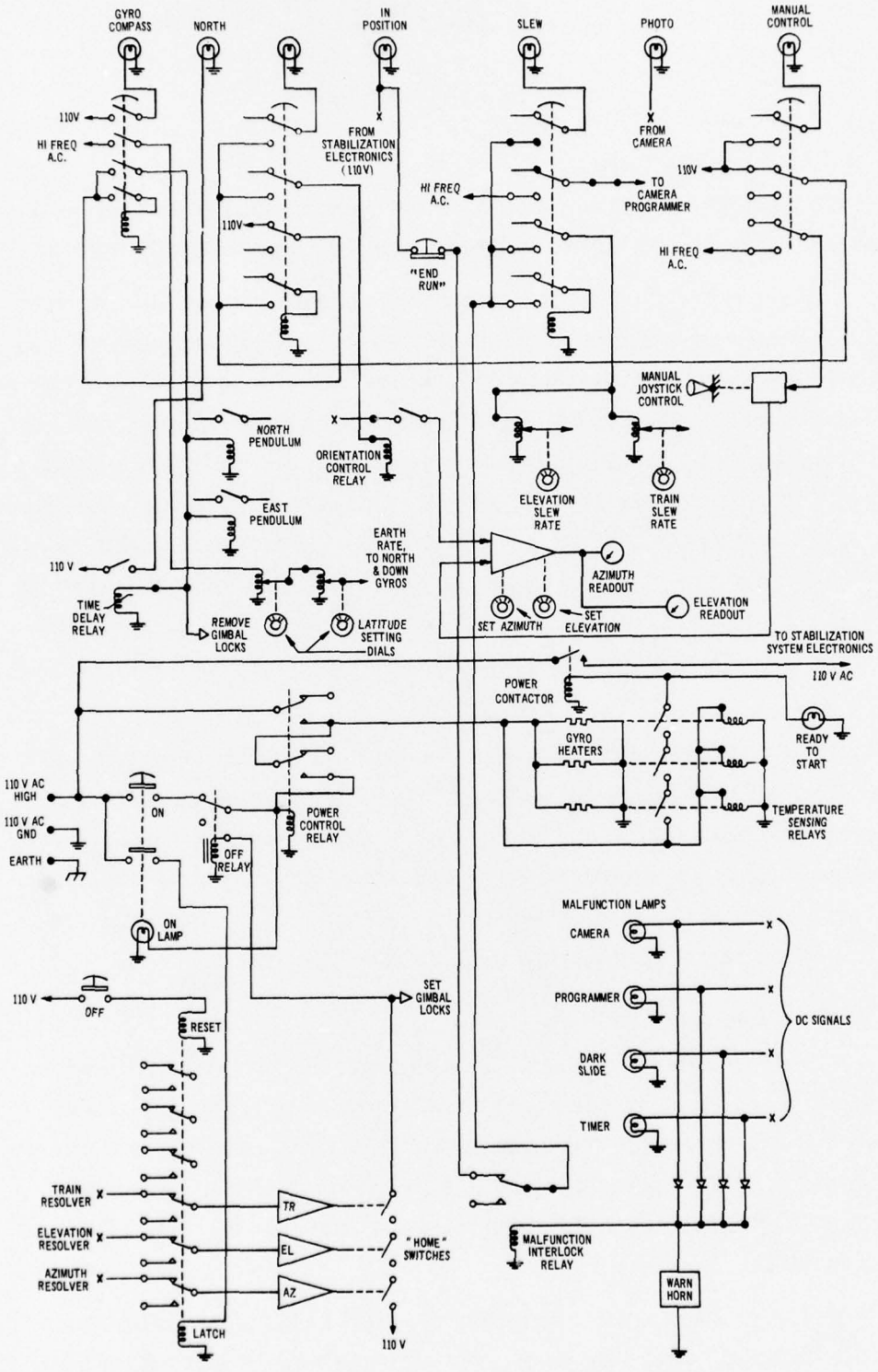


Fig. F-1. Stabilization system control panel.

APPENDIX G

GYROCOMPASSING

1. A Gyrocompassing System

By adding two accelerometers (or pendulums) to the camera stabilization system a gyrocompassing mode can be instrumented.

Figure G-1 is a functional diagram of an acceleration coupled gyrocompassing system. The gimbal drive system is the three axis stabilization system described in Section 3 of Chapter II. Two accelerometers have been rigidly attached to the gyro enclosure. The input axis of the x accelerometer is perpendicular to both the optical axis of the camera and the pitch axis. The input axis of the y accelerometer is perpendicular to the optical axis of the camera and parallel to the pitch axis. The optical axis will be called the z axis and is positive pointing from lens to plate holder. The x y z axis system will be called instrument coordinates. Table G-1 is a glossary of symbols.

The outputs of the x and y accelerometers are connected to their respective gyros by filters. These two loops operate so as "level" the camera, i.e., erect the -z axis to the vertical. Gyrocompassing is accomplished by connecting the output of the x accelerometer to the z gyro as shown in Fig. G-1. The motivations behind this particular design may be found in Ref. 13.

2. Assumed Boundary Conditions

The instrument axes will be misaligned with respect to geographic axes prior to the start of alignment. Figure G-2 illustrates the three error angles that will be used to identify this misalignment. The magnitude and sign of these angles at the time alignment begins are a function of ships motion and, accordingly, are random.

Prior to the start of alignment the gimbal system will be caged in the "stored" position, i.e., all gimbals will be orthogonal and the camera will be facing up. The train plate will be positioned

Table G-1. Glossary of symbols.

A_x, A_y, A_z	Platform error angles (See Fig. G-2) (radians)
a_x, a_y, a_z	Acceleration components in geographic coordinates (ft/sec^2)
$[a_{x_i}]$ sg, $[a_{y_i}]$ sg, $[a_{z_i}]$ sg	Inertially referred accelerometer output signals (volts)
E_{ax}	x-axis accelerometer bias ("g's")
E_{ay}	y-axis accelerometer bias ("g's")
E_{gx}, E_{gy}, E_{gz}	Gyro drift (rad/sec). (This is platform drift resulting from a constant torque unbalanced about the gyro output axis.)
G	Magnitude of the gradient of the earth's gravitational field.
g	Magnitude of the gradient of the earth's gravity field.
$K_1 G_1(p)$	Transfer function of the level axes filters (units depend on choice of filter).
$K_2 G_2(p)$	Transfer function of the gyrocompassing filter (volt/volt).
ℓ	Geographic longitude (rad).
L	Geographic Latitude (rad).
L'	Computed or hand set value of latitude.
R	Radius of earth (ft).
S_{au}	Sensitivity of accelerometer (volts/ft/sec^2)
S_{GD}	Sensitivity of platform drive system about x_i and y_i and z_i (rad/sec/volt)
S_{GL}	Gyrocompass loop component sensitivity product = $S_{au}\ S_{GD}\ K_1\ K_2\ \frac{rad/sec}{ft/sec^2}$
S_{LL}	Level loop component sensitivity product = $S_{au}\ S_{GD}\ K_1 \frac{rad/sec}{ft/sec^2}$

Table G-1. Glossary of symbols. (Cont.)

$\left[\frac{V_N}{R}\right]_{sg}$	Latitude rate compensation signal (volts)
$\left[\frac{V_E}{R}\right]_{sg}$	Longitude rate, horizontal component, compensation signal (volts)
$\left[\frac{V_E \tan L'}{R}\right]_{sg}$	Longitude rate, vertical component, compensation signal (volts)
x, y, z	Geographic coordinates (no units)
x_i, y_i, z_i	Platform coordinates (no units)
ω_{E_x}, ω_{E_y}, ω_{E_z}	Angular velocity components in geographic coordinates with respect to earth (rad/sec)
ω_{I_x}, ω_{I_y}, ω_{I_z}	Angular velocity components in geographic coordinates with respect to inertial space (rad/sec)
$\omega_{I_{x_i}}$, $\omega_{I_{y_i}}$, $\omega_{I_{z_i}}$	Angular velocity components in platform coordinates with respect to inertial space (rad/sec)
$[\omega_{I_{x_i}}]_{sg}$, $[\omega_{I_{y_i}}]_{sg}$, $[\omega_{I_{z_i}}]_{sg}$	Angular velocity command signals to platform drive system (volts)
ω_{IE}	Angular velocity of the earth (rad/sec)
$[\omega_{IE} \cos L']_{sg}$, $[\omega_{IE} \sin L']_{sg}$	Earth rate compensation signals (volt)

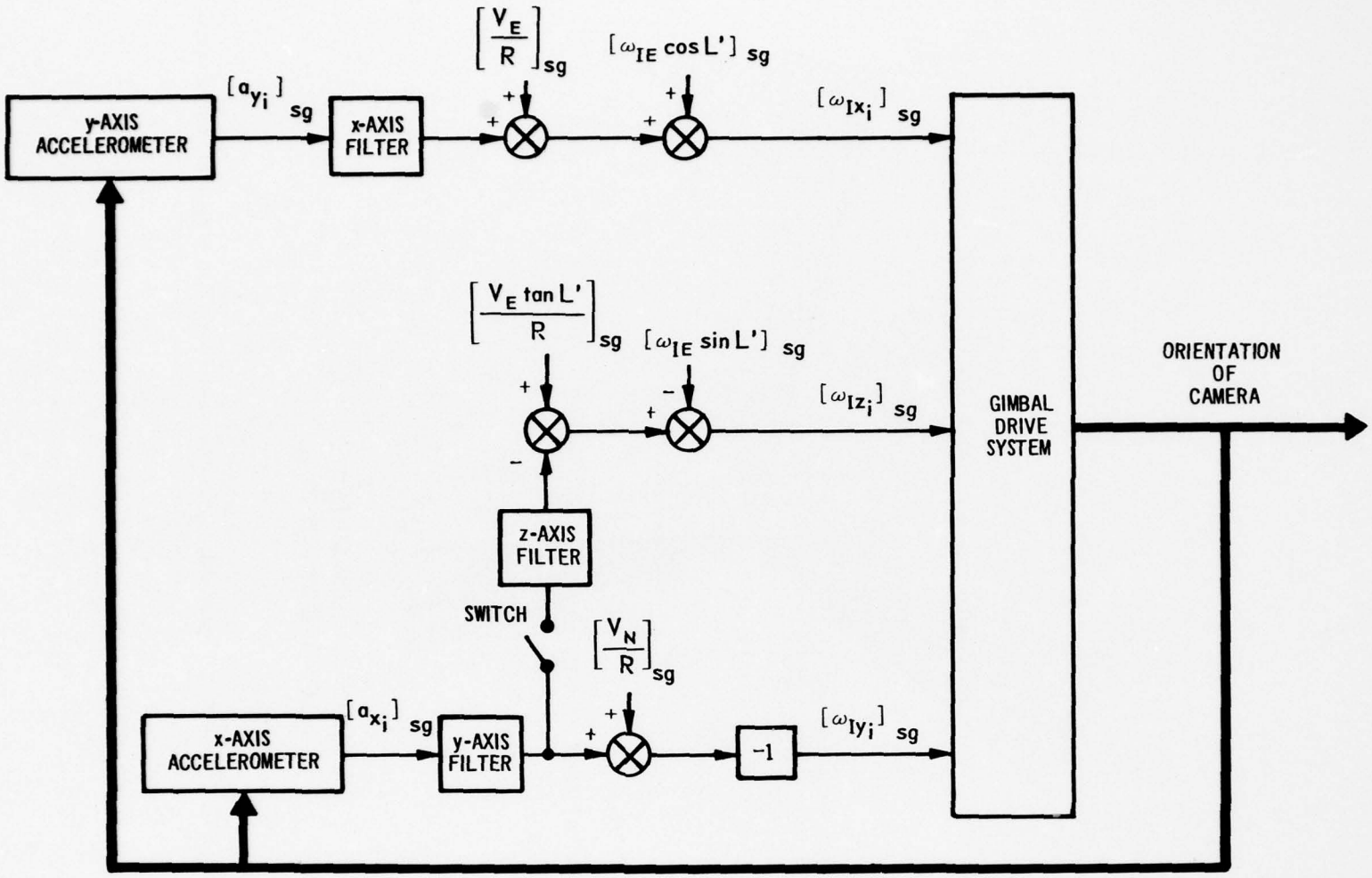


Fig. G-1. Functional diagram for an acceleration- coupled gyrocompassing system.

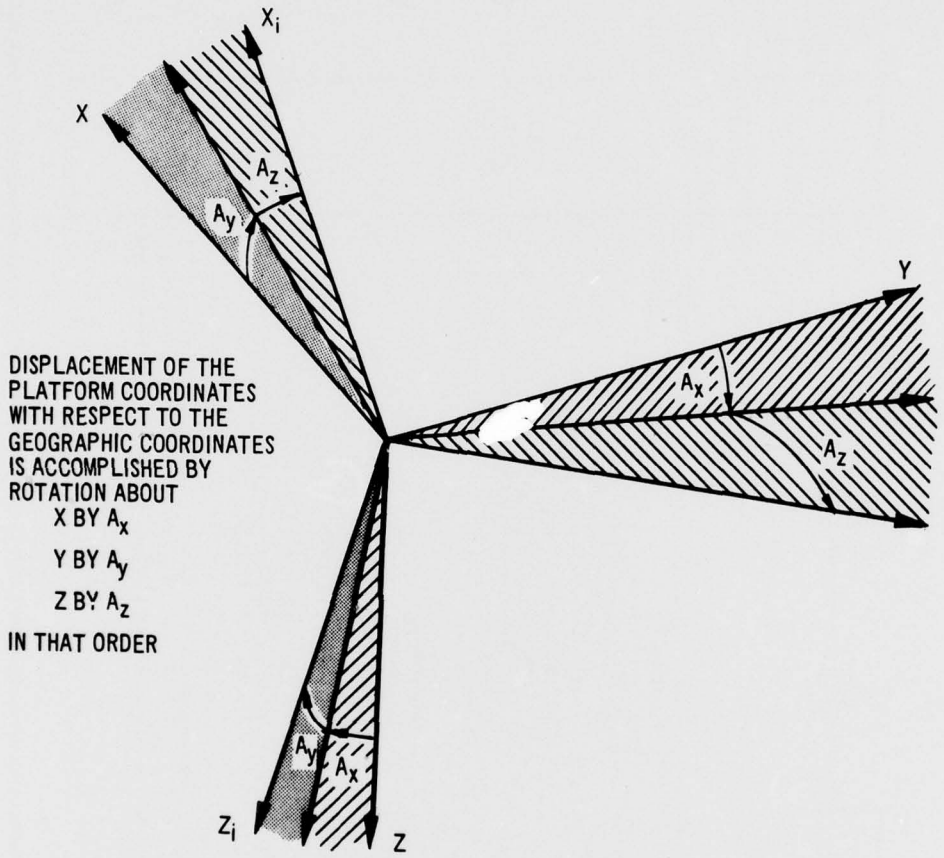


Fig. G-2. Orientation of platform coordinates with respect to geographic coordinates.

port or starboard depending on the satellite ephemeris. The gimbals will be unpinned;* the stabilization servos will be turned on, and gyrocompassing will begin.

Given these misalignment angles as initial conditions, the platform coordinates would eventually settle into geographic coordinates if no component inaccuracies were present, and all external data introduced into the system were perfect. Component inaccuracies such as gyro drift and accelerometer bias can be assumed constant during the short alignment time. In the absence of quantitative data, the inaccuracy in each externally-derived signal shown in Fig. G-1 will be assumed constant. The nature of these signals is, of course, a function of the base motion environment. A few comments on this subject follow.

A gyrocompassing system is sensitive to the translational motion of its supporting base. One method of specifying this motion is in terms of the power spectral density of attendant acceleration components. In the case of a ship, this spectrum would depend on roll, pitch, and yaw rotations as well as on wander in ship's heading. It is reasonable to assume that the spectrum is split into two parts: one contains energy at roll and pitch frequencies, while the other characterizes the wander in heading which is of much lower frequency and more broadband than the rather sharply defined roll and pitch motion.

An alignment time of 20 minutes will be assumed. It is desirable, of course, to gyrocompass in as short a time as possible. It tunrs out that 20 minutes is a good comprimise for the problem of minimizing both gyrocompassing time and forced dynamic errors. This subject is pursued in the following sections. First alignment on a stationary base is studied. Then ships motion is admitted in three steps.

---

*As stated in Section 3 of Chapter II the system will have been turned on and placed in the ready mode prior to this action.

3. Gyrocompassing on a Stationary Base

In Derivation Summary 1 the equations of motion of the system shown in Fig. G-1 are derived for a stationary base. The transient behavior and steady-state values of the dependent variables A_x, A_y, and A_z are of interest. The former will be considered first.

The error angles as functions of time can be determined from Eqs. (D. S. 1. 7). It turns out that A_y and A_z are almost independent of A_x (except at high latitude) and a simplified model can be introduced for design purposes. The data presented in this paper, however, are based on analogue computer studies with a three-axis model. A functional diagram of this system is given in Fig. G-3. The dynamics of the y and z axis filters are neglected as irrelevant to the following design synthesis. In D. S. -2 the equation for $A_z(t)$ using this model is derived, and it is shown that

$$A_z(t) = \left[\frac{g S_{LL}}{2} A_z(0) - g S_{GL} A_y(0) \right] t \, e \exp -\frac{t}{\tau} + A_z(0) \, e \exp -\frac{t}{\tau}$$

if the roots of the second-order characteristic equation are equal and

$$A_z(t) = \frac{\tau_1 \tau_2}{\tau_1 - \tau_2} \left\{ \left[g S_{LL} A_z(0) - g S_{GL} A_y(0) - \frac{A_z(0)}{\tau_1} \right] e \exp -\frac{t}{\tau_1} \right.$$

$$\left. - \left[g S_{LL} A_z(0) - g S_{GL} A_y(0) + \frac{A_z(0)}{\tau_2} \right] e \exp -\frac{t}{\tau_2} \right\}$$

if the roots are greatly separated. In order to minimize solution time, it follows that, for any given set of initial conditions on the angles, certain values for leveling loop gain, S_{LL}, and gyrocompassing loop gain, S_{GL}, can be chosen. Since $A_y(0)$ and $A_z(0)$ are random, however, the choice is not obvious.

Three questions arise from a consideration of the preceding equations:

(1) How are S_{LL} and S_{GL} selected to minimize solution time?

DERIVATION SUMMARY 1

DERIVATION OF SYSTEM EQUATIONS

The errors in vertical and north indication are expressed in terms of the angles shown in Fig. G-2. Differential equations in operational form involving these angles as dependent variables are obtained from an inspection of Fig. G-2.

The angular velocity commands to the gimbal drive system are

$$[\omega_{Ix_i}]_{sg} = \left\{ [a_{y_i}]_{sg} - [a_{y_c}]_{sg} \right\} K_1 G_1(p) + \left[\frac{V_E}{R} \right]_{sg} + [\omega_{IE} \cos L]_{sg}$$

$$-[\omega_{Iy_i}]_{sg} = \left\{ [a_{x_i}]_{sg} - [a_{x_c}]_{sg} \right\} K_1 G_1(p) + \left[\frac{V_N}{R} \right]_{sg} \qquad \text{(D.S.1-1)}$$

$$[\omega_{Iz_i}]_{sg} = - \left\{ [a_{x_i}]_{sg} - [a_{x_c}]_{sg} \right\} K_1 G_1(p) K_2 G_2(p) - \left[\frac{V_E \tan L'}{R} \right]_{sg}$$

$$- [\omega_{IE} \sin L']_{sg}$$

Since,

$$\omega_{Ix_i} = S_{GD} \; [\omega_{Ix_i}]_{sg}$$

$$\omega_{Iy_i} = S_{GD} \; [\omega_{Iy_i}]_{sg} \qquad \text{(D.S.1-2)}$$

$$\omega_{Iz_i} = S_{GD} \; [\omega_{Iz_i}]_{sg}$$

relating the angular velocity in indicated coordinates to the angular velocity in geographic coordinates through error angle rates will provide a relationship between the error angles and the sensed acceleration components.

Referring to Fig. G-2, the following equations may be written assuming small angle approximations:

$$\omega_{Ix_i} = \omega_{Ix} - \omega_{Iz} A_{y,} + \omega_{Iy} A_z + \dot{A}_x \qquad \text{(D.S.1-3)}$$

$$\omega_{Iy_i} = \omega_{Iy} - \omega_{Iz} A_x - \omega_{Iy} A_z + \dot{A}_x$$
$$\omega_{Iz_i} = \omega_{Iz} - \omega_{Iy} A_x + \omega_{Ix} A_y + \dot{A}_z \qquad \text{(D.S.1-3) cont.}$$

Acceleration components in indicated coordinates are related to components in geographic coordinates as follows:

$$a_{x_i} = a_x - a_z A_y + a_y A_z$$
$$a_{y_i} = a_y + a_z A_x - a_x A_z \qquad \text{(D.S.1-4)}$$
$$a_{z_i} = a_z - a_y A_x + a_x A_y$$

If the ship is stationary:

$$\omega_{Ix} = \omega_{IE} \cos L$$
$$\omega_{Iy} = 0 \qquad \text{(D.S.1-5)}$$
$$\omega_{Iz} = -\omega_{IE} \sin L$$

and, from Equations (D.S.1-4)

$$[a_{x_i}]_{sg} = S_{au} (a_{x_i} - G_{x_i}) = S_{au} g A_y$$
$$[a_{y_i}]_{sg} = S_{au} (a_{y_i} - G_{y_i}) = -S_{au} g A_x \qquad \text{(D.S.1-6)}$$

Combining Equations (D.S.1-1), (D.S.1-2), (D.S.1-3), (D.S.1-5) and (D.S.1-6) yields

$$(p + S_{au} g K_1 G_1 (p) S_{GD}) A_x + (\omega_{IE} \sin L) A_y$$
$$= [\omega_{IE} \cos L']_{sg} S_{GD} - \omega_{IE} \cos L$$
$$-(\omega_{IE} \sin L) A_x + (p + S_{au} g K_1 G_1 (p) S_{GD}) A_y \qquad \text{(D.S.1-7)}$$
$$- (\omega_{IE} \cos L) A_z = 0$$
$$(\omega_{IE} \cos L) A_y + S_{au} g K_1 G_1 (p) K_2 G_2 (p) S_{GD} A_y + p A_z$$
$$= \omega_{IE} \sin L - [\omega_{IE} \sin L']_{sg} S_{GD}$$

since,

$$\left[\frac{V_E}{R}\right]_{sg} = \left[\frac{V_N}{R}\right]_{sg} = \left[\frac{V_E \tan L'}{R}\right]_{sg} = 0$$

and all acceleration compensation terms are zero.

If the ship is moving the equations of motion are:

$$p A_x + (\omega_{IE} \sin L) A_y - \frac{V_N}{R} A_z + \frac{V_E \tan L}{R} A_y$$
$$= \left([a_{y_i}]_{sg} - [a_{y_c}]_{sg}\right) K_1 G_1(p) S_{GD} + S_{GD} [\omega_{IE} \cos L']_{sg}$$
$$- \omega_{IE} \cos L + \left[\frac{V_E}{R}\right]_{sg} S_{GD} - \frac{V_E}{R}$$

$$- (\omega_{IE} \sin L) A_x + pA_y - \frac{V_E \tan L}{R} A_x - (\omega_{IE} \cos L) A_z - \frac{V_E}{R} A_z$$
$$= \left(- [a_{x_i}]_{sg} + [a_{x_c}]_{sg}\right) K_1 G_1(p) S_{GD} + \frac{V_N}{R} - \left[\frac{V_N}{R}\right]_{sg} S_{GD} \qquad \text{(D.S.1-8)}$$

$$\frac{V_N}{R} A_x + (\omega_{IE} \cos L) A_y + \frac{V_E}{R} A_y + p A_z$$
$$= \left(- [a_{x_i}]_{sg} + [a_{y_c}]_{sg}\right) K_1 G_1(p) K_2 G_2(p) S_{GD}$$
$$+ \omega_{IE} \sin L - [\omega_{IE} \sin L'] S_{GD}$$
$$- \left[\frac{V_E \tan L'}{R}\right]_{sg} S_{GD} + \frac{V_E \tan L}{R}$$

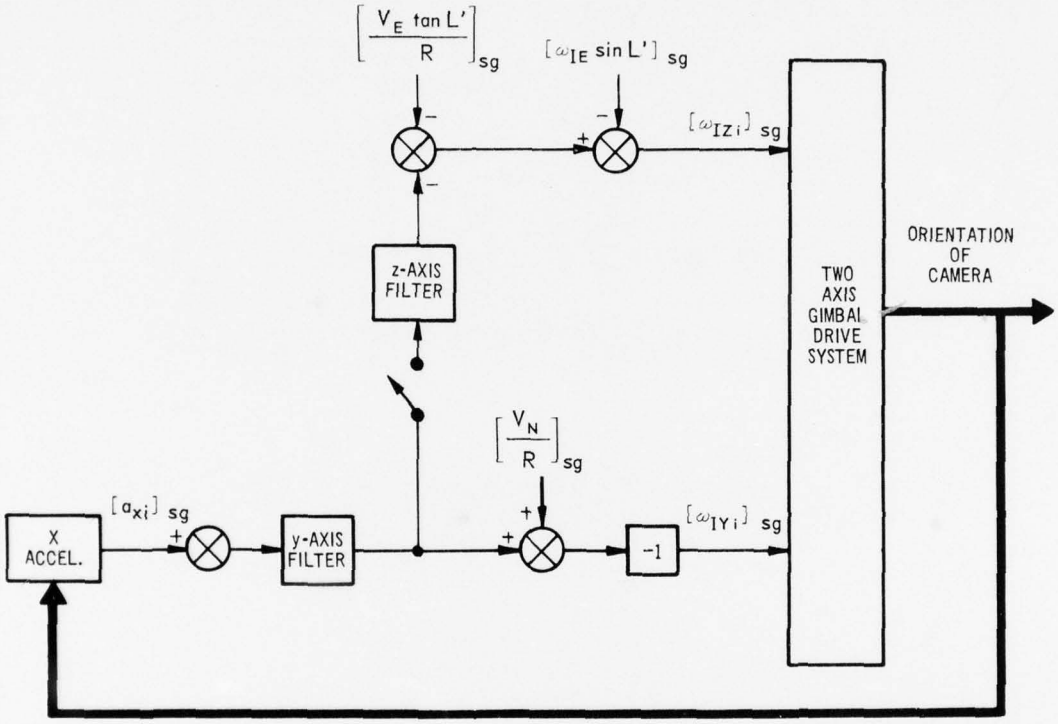


Fig. G-3. Functional diagram of a simplified model of an acceleration coupled gyrocompassing system.

DERIVATION SUMMARY 2

DERIVATION OF THE TRANSIENT BEHAVIOR OF THE SIMPLIFIED MODEL

Referring to Fig. G-3 and D.S.1, the following equations may be written:

$$\omega_{Iy_i} = \omega_{Iy} - \omega_{Ix} A_z + \dot{A}_y$$

$$\omega_{Iz_i} = \omega_{Iz} + \omega_{Ix} A_y + \dot{A}_z$$

$$g A_y S_{LL} = -\omega_{Iy_i}$$

$$g A_y S_{GL} + [\omega_{IE} \sin L']_{sg} S_{GD} = -\omega_{Iz_i}$$

where zero component errors and perfect earth rate compensation are assumed. Also, the dynamic characteristics of the x and y axis filters are neglected. The bandwidth of these filters, discussed in the text, is large compared with that of the level and gyrocompassing loops.

Taking the Laplace transform of Eqs. (D.S.2-1)

$$\begin{vmatrix} g S_{LL} + S & -\omega_{IE} \cos L \\ g S_{GL} + \omega_{IE} \cos L & S \end{vmatrix} \begin{vmatrix} A_y \\ A_z \end{vmatrix} = \begin{vmatrix} A_y(0) \\ A_z(0) \end{vmatrix}$$

The characteristic equation is

$$\Delta = S^2 + g S_{LL} S + g S_{GL} \omega_{IE} \cos L$$

where it is assumed that

$$g S_{GL} \omega_{IE} \cos L >> \omega_{IE}^2 \cos^2 L$$

the roots are

$$-r_1 = -\frac{g S_{LL}}{2} + \frac{1}{2} \sqrt{g^2 S_{LL}^2 - 4 g S_{GL} \omega_{IE} \cos L}$$

and

$$-r_2 = -\frac{g S_{LL}}{2} - \frac{1}{2}\sqrt{g^2 S_{LL}^2 - 4g S_{GL}\,\omega_{IE}\cos L}$$

Two cases will be considered. If the roots are equal

$$r_1 = r_2 = \frac{g S_{LL}}{2}$$

Defining

$$\tau = \frac{1}{r}$$

we have

$$A_z(t) = \left[\frac{g S_{LL}}{2} A_z(0) - g S_{GL} A_y(0)\right] t\,\epsilon \exp\frac{-t}{\tau} + A_z(0)\,\epsilon \exp\frac{-t}{\tau} \quad \text{(D.S.2-2)}$$

If the roots are greatly separated,

$$-r_1 = -\frac{S_{GL}}{S_{LL}}\,\omega_{IE}\cos L = -K_2\,\omega_{IE}\cos L$$

$$-r_2 = -g S_{LL} + K_2\,\omega_{IE}\cos L$$

Defining

$$\tau_1 = \frac{1}{r_1}$$

and

$$\tau_2 = \frac{1}{r_2}$$

we have

$$A_z(t) = \frac{\tau_1\,\tau_2}{\tau_1 - \tau_2}\left\{\left[g S_{LL} A_z(0) - g S_{GL} A_y(0) - \frac{A_z(0)}{\tau_1}\right]\epsilon \exp\frac{-t}{\tau_1}\right.$$

$$\left. - \left[g S_{LL} A_z(0) - g S_{GL} A_y(0) - \frac{A_z(0)}{\tau_2}\right]\epsilon \exp\frac{-t}{\tau_2}\right\} \quad \text{(D.S.2-3)}$$

(2) Is it possible to choose values of S_{LL} and S_{GL} that yield a solution time invariant to different initial conditions on the platform error angles?

(3) Should the random nature of $A_y(0)$ be eliminated by throwing the switch in Fig. G-1 only after the platform has become level to within a certain tolerance?

The problem of parameter selection is simplified if a value of SS_{LL} can be chosen and held constant while S_{GL} varies. It turns out that S_{LL} can be chosen in order to achieve a compromise between desired dynamic response characteristics and solution time. At this point a value of 3.5×10^{-4} rad/sec/ft/sec^2 will be chosen with admitted foreknowledge. Later, the reason for this choice will be apparent.

By way of preliminary design, Table G-2 shows the variation of gyrocompassing time, between + and − values of initial azimuth error, with $A_y(0)$ at the start of gyrocompassing. Leveling time is the time required for A_y to decrease from +2° to the particular value of $A_y(0)$. The values of loop gain ratio shown were selected to give minimum gyrocompassing time for positive values $A_z(0)$. Gyrocompassing time is the time required for A_z to decrease to and stay within 0.1°. Equation (D. S. 2-3) can be used to predict these results. At low values of loop gain ratio, the system is highly damped and the roots are greatly separated. For a given set of initial error angles the coefficient of the dominant exponential mode has been made small by the particular choice of loop gain ratio. If, however, $A_z(0)$ changes sign, this coefficient is no longer small and the change in gyrocompassing time is pronounced. At the large values of loop gain ratio, the system approaches critical damping. With the given value of S_{LL}, critical damping occurs at a loop gain ratio of 55. In this case, Eq. (D. S. 2-2) applies and it may be seen that the gyrocompassing time is less affected by a change in sign of $A_z(0)$.

Figure G-4 shows the variation of gyrocompassing time with $A_z(0)$ with a given S_{GL} − one which is chosen to minimize gyrocompassing time for $A_z(0) = +4°$. Similar curves would apply for any row in Table G-2.

Table G-2. Variation of leveling and gyrocompassing time with sign reversal of initial azimuth error.

$A_y(0)$	$\frac{S_{GL}}{S_{LL}}$	$A_z(0) = +4°$		$A_z(0) = -4°$	
		LEVELING TIME (SEC)	GYROCOMPASSING TIME (SEC)	LEVELING TIME (SEC)	GYROCOMPASSING TIME (SEC)
1.5°	2.298	55	225	55	*
1.0°	3.207	85	210	85	*
0.5°	6.075	125	210	125	*
0.2°	14.625	180	210	170	5800
0.1°	28.23	215	250	200	2300
0.05°	50.1	265	340	225	1300

Notes:

1) Values of $A_y(0)$ shown are for gyrocompassing
2) $A_y(0)$ and $A_x(0)$ for leveling are constant at $+2°$
3) *Values are too large to be accurately determined on the analogue computer with particular scaling used.
4) Latitude is 45°

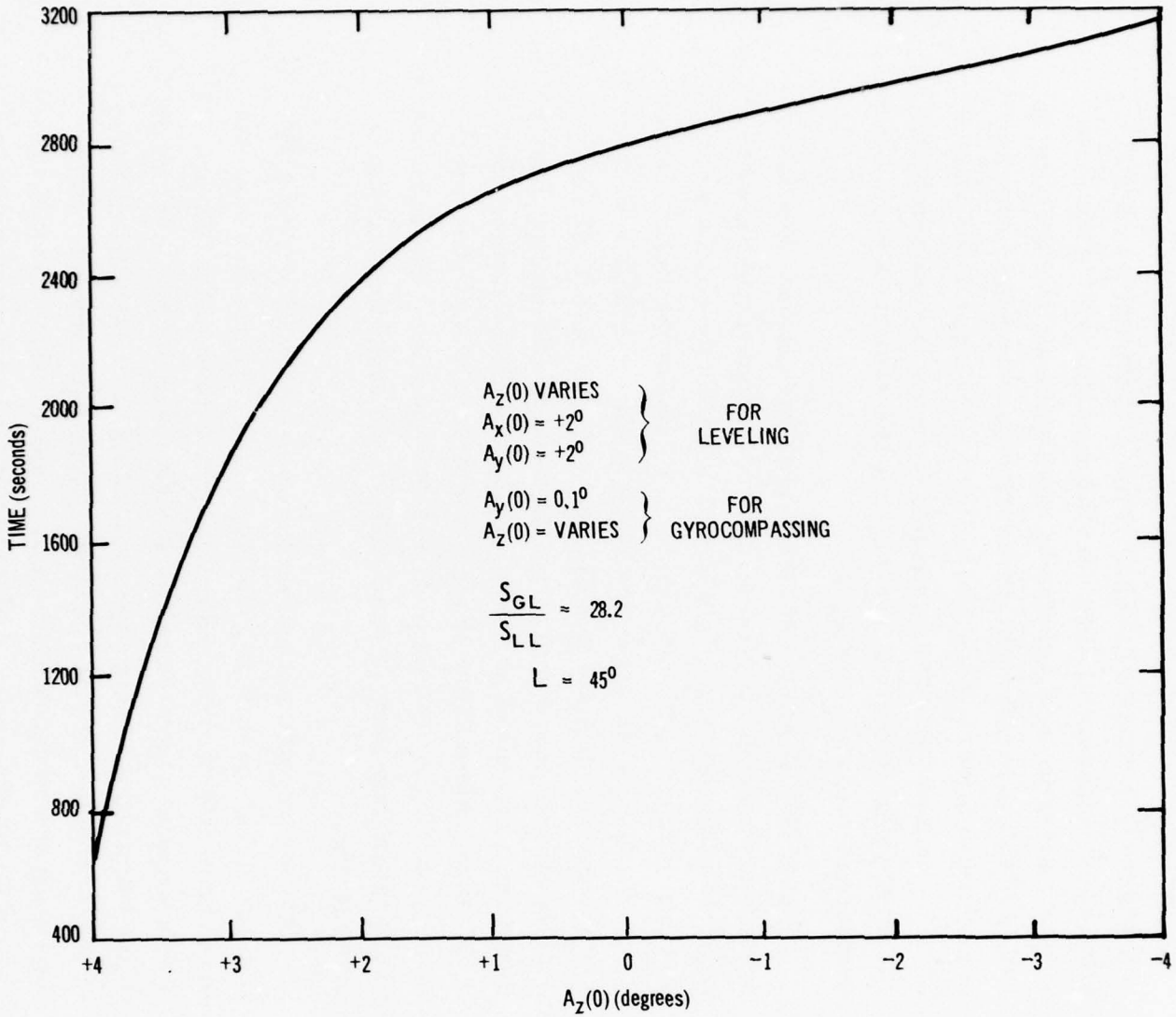


Fig. G-4. Variation of gyrocompassing time with initial azimuth error.

The preceding results suggest a more detailed study of the variation of solution time with loop gain ratio for different values of $A_z(0)$. For the moment the value of $A_y(0)$ at the start of gyrocompassing is chosen to be 0.1°. The consequence of this choice will be examined later.

Figure G-5 shows a loop gain ratio of 70 minimizes the variation of gyrocompassing time with the sign of $A_z(0)$. This value is near that for critical damping as was expected. For decreasing values of loop gain ratio, the solution time is unbounded (in the 2-axis model) because the coupling between the y-axis loop and the azimuth drive is diminishing. For increasing values of loop gain ratio, the gyrocompassing time is again unbounded because the damping ratio approached zero (S_{LL} is fixed).

Figure G-6 shows the variation of alignment time with initial conditions on all platform error angles. Alignment time is the time required to go to and stay within 0.1° in azimuth from the start of leveling. For the solid curves $A_x(0)$ is 2°, and for the dashed curves it is −2°. If $A_y(0)$ is large, no change in aligment time occurs if $A_x(0)$ is minus. If $A_y(0)$ is small, the two-axis model does not apply because of the coupling from the x-axis. The changes in alignment time in this case are shown. Also, if $A_y(0)$ is greater than 0.05°, the alignment time is almost invariant to $A_z(0)$ because the term containing $A_y(0)$ in Eq. (D.S.2-2) dominates. The increase in alignment time as $A_y(0)$ approaches 2° is due to the increase in leveling time.

It is now possible to consider the consequence of setting $A_y(0)$ equal to 0.1° at the start of gyrocompassing. Figure G-6 suggests the alignment time can be reduced if $A_y(0)$ is made small. Figure G-7 shows a typical case. The shape of this curve for small values of $A_y(0)$ would depend on the magnitude and sign of the initial conditions of the other error angles because of interaxial coupling. Nevertheless, it seems desirable to choose a small value for $A_y(0)$ at the start of gyrocompassing. Unfortunately, it is not practical to assume that $A_y(0)$ can be arbitrarily small because of component errors, forced dynamic errors on a moving base (discussed in the

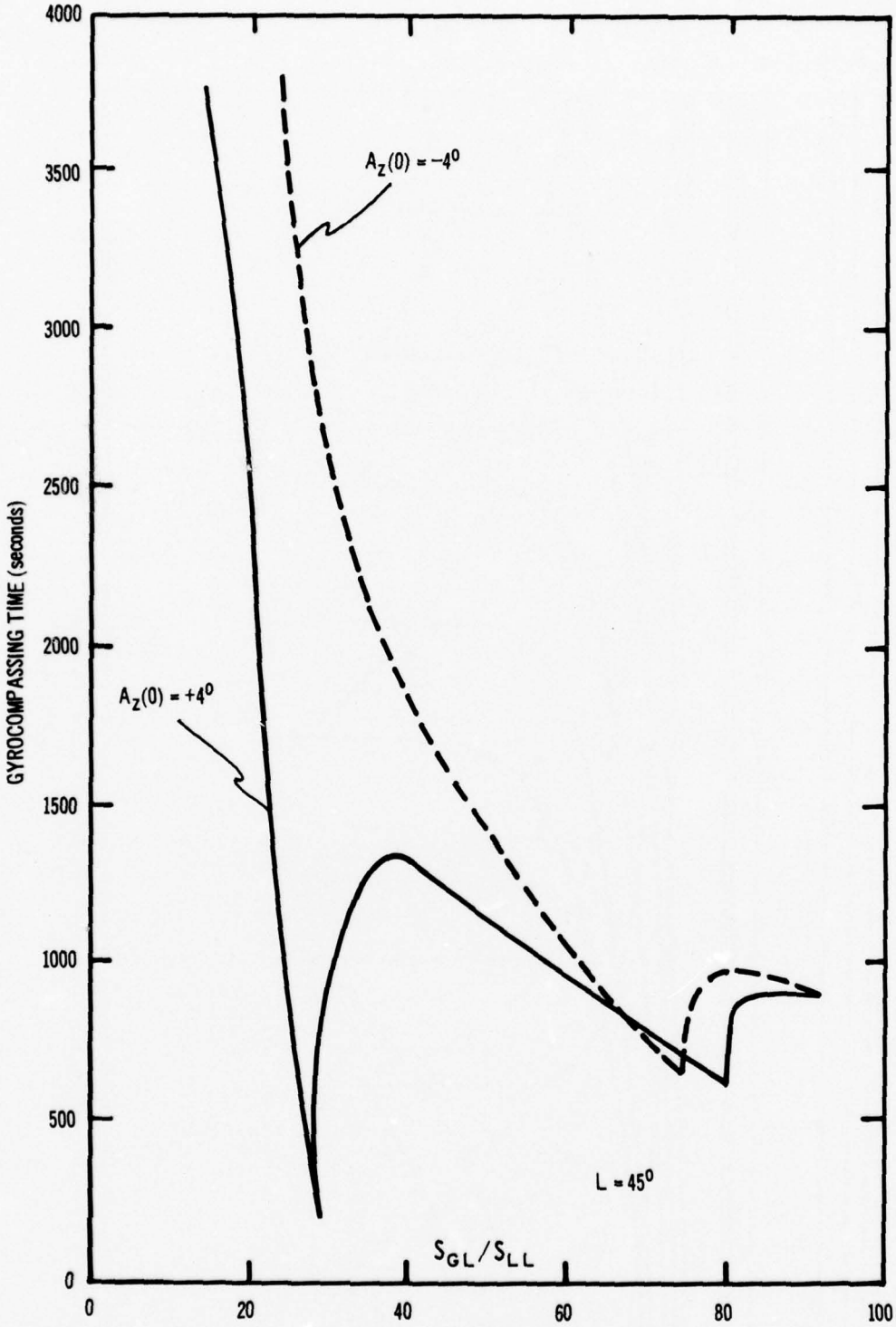


Fig. G-5. Variation in gyrocompassing time between + and − values of $A_z(0)$ with loop gain ratio.

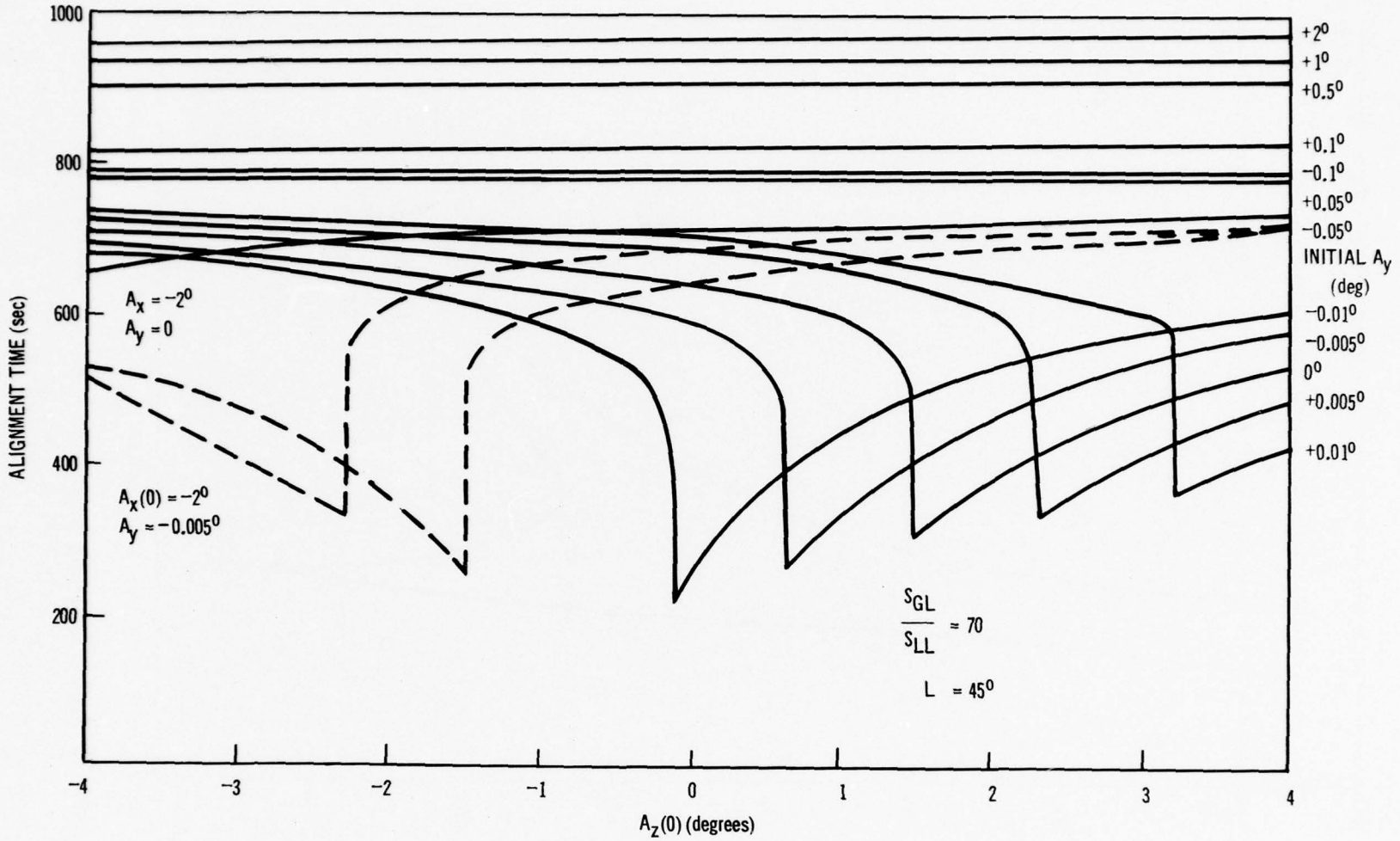


Fig. G-6. Variation in alignment time with initial conditions on platform error angles.

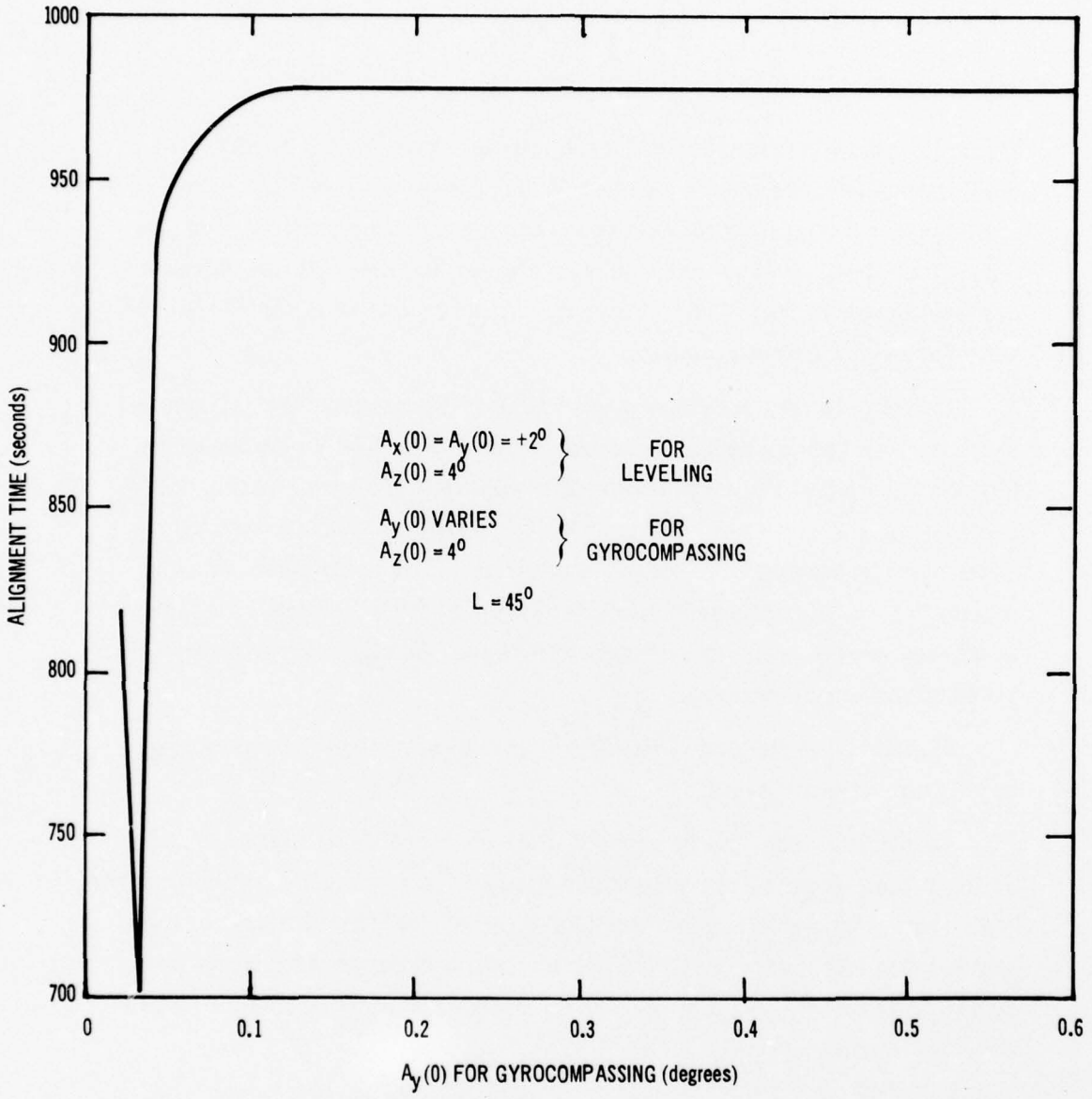


Fig. G-7. Variation of alignment time with $A_y(0)$ for gyrocompassing.

next section), and $A_z(0)$. From Eq. (D.S.1-7) it may be seen that the steady-state value of A_y with the platform in a level mode is

$$\frac{\omega_{IE} \cos L}{S_{LL}\, g} A_z(0)$$

With the given numbers the steady-state value of A_y might not be less than 1 minute of arc on a stationary base. In the presence of base motion a considerably larger forced error is possible, depending, of course, on the parameters chosen for the system (this is discussed in the following section). It turns out that the choice of 0.1° for $A_y(0)$ is reasonable.

The choice of a large loop gain ratio (70) creates large angular velocity commands to the azimuth drive. For the worst case in Fig. G-6, an azimuth command for approximately 50 earth rates is developed. It is not uncommon for "inertial quality" gyros to have limited torque generator capability. Consequently, it is of interest to determine how the preceding results change if a limit is placed on the azimuth drive command. Arbitrarily a value of 10 earth rates is chosen.

Figure G-8 shows the results in this case. No adverse changes in alignment time occur.

Admitting component errors such as gyro drift and accelerometer bias does affect alignment time. As a result of choosing the high loop gain ratio a gyro drift of + or −0.33°/hr and an accelerometer bias of + or -1×10^{-3} "g's" do not change alignment time by more than 5%. At low values of loop gain ratio this invariance does not occur.

Finally, the subject of steady-state error angles is to be discussed. During the gyrocompassing action the platform will approach some equillibrium orientation relative to geographic coordinates. In the absence of component errors and with correct earth

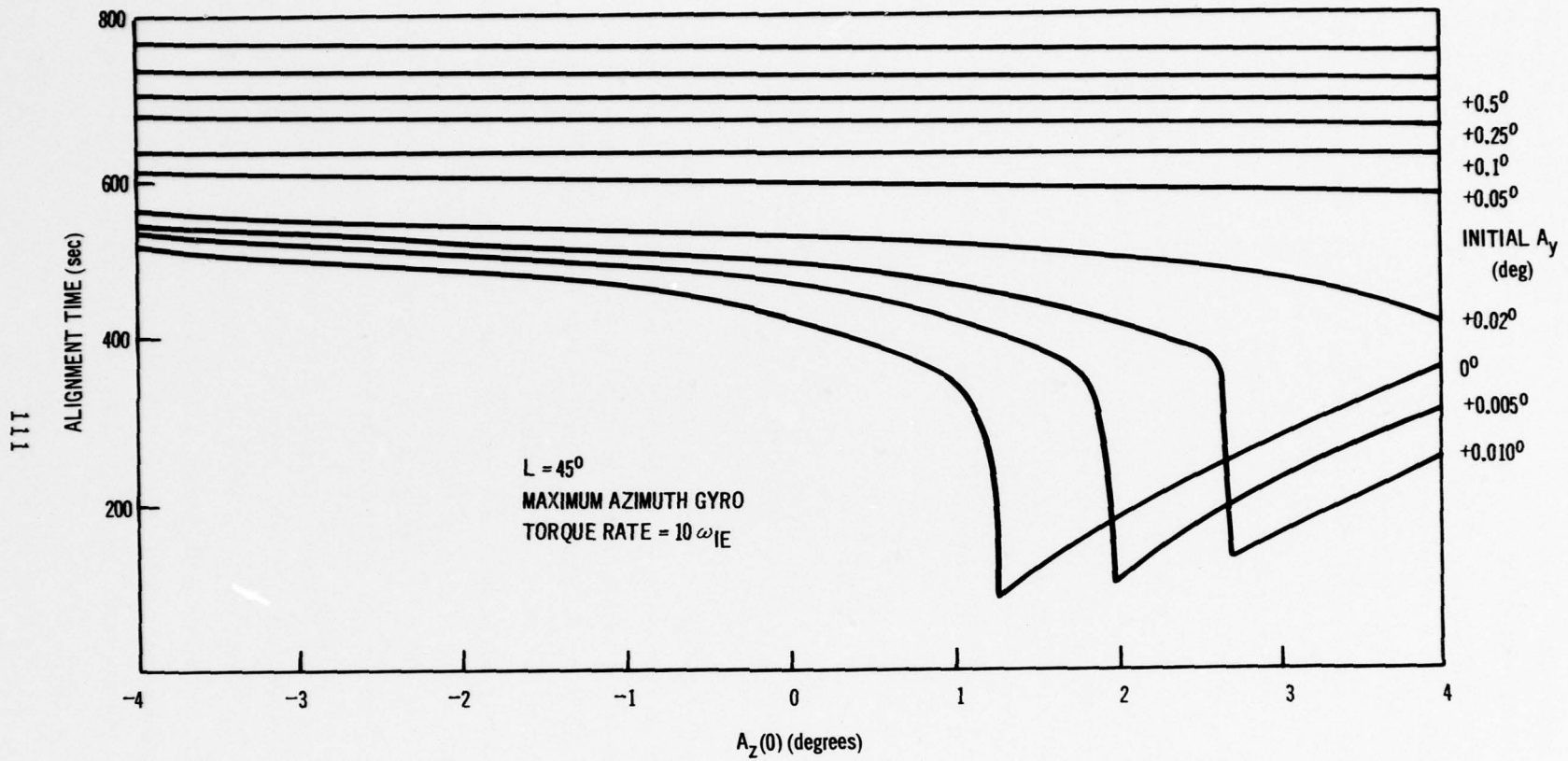


Fig. G-8. Variation in alignment time with initial conditions with rate limiting for the azimuth gyro.

rate compensation, Eqs. (D. S. 1-1) and (D. S. 1-3) show that the platform coordinates will be aligned with respect to geographic coordinates in steady-state. If such errors are present, the final values of the resulting error angles can be determined by assuming the time derivatives of the dependent variables are zero. The result is derived in D. S. 3 and presented in Table G-3. The values shown are based on a loop gain ratio of 70. The error angles' tolerances assumed in the preceding section are seen to be compatible with a gyro drift of 10 meru that was assumed in the preceding section.

In summary, a gyrocompassing system which will become aligned to geographic coordinates in less than twenty minutes has been synthesized. The ratio of gyrocompassing loop gain to level loop gain determines the sensitivity of alignment time to random initial conditions on the platform error angles. With a given S_{LL} a loop gain ratio can be chosen to minimize this sensitivity, and the result is a nearly critically damped system. From Eq. (D. S. 2-2) it would appear possible to suppress the upper boundary of alignment time in Fig. G-7 by choosing a higher value of S_{LL} while maintaining a constant loop gain ratio. This subject is pursued in the following section.

4. Shipboard Alignment

When base motion is introduced alignment of a linear system can be regarded as a superposition of the results of the preceding section with forced dynamic errors. In a preceding section the base motion spectrum was assumed to be split between high and low frequency portions. Because of this, ship's motion will now be introduced into the problem in three steps. They are: (1) pitch and roll only, (2) pitch and roll which steaming at constant heading, and (3) pitch and roll while wandering in heading.

In D. S. 4 the performance functions relating azimuth and vertical errors to northerly acceleration are derived. Longitude acceleration is not admitted because the forced errors in azimuth are small compared with those due to latitude acceleration. Assuming typical values for the displacement of the platform from the ship's metacenter and for roll and pitch frequencies yields fore

DERIVATION SUMMARY 3

ALIGNMENT ERRORS ON A STATIONARY BASE

In the absence of component errors and with correct earth rate compensation, Equations D.S.1-7 show the platform coordinates will be aligned with geographic coordinates in steady-state. If these errors are assumed the platform coordinates will be misaligned with geographic coordinates in steady-state. In this case, the steady-state values of A_x, A_y and A_z can be obtained from Equations D.S.1-7 by assuming the time derivatives of the dependent variables are zero. The equations may then be written in matrix form as follows:

$$\begin{vmatrix} -\omega_{IE} \sin L & S_{au} g K_1 S_{GD} & -\omega_{IE} \cos L \\ S_{au} g K_1 S_{GD} & \omega_{IE} \sin L & 0 \\ 0 & S_{au} g K_1 K_2 S_{GD} + \omega_{IE} \cos L & 0 \end{vmatrix} \begin{vmatrix} A_x \\ A_y \\ A_z \end{vmatrix} = \begin{vmatrix} E_{gy} - S_{au} K_1 E_{ax} S_{GD} \\ E_{gx} + S_{au} K_1 E_{ay} S_{GD} \\ E_{gz} - S_{au} K_1 E_{ax} S_{GD} \end{vmatrix}$$

where the E_g's are gyro drifts and the E_a's are accelerometer biases.

The solutions of this equation for A_x, A_y and A_z as function of gyro drift and accelerometer bias are summarized in Table 2. Incorrect earth rate compensation is considered to be combined with gyro drift since, as may be seen from Equations D.S.1-1 and D.S.1-2, the two cannot be separated under the assumption stated in Section III. The values listed in this table were corroborated by REAC solutions.

An interpretation of Table 2 is summarized as follows:

x gyro drift

(1) the platform rotates in a + sense about the x axis to develop a signal to balance the gyro drift.

(2) the y gyro then senses $A_x \omega_{IE} \sin L$

(3) the platform then rotates about the z axis by

$$\frac{-A_x \omega_{IE} \sin L}{\omega_{IE} \cos L} = -\tan L \, A_x$$

to null the angular velocity about the y axis.

y gyro drift

The platform rotates about the vertical by

$$\frac{+E_{gy}}{\omega_{IE} \cos L}$$

to create an angular velocity about the y axis equal to the gyro drift.

z gyro drift

(1) the platform rotates in a + sense about the y axis to develop a signal to balance the gyro drift.

(2) the command to the y gyro is then $-S_{au}\, g K_1 A_y$ so the platform rotates about the vertical by

$$\frac{-S_{au}\, g K_1 S_{GD} A_y}{\omega_{IE} \cos L} = \frac{-S_{LL}\, g}{\omega_{IE} \cos L} A_y$$

to satisfy the commanded angular velocity about the y axis.

x accelerometer bias

(1) the platform rotates in a + sense about the y axis to null the accelerometer bias.

(2) the change in A_x and A_z is second order since the change in the ω_{IE} projection along x and z is of second order.

y accelerometer bias

(1) the platform rotates about the x axis in the positive sense to null the accelerometer output.

(2) then the y gyro senses $-A_x\, \omega_{IE} \sin L$

(3) the platform rotates about the vertical by

$$\frac{-A_x\, \omega_{IE} \sin L}{\omega_{IE} \cos L} = -\tan L\, A_x$$

to create zero angular velocity about the y axis.

Table G-3. Steady-state platform error angles (A_x, A_y, A_z,) as a function of gyro drift (E_{gx}, E_{gy}, E_{gz}) and accelerometer bias (E_{ax}, E_{ay})

	(E_{gx})	(E_{gy})	(E_{gz})	(E_{ax})	(E_{ay})
$\frac{\delta A_x}{\delta(\ )}$	$\frac{1}{S_{LL}\, g}$ $+2.46 \times 10^{-2}$ deg/deg/hr	0	$\frac{-\omega_{IE} \sin L}{S_{LL}\, g\, [S_{GL}\, g + \omega_{IE} \cos L]}$ $-1.6 \times 10^{-6} \times \frac{S_{LL}}{S_{GL}}$ deg/deg/hr	$\frac{\frac{S_{GL}}{S_{LL}}\, \omega_{IE} \sin L}{g\, [S_{GL}\, g + \omega_{IE} \cos L]}$ 4.55×10^{-3} rad/"g"	$\frac{1}{g}$ 1 rad/"g"
$\frac{\delta A_y}{\delta(\ )}$	0	0	$\frac{1}{S_{GL}\, g + \omega_{IE} \cos L}$ 3.52×10^{-4} deg/deg/hr	$\frac{-S_{GL}}{S_{GL}\, g + \omega_{IE} \cos L}$ -1 rad/"g"	0
$\frac{\delta A_z}{\delta(\ )}$	$\frac{-\tan L}{S_{LL}\, g}$ -2.46×10^{-2} deg/deg/hr	$\frac{-1}{\omega_{IE} \cos L}$ -5.4 deg/deg/hr	$\frac{[S^2_{LL}\, g^2 + \omega^2_{IE} \sin^2 L]}{S_{LL}\, g\, \omega_{IE} \cos L\, [S_{GL}\, g + \omega_{IE} \cos L]}$ 7.7×10^{-2} deg/deg/hr	$\frac{S_{LL}}{\omega_{IE} \cos L}$ $\frac{K_2\, [S^2_{LL}\, g^2 + \omega^2_{IE} \sin^2 L]}{g\, \omega_{IE} \cos L\, [S_{GL}\, g + \omega_{IE} \cos L]}$ ~ 0	$\frac{\tan L}{g}$ -rad/"g"

DERIVATION SUMMARY 4

DERIVATION OF PERFORMANCE FUNCTIONS RELATING PLATFORM ERROR ANGLES TO NORTHERLY ACCELERATIONS

The equations of motion are derived in D.S.1 and summarized in D.S.1-8. Using a two axis model and assuming perfect velocity and earth rate compensation, the equations are

$$\dot{A}_y - A_z \left(\omega_{IE} \cos L + \frac{V_E}{R}\right) = + a_{x_i} S_{LL} \qquad \text{(D.S.4-1)}$$

$$A_y \left(\omega_{IE} \cos L + \frac{V_E}{R}\right) + \dot{A}_z = + a_{x_i} S_{GL} \qquad \text{(D.S.4-2)}$$

where

a_{x_i} = northerly acceleration resolved into indicated (platform) coordinates

$$= \dot{V}_N + g A_y = R\ddot{L} - g A_y$$

and R is the earth radius. The assumption of perfect velocity compensation is not realistic but the change in the performance function (from the case of no compensation) occurs at such low frequency as to be irrelevant. Rewriting the above equations yields

$$\begin{vmatrix} p + S_{LL}\, g & -\omega_{IE} \cos L \\ g S_{GL} + \omega_{IE} \cos L & p \end{vmatrix} \begin{vmatrix} A_y \\ A_z \end{vmatrix} = \begin{vmatrix} + S_{LL}\, R p^2 L \\ + S_{GL}\, R p^2 L \end{vmatrix}$$

The performance function relating A_y to northerly acceleration is:

$$\frac{A_y}{a_{x_i}} = \frac{A_y}{R p^2 L} = \frac{+ S_{LL}\, p + S_{GL}\, \omega_{IE} \cos L}{p^2 + p S_{LL}\, g + S_{GL}\, g\, \omega_{IE} \cos L}$$

or in a form convenient for frequency analysis:

$$\frac{A_y}{a_{x_i}}(\omega) = \frac{+1}{g} \; \frac{\dfrac{S_{LL}}{S_{GL}\, \omega_{IE} \cos L} j\omega + 1}{\dfrac{j\omega^2}{S_{GL}\, g\, \omega_{IE} \cos L} + \dfrac{S_{LL}\, j\omega}{S_{GL}\, \omega_{IE} \cos L} + 1} \qquad \text{(D.S.4-3)}$$

The transfer function relating azimuth error, A_z, to northerly acceleration is

$$\frac{A_z}{a_{x_i}}(\omega) = \frac{-S_{LL}}{S_{GL}\, g} \; \frac{\dfrac{-S_{GL}}{S_{LL}\, \omega_{IE} \cos L}\, j\omega + 1}{\dfrac{\overline{j\omega}^2}{S_{GL}\, g\, \omega_{IE} \cos L} + \dfrac{S_{LL}\, j\omega}{S_{GL}\, \omega_{IE} \cos L} + 1} \qquad \text{(D.S.4-4)}$$

and aft and athwartship acceleration components of approximately 3 ft/sec^2. From Eqs. (D.S. 4-3) and (D.S. 4-4) it may be seen that level and azimuth error angles of 0.01° and 0.1° respectively will be exceeded. If filters are introduced in the level and gyrocompassing loops, the forced errors can be reduced to values well within these tolerances. The chosen performance functions are

$$\frac{K_1}{(13p + 1)^2}$$

for the y-axis filter and

$$\frac{K_2}{(7p + 1)^2}$$

for the z-axis filter.

Assume, now, the ship is steaming east at 25 knots* The angular velocity components of the platform differ from those on a stationary base only in that the longitude rate is added to earth rate. If accelerometer bias is considered to contain Coriolis acceleration compensation error, and gyro drift is considered to contain velocity compensation error, the results of Table G-3 apply because the longitude rate is small compared to earth rate. This means that the interaxial velocity terms in Eq. (D.S. 1-8) are almost the same as those in Eq. (D.S. 1-7). If the ship is steaming north at 25 knots, the results of Table G-3 could be expected, provided gyro drift contains velocity compensation error and accelerometer bias contains acceleration compensation error, since the interaxial angular velocity terms are not significantly different from those steaming east. The alignment time discussed in the previous section is not affected by this small vehicle velocity.

*This is probably a worst case in that the ship most likely will be steaming at less than 10 knots.

The frequency characteristics for that portion of the spectrum due to heading wander are more difficult to determine because of the lack of a suitable model. From admittedly brief experimental results (see Ref. 18) it is assumed that the ship will wander sinusoidally about an average heading at an amplitude of one degree.

Figure G-9 shows the level and azimuth response in this case, and it may be seen that the 0.01° tolerance in level is achieved. The 0.1° tolerance in azimuth is exceeded, however.

Equation (D.S. 4-4) shows that decreasing S_{GL} would reduce the magnitude of the forced errors in azimuth. Varying S_{LL} would have little effect since the product of the static sensitivity and time constant of the first-order factor is constant at a given latitude. If S_{GL} is halved, the peak error in A_z is reduced by about 65%. In order to maintain critical damping, however, S_{LL} would be reduced by 70% and the alignment time would increase by 40%. In this case the assumed maximum value of 20 minutes could be exceeded.

An alternate method of suppressing the forced error in azimuth is to deliberately increase the rate limiting in the azimuth drive. However, analogue computer studies show that the level of rate limiting required to reduce the peak azimuth error in Fig. G-9 to 0.1° decouples the azimuth drive from the northy accelerometer thereby increasing the alignment time well beyond 20 minutes. A more detailed study without specific data on base motion is not justifiable.

If external acceleration compensation data are available, the forced error in azimuth can be reduced. It is not likely that data of sufficient precision can be derived from a ship's velocity sensor.

As a final point, Eq. (D.S. 4-4) shows that the frequency response characteristics in azimuth are a function of latitude unless S_{GL} varies as the secant of latitude. Figure G-10 shows that this relationship is necessary in order to keep alignment reasonably invariant to latitude.

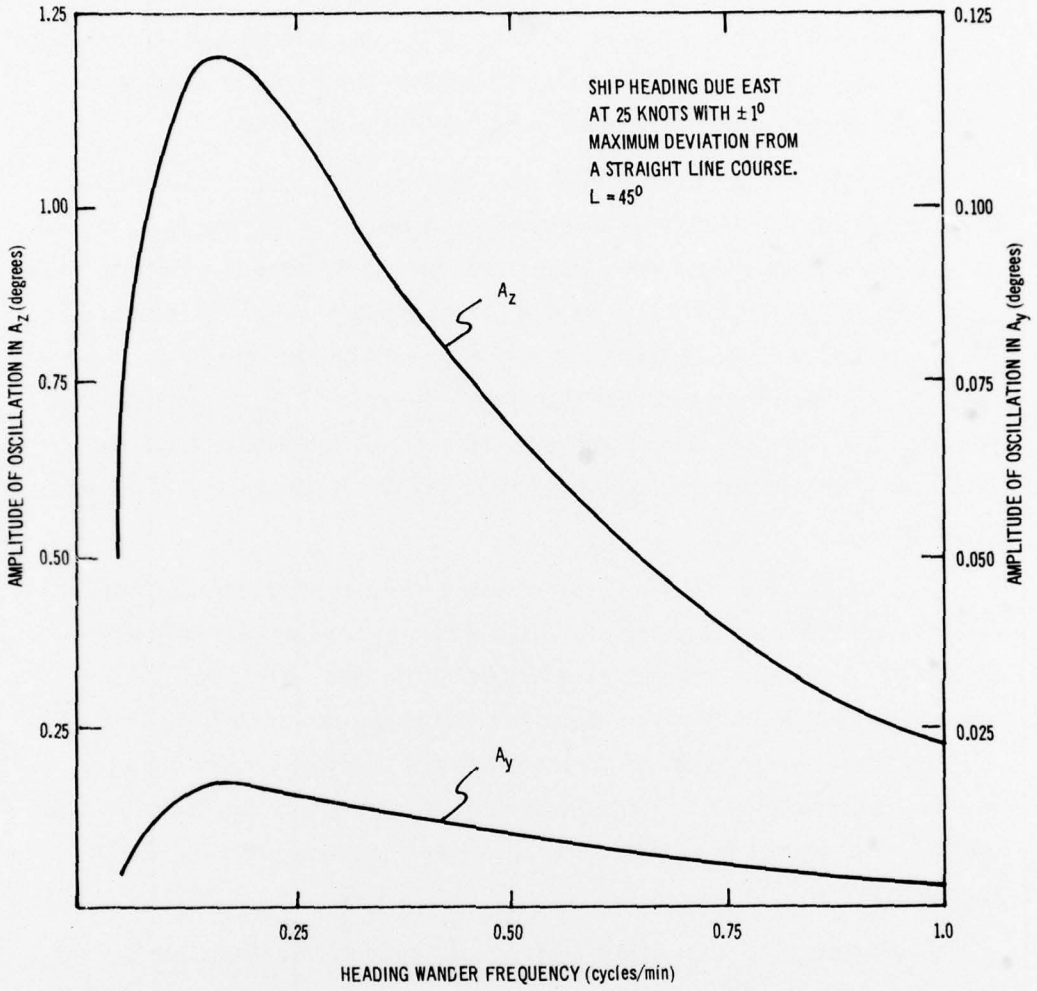


Fig. G-9. Variation of platform error angle magnitude with frequency of heading wander.

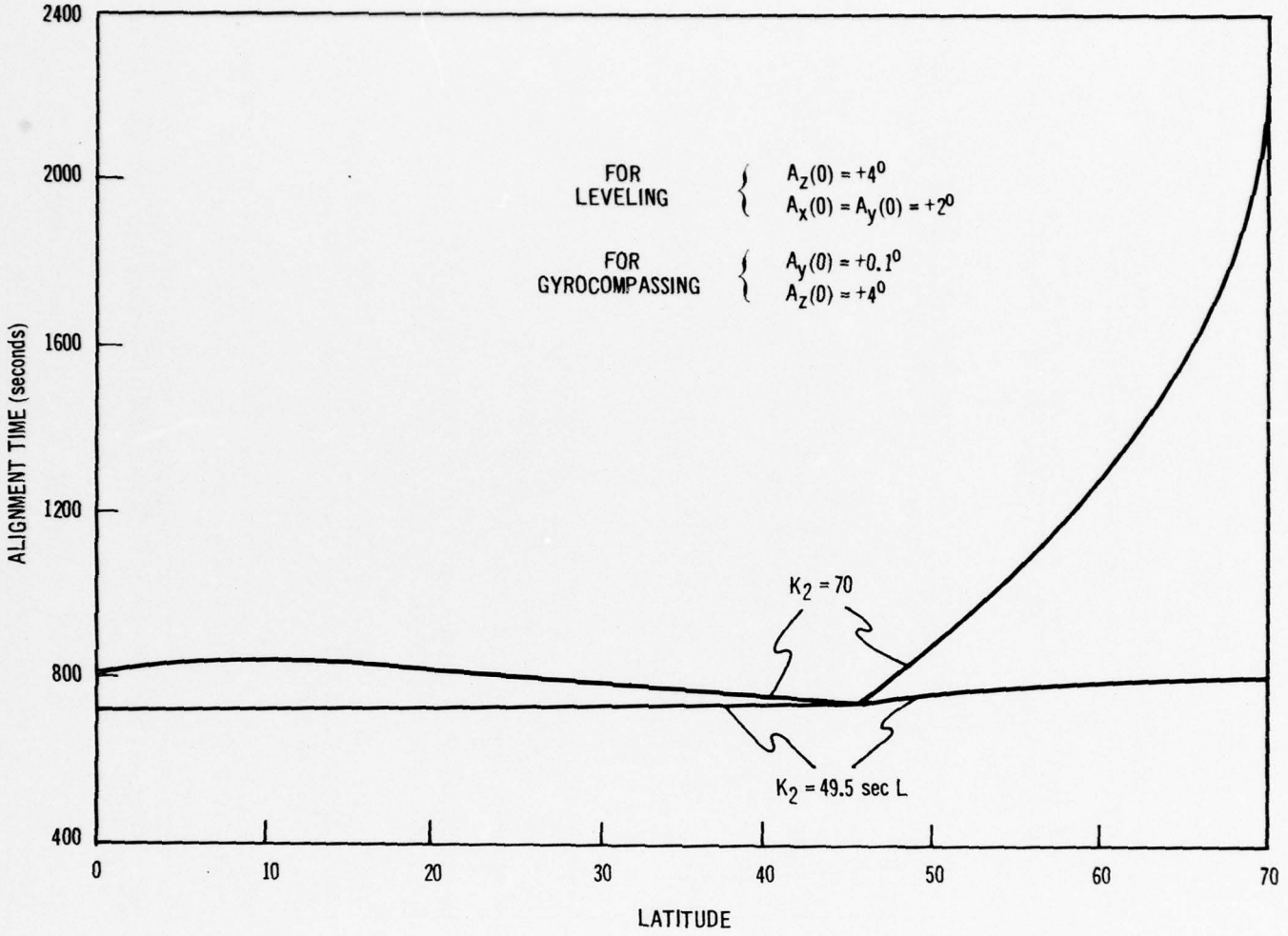


Fig. G-10. Variation of alignment time with latitude on a stationary base.

REFERENCES

1. SAO Ephemeris 6, Special Bulletin No. 72, Smithsonian Astrophysical Observatory, Cambridge, Massachusetts, April, 1963

2. U.S. Coast & Geodetic Survey Satellite Triangulation, U.S. Department of Commerce, Washington, D.C., 1962.

3. Brown, Duane C. Results in Geodetic Photogrammetry - I, RCA Data Processing Technical Report No. 54, AFMTC-TR-59-25, 27 October 1959.

4. Jury, H. L., Photogrammetric Ocean Survey Equipment (POSE) Program - Preliminary Report, AFMTC-PAA Report MTVRP 63-4, October, 1963.

5. Eto, D. K., Analysis of an Astro-Photogrammetric Ship Positioning System, Experimental Astronomy Laboratory, Thesis TE-3, Massachusetts Institute of Technology, Cambridge 39, Massachusetts, June, 1963.

6. Brown, Duane C., Results in Geodetic Photogrammetry - II, RCA Data Processing Technical Report No. 65, AFMTC-TR-61-2, 15 September 1960.

7. Sixby, S.R., et al, Long Focal Length Ballistic Camera Study, Perkin - Elmer Corporation, Engineering Report, No. 5942, Norwalk, Conn., 2 October 1961.

8. Nettelblad, F., Studies of Astronomical Scintillation, Lund Observatory, Series II, No. 130, Lund, Sweden, 1953.

9. Morgan, A. H., Precise Time Synchronization of Widely Separated Clocks, National Bureau of Standards, Technical Note, No. 22, Washington, D.C., July, 1959.

10. Wyckoff, C. W., An Experimental Extended Exposure Response Film, S.P.I.E. Newsletter, June - July, 1962, pp. 16-20.

11. Hendriksen, S. W., Camera Design for Photography of Artificial Satellites, Photographic Science and Engineering, pp. 318-323, VI-6, Nov. - Dec., 1962.

12. Draper, C. S., and Woodbury, R. B., Geometric Stabilization Based on Servodriven Gimbals and Integrating Gyro Units, Instrumentation Laboratory, Massachusetts Institute of Technology, Cambridge 39, Massachusetts, September, 1956.

13. Markey, W. R., and Hovorka, J. The Mechanics of Inertial Position and Heading Indication, Methuen, London, 1961.

REFERENCES (Cont.)

14. Bumstead, R. M., Optimum Bandwidth for a Gyro Stabilized Startracker, Instrumentation Laboratory, Massachusetts Institute of Technology, Thesis T-263, Cambridge 39, Massachusetts, August, 1960.

15. MIL-STD 167 (Ships), Mechanical Vibrations of Shipboard Equipment, Navy Dept., Bureau of Ships, Washington, D.C., December, 1954.

16. Woodson, G., Human-Engineering Guide for Equipment Designers, University of California Press, Berkely, California, 1960.

17. Hynek, J. A., On the Effects of Image Motion on the Accuracy of Measurement of a Flashing Satellite, Smithsonian Astrophysical Observatory, Special Report, No. 33, Cambridge, Massachusetts, February, 1960.

18. Seeley, R. B., et al, Alignment of Moving Inertial Navigation Systems, December, 1957.